Activation of an LTR12D repeat by HIV and other stress inducers leads to DHRS2-mediated cellular senescence

Dissertation

der Mathematisch-Naturwissenschaftlichen Fakultät
der Eberhard Karls Universität Tübingen
zur Erlangung des Grades eines
Doktors der Naturwissenschaften
(Dr. rer. nat.)

vorgelegt von
Daksha Navneetkumar Munot
aus Kelshi, Indien (Bharat)

Tübingen
2025

Gedruckt mit Genehmigung der Mathematisch-Naturwissenschaftlichen Fakultät der Eberhard Karls Universität Tübingen.

Tag der mündlichen Qualifikation:	06.08.2025
Dekan:	Prof. Dr. Thilo Stehle
1. Berichterstatter/-in:	Prof. Dr. Daniel Sauter
2. Berichterstatter/-in:	Prof. Dr. Michael Schindler

Dedicated to:

To my beloved **husband Shubham**,
my guiding lights **Mommy and Papa**
(mother, mother-in-law, father, father-in-law),
my pillars **Gaurav, Sahil, Sejal and Shrushti** (siblings),
and to **Bharat**, my sacred motherland,
each of you has shaped the person I am today.

To my **Gurus** and **friends**,
whose blessings and presence continue to illuminate my path,
I remain forever grateful.

With reverence and humility, I offer this timeless prayer:
"Khamemi Savve Jiva, Savve Jiva Khamantu Me,
Mitti Me Savve Bhūesu, Veram Majjha Na Kenai."
I forgive all living beings, may all living beings forgive me.
My friendship is with all, I harbor enmity toward none.

Table of Contents

Abbreviations

Abbreviation	Meaning
°C	Degree Celsius
µ	Micro
ADC	AIDS dementia complex
AIDS	Acquired immunodeficiency syndrome
AIM2	Absent in melanoma 2
AKT	Protein kinase B
ALS	Amyotrophic lateral sclerosis
AMP	Adenosine monophosphate
AmpR	Ampicillin resistance
APOBEC	Apolipoprotein B mRNA editing enzyme-catalytic polypeptide-like
ART	Antiretroviral therapy
ATCC	American Type Culture Collection
ATF4	Activating Transcription Factor 4
ATM	Ataxia-telangiectasia mutated
ATP	Adenosine triphosphate
BANCR	BRAF-activated-non-protein coding RNA
BCL-2	B-cell lymphoma 2
BFP	Blue fluorescent protein
BSA	Bovine serum albumin
β-hCG	Beta-human chorionic gonadotropin
C/EBPβ	CCAAT/enhancer-binding protein beta
CA	Capsid protein
$CaCl_2$	Calcium chloride
CAGE	Cap analysis of gene expression
cAMP	Cyclic adenosine monophosphate
CCR5	C-C chemokine receptor type 5
CD	Cluster of differentiation

CDKI	Cyclin-Dependent Kinase Inhibitor
CDKN1A	Cyclin-Dependent Kinase Inhibitor 1A
CDKs	Cyclin-dependent kinases
cDNA	Complementary DNA
CHKα	Choline kinase alpha
cGAMP	Cyclic GMP-AMP
cGAS	Cyclic GMP-AMP Synthase
CMV	Cytomegalovirus
CNS	Central nervous system
CO_2	Carbon dioxide
CpG	Cytosine-phosphate-guanine
CrFK	Crandell feline kidney cells
CRISPR	Clustered Regularly Interspaced Short Palindromic Repeats
CSF1R	Colony stimulating factor 1 receptor
CXCR4	C-X-C chemokine receptor type 4
CyTOF	Cytometry by Time-of-Flight
dCas9	Dead Cas9 or catalytically inactive Cas9
dCas9-HSF1	Dead Cas9/ Heat Shock Factor 1
dCas9-Rta	Dead Cas9/Replication Transactivator
DDR	DNA damage response
DEAE	Diethylaminoethyl
DENV	Dengue virus
DHRS2	Dehydrogenase/reductase SDR family member 2
DMEM	Dulbecco's modified eagle medium
DMSO	Dimethyl sulfoxide
DNA	Deoxyribonucleic acid
DNMT	DNA methyl transferase
dNTP	Deoxynucleotide triphosphate
dNTPase	Deoxynucleotide triphosphatase
dPBS	Dulbecco's phosphate buffered saline

d.p.i.	Days post-infection
d.p.t.	Days post-transduction
dsRNA	Double-stranded RNA
E. coli	*Escherichia coli*
E2F	E2F transcription factor
E3	Ubiquitin ligase
EBV	Epstein Barr virus
ECM	Extracellular matrix
EDTA	Ethylenediaminetetraacetate
eGFP	Enhanced green fluorescent protein
ELISA	Enzyme-linked immunosorbent assay
Env	Envelope
ER	Endoplasmic reticulum
ERV	Endogenous retrovirus
ETV5	ETS (E26 transformation-specific) variant transcription factor 5
ESCC	Esophageal squamous cell carcinoma
ex vivo	Experiments or procedures performed on living tissue or cells that have been removed from an organism
FACS	Fluorescence-activated cell sorting
FCS	Fetal calf serum
Fig.	Figure
FISH	Fluorescence In Situ Hybridization
FITC	Fluorescein isothiocyanate
FOXO	Forkhead Box
FRD	Friend-related
Fw	Forward
G	Gram; gravitational acceleration
G0	Gap 0 phase
G1	First gap phase
G2	Second gap phase

GADD45	Growth Arrest and DNA Damage-inducible 45
Gag	Group-specific antigen
Gal	Galactosidase
GAPDH	Glyceraldehyde 3-phosphate dehydrogenase
GBP	Guanylate-binding protein
GCM1	Glial cells missing transcription factor 1
GDP	Guanosine diphosphate
GFP	Green fluorescent protein
GMP	Guanosine monophosphate
GP, gp	Glycoprotein
GREAT	Genomic Regions Enrichment of Annotations Tool
GRO	Growth-Regulated Oncogenes
gRNA	Guide RNA
GTAp63	Germ cell-associated, transcriptionally active p63
GTP	Guanosine triphosphate
GTPase	Guanosine triphosphatase
h	Hour; human
H_2O_2	Hydrogen peroxide
H_2SO_4	Sulfuric acid
HAT	Histone acetyl transferase
HBS	HEPES buffered saline
HBV	Hepatitis B virus
HDAC	Histone deacetylase
HDACi	Histone deacetylase inhibitor
HDIS	HSF1 depletion-induced senescence
HEK	Human embryonic kidney
HEPES	4-(2-hydroxyethyl) -1-piperazine-ethanesulfonic acid
HERV	Human endogenous retrovirus
HIF	Hypoxia-inducible factor
HIV	Human immunodeficiency virus

HML	Human Mouse Mammary Tumor Virus-like
HOXA13	Homeobox A13
hRAS^{G12V}	Human *RAS* gene, harboring a mutation that results in an exchange of glycine to valine at position 12 of the protein
HRP	Horseradish peroxidase
HSP	Heat shock protein
HSV	Herpes simplex virus
HTLV	Human T-cell leukemia virus
IAV	Influenza virus
IFI6	Interferon alpha-inducible protein 6
IFN	Interferon
IgG	Immunoglobulin G
IL	Interleukin
in vivo	in the living
in vitro	in glass
IN	Integrase
IRES	Internal ribosome entry site
IRF	Interferon regulatory factor
ISG	Interferon-stimulated gene
JAK	Janus Kinase
kanaR	Kanamycin resistance
KCl	Potassium chloride
kDa	kilodalton
ko	knockout
l	Liter
LB	Lysogeny broth
LINE	Long interspersed element
LTR	Long terminal repeat
LVPs	Lentiviral particles
M	Molarity (mol/l)

MA	Matrix protein
MAPK	Mitogen-activated protein kinase
MAVS	Mitochondrial antiviral signaling protein
MCPs	Monocyte Chemoattractant Proteins
MDA5	Melanoma differentiation-associated protein 5
MDDCs	Monocyte-derived dendritic cells
MDM2	Mouse double minute 2 homolog
MEM	Minimal essential medium
MFI	Mean fluorescence intensity
$MgCl_2$	Magnesium chloride
MHC	Major histocompatibility complex
MiDAS	Mitochondrial dysfunction-associated senescence
min	Minute
ml	Milliliter
MMP	Matrix metalloproteinase 14
mRNA	Messenger RNA
MS	Multiple sclerosis
mtDNA	Mitochondrial DNA
mTOR	Mammalian target of Rapamycin
M-tropic	macrophage-tropic
MW	Molecular weight
n	Number of experiments
N	Nitrogen; amino
Na_2HPO_4	Disodium phosphate
NaCl	Sodium chloride
NADPH	Nicotinamide adenine dinucleotide phosphate
$NaHCO_3$	Sodium bicarbonate
NC	Nucleocapsid
NEAA	Non-essential amino acids

Nef	Negative regulatory factor
NF-Y	Nuclear transcription factor Y
NF-κB	Nuclear factor kappa-light-chain-enhancer of activated B cells
NK	Natural killer
NOTCH1	Neurogenic locus notch homolog protein 1
NRF2	Nuclear factor erythroid 2-related factor 2
nt	Nucleotide
NT	Non-targeting
OIS	Oncogene-induced senescence
ORF	Open reading frame
$p16^{INK4A}$	Protein with a molecular weight of 16 kilodaltons (kDa); inhibitor of cyclin-dependent kinase 4a
$p21^{WAF1/CIP1}$	Protein with a molecular weight of 21 kilodaltons (kDa); wild-type p53-activated fragment 1, CDK-interacting protein 1
p24	Protein with a molecular weight of 24 kilodaltons (kDa)Viral capsid protein
p53	Protein with a molecular weight of 53 kilodaltons (kDa)Tumor protein 53
PAMP	Pathogen-associated molecular pattern
PASP	p21-associated secretory phenotype
PBMC	Peripheral blood mononuclear cell
PBS	Phosphate-buffered saline
PC	Phosphorylcholine
PCR	Polymerase chain reaction
PDGF	Platelet-derived growth factor
PE	Pre-eclampsia
PFA	Paraformaldehyde
PHA	Phytohemagglutinin
PI3K	Phosphoinositide 3-kinase
PLHIV	People living with HIV
PLL	Poly-L-Lysine

PLWH	People Living With HIV
Pol	Polymerase
Poly(I:C)	Polyinosinic:Polycytidylic acid
PP13/LGALS13	Placental Protein 13/Galectin-13
PR	Protease protein
pRb	Retinoblastoma protein
PRR	Pattern recognition receptor
PVDF	Polyvinylidene difluoride
R	Repeat
R	Regulatory
R5	C-C chemokine receptor type 5
RAB11B	Ras-related protein Rab-11B
RAE1	Ribonucleic acid export 1
RcRE	Rec-responsive element
Rev/rev	Regulator of expression of virion protein/Reverse
rh	Rhesus monkey (*Macaca mulatta*)
RIG-I	Retinoic acid-inducible gene I
RING	Really interesting new gene
RLR	RIG-I-like receptor
RNA	Ribonucleic acid
RNase	Ribonuclease
ROS	Reactive oxygen species
RPMI	Roswell park memorial institute
RT	Reverse transcriptase
S.O.C.	Super optimal broth with catabolite repression
SA-β-gal	Senescence-associated-β-galactosidase
SAHF	Senescence-associated heterochromatin foci
SAM	Synergistic Activation Mediator
SAMHD1	Sterile Alpha Motif and Histidine-Aspartate Domain-containing protein 1

SASP	Senescence-associated secretory phenotype
SCAP	Senescent cell anti-apoptotic pathways
SchLAP1	Second chromosome locus associated with prostate cancer 1
SDR	Short-chain dehydrogenase/reductase
SDS	Sodium dodecyl sulfate
s	Second
sec	Second
SEM	Standard error of the mean
SEMA4D	Semaphorin 4D
SERCA	Sarco/endoplasmic reticulum Ca^{2+}-ATPase
SINE	Short interspersed element
SIPS	Stress-induced premature senescence
SLE	Systemic lupus erythematosus
ssRNA	single stranded RNA
STAT	Signal transducers and activators of transcription
STING	Stimulator of interferon genes
SU	Surface protein
SUPYN	Suppressyn
SV40	Simian virus 40
SWI/SNF	Switch/sucrose non-fermentable
TAE	Tris-acetate-EDTA
TAL	Transcription activator-like
Tat	Transactivator of transcription
TCN	Trichothecin
TCR	T cell receptor
TE	Transposable element
tetR	Tetracycline resistance
TF	Transcription factor
TFBS	Transcription factor binding site
TGF-β	Transforming growth factor beta

Th1	T helper type 1
TIMP	Tissue inhibitor of metalloproteinases
TIS	Therapy-induced senescence
TM	Transmembrane
TMD	Transmembrane domain
TNFRSF10B	Tumor necrosis factor receptor superfamily member 10B
TNF-α	Tumor necrosis factor-alpha
TRIM	Tripartite-motif-containing protein
TSS	Transcription start site
TZM-bl	Tranzyme Inc., β-galactosidase and luciferase
U3	Unique 3'
U5	Unique 5'
UCSC	University of California Santa Cruz
unstim.	Unstimulated
UPR	Unfolded protein response
UV	Ultra violet
v	Volume
VEGF-C	Vascular endothelial growth factor C
Vif	Virion infectivity factor
Vpr	Viral protein R
Vpu	Viral protein U
Vpx	Viral protein X
VSV	Vesicular stomatitis virus
VSVG	Glycoprotein of vesicular stomatitis virus
X4	C-X-C chemokine receptor type 4

1 Introduction

1.1 Exogenous retroviruses

1.1.1 Overview

Retroviruses are a diverse family of RNA viruses that have co-evolved with their hosts for millions of years, leaving a lasting impact on both viral evolution and host genomes. They are broadly classified into exogenous and endogenous retroviruses [1-3]. Exogenous retroviruses spread through horizontal transmission, infecting new hosts via direct contact, bodily fluids, or other transmission routes [4]. Among these, the *Orthoretrovirinae* subfamily includes several clinically significant human pathogens, such as the human immunodeficiency viruses (HIV-1 and HIV-2) and the human T-cell leukemia viruses (HTLV-1 and HTLV-2) [5]. HIV-1 is responsible for the global AIDS pandemic due to its high transmission efficiency and ability to weaken the immune system by targeting $CD4^+$ T cells [6, 7]. In contrast, HIV-2 has a lower transmission rate and is primarily confined to West Africa [8, 9]. HTLV-1, though less widely known, is linked to aggressive leukemias and neurological disorders, particularly in endemic regions such as Japan, the Caribbean, and parts of Africa [10]. These exogenous retroviruses continue to pose significant public health challenges, requiring ongoing research into treatment, prevention, and epidemiology.

1.1.2 Epidemiology of HIV

Despite advances in antiretroviral therapy (ART), retroviral infections remain a major public health challenge. In 2023, approximately 39.9 million people were living with HIV globally, with 1.3 million new infections and 630,000 AIDS-related deaths [11]. While antiretroviral therapy improves survival, it is not a cure, and access remains unequal [12]. The high mutation rate and immune evasion of HIV complicate vaccine development and treatment [13].

1.1.3 HIV proteins

HIV-1 and HIV-2 encode several structural, accessory, and regulatory proteins that play crucial roles in viral replication, immune evasion, and pathogenesis [14]. The structural proteins include Gag, Pol, and Env, which form the viral core, enzymes, and envelope, respectively (Fig. 1.1) [15]. Gag is responsible for assembling the viral particle and includes components such as matrix (MA), capsid (CA), and nucleocapsid (NC) [16]. *pol* encodes the viral enzymes reverse transcriptase (RT), integrase (IN), and protease (PR),

which are required for viral replication [17]. Env, the envelope glycoprotein, is crucial for viral entry into host cells. In HIV-1, it consists of the Gp120 and Gp41 subunits [18], while in HIV-2, it comprises Gp125 (which is functionally similar to Gp120) and Gp36 [19].

In addition to structural proteins, HIV-1 and HIV-2 encode the regulatory proteins Tat and Rev [20]. Tat enhances transcription from the viral long terminal repeat (LTR), while Rev facilitates the export of incompletely spliced transcripts from the nucleus to the cytoplasm, allowing for the synthesis of structural and enzymatic proteins [21].

HIV also produces the accessory proteins Nef, Vif, Vpu (in HIV-1) or Vpx (in HIV-2), and Vpr, which modulate host cell functions to enhance viral replication and immune evasion [22-25]. Nef downregulates CD4 and MHC class I molecules to escape immune detection [26, 27], Vif counteracts the antiviral effects of the host APOBEC3G enzyme [28], Vpu (in HIV-1) inhibits the host restriction factor tetherin and degrades CD4 [27, 29, 30], and Vpx (in HIV-2) enhances viral replication by degrading the restriction factor SAMHD1 [31]. Vpr contributes to cell cycle arrest and enhances viral replication in non-dividing cells [32].

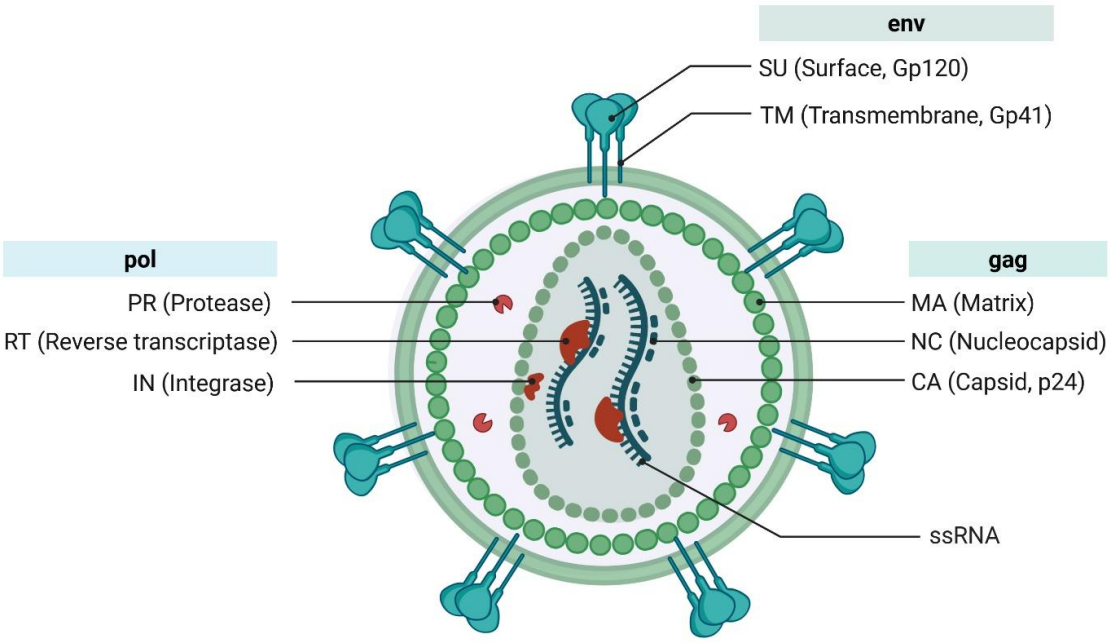

Figure 1.1: HIV-1 virion (**Created with BioRender.com):** The HIV-1 virion is a complex retrovirus characterized by an outer lipid envelope embedded with Env glycoproteins, GP120 (Surface) and GP41 (Transmembrane), crucial for host cell attachment and entry. Encased within this envelope is a conical capsid, primarily composed of Gag proteins

such as the p24 Capsid (CA) and Matrix (MA), which encloses the viral core. This core houses two copies of the single-stranded RNA (ssRNA) genome along with essential Pol enzymes: reverse transcriptase (RT) for converting RNA to DNA, protease (PR) for viral protein processing, and integrase (IN) for viral DNA integration.

1.1.4 Cell tropism of HIV-1

The Envelope (Env) protein is the only viral protein exposed on the lipid membrane of HIV-1, functioning as a transmembrane protein. Synthesized in the rough ER as a type I integral membrane protein, it undergoes cleavage to form a heavily glycosylated Gp160 precursor. This precursor trimerizes and is processed in the ER and Golgi, where a furin-like protease or furin itself cleaves it into Gp120 and Gp41 [33]. Gp120, the Surface (SU) protein, mediates receptor and coreceptor binding, while Gp41, the Transmembrane (TM) protein, facilitates membrane fusion during viral entry. The Gp120/Gp41 complex remains a trimer, first on the host cell and later in the mature virions. Extensive glycosylation on Gp120 shields key epitopes from neutralizing antibodies [33-35].

HIV-1 entry is mediated by the CD4 receptor, which was identified as essential when antibodies against it were found to block infection [36]. CD4 is primarily expressed on T helper cells and plays a key role in stabilizing T cell receptor (TCR) and MHC class II interactions [37]. HIV-1 predominantly targets CD4+ T cells due to the high affinity of its envelope glycoprotein (Env) for CD4, leading to the progressive depletion of these cells during infection [38, 39]. For successful entry, the virus also requires a coreceptor, most commonly CCR5. The transmitted and most prevalent form of HIV-1 is CCR5-tropic (R5) and infects CD4+ memory T cells with high CD4 expression. These R5 viruses are typically found in blood and lymphoid tissues and are responsible for reactivation from latency [40].

When CD4+CCR5+ T cells become limited, such as in specific tissue environments, HIV-1 adapts by evolving to infect alternative cell types. In the central nervous system (CNS), the virus may target macrophages or microglial cells, which express lower levels of CD4 but still use CCR5 [41]. This variant is referred to as macrophage-tropic (M-tropic). In late-stage disease, a coreceptor switch often occurs from CCR5 to CXCR4, allowing the virus to infect a different subset of $CD4^+$ T cells. These are known as CXCR4-tropic (X4) viruses. Thus, HIV-1 displays remarkable flexibility in coreceptor usage to sustain replication in diverse tissue environments. Its entry phenotypes are classified as R5 T

cell-tropic, X4 T cell-tropic, and M-tropic. While X4 viruses remain distinct, most viruses previously classified as M-tropic are now recognized as R5 T cell-tropic, with truly macrophage-tropic strains being relatively rare [42].

1.1.5 AIDS

HIV-1 and HIV-2 progressively weaken the immune system, and if untreated, lead to AIDS, a condition marked by severe immunodeficiency, recurrent opportunistic infections, malignancies, and systemic complications [43].

Beyond its impact on immune function, chronic HIV infection, even before progression to AIDS, has been increasingly recognized as a driver of accelerated aging. Persistent viral replication, chronic immune activation, and inflammation (often termed inflammaging) contribute to premature cellular senescence, telomere shortening, mitochondrial dysfunction, and dysregulated repair pathways [44-46]. These biological changes mirror those observed in natural aging, but occur at a younger age in people living with HIV (PLWH).

As a result, PLWH, especially those with a history of advanced immunodeficiency, face an elevated risk of aging-associated diseases such as cardiovascular disorders, neurocognitive decline, osteoporosis, frailty, and certain cancers, even when viral replication is controlled with antiretroviral therapy [47-49]. The chronic immune activation and reduced immune surveillance in AIDS further accelerate these age-related pathologies by allowing latent infections and cellular stress responses to persist unchecked [49].

1.1.6 Accelerated Aging under ART

Although ART has successfully transformed HIV infection from a fatal illness into a manageable chronic condition, PLWH continue to experience signs of premature aging such as cardiovascular disease, bone density loss, metabolic disorders, and neurocognitive decline [49, 50]. Despite effective viral suppression, ART does not fully restore immune health or prevent the onset of metabolic and mitochondrial dysfunctions, which are central to the aging process in this population [51, 52].

A key factor driving aging in ART treated individuals is mitochondrial dysfunction. Both HIV infection and long-term ART impair mitochondrial integrity by disrupting mitochondrial DNA (mtDNA) maintenance, inhibiting polymerase gamma (Pol-γ)

activity, and increasing oxidative stress. These disruptions lead to reduced ATP production, deregulated respiration, and accumulation of mtDNA mutations. Unlike nuclear DNA, mtDNA lacks protective histones and efficient repair mechanisms, making it particularly susceptible to damage. Over time, this results in impaired energy metabolism and contributes to hallmarks of aging such as cellular senescence and systemic inflammation [51, 53, 54].

Moreover, chronic immune activation persists even under ART, leading to immunosenescence, where immune cells such as T cells lose their functional capacity [55, 56]. This is exacerbated by mitochondrial defects in immune cells, which further compromise their energy-dependent functions such as proliferation and cytokine production [57]. The interplay between mitochondrial damage, telomere shortening, and p53 activation establishes a cycle of cellular stress and aging.

Therefore, while ART remains indispensable for managing HIV, the persistent chronic inflammation and immune activation driven by the HIV infection itself, even under ART, along with some indirect effects of ART, inadvertently contribute to aging-related complications. Understanding these mechanisms is essential for developing adjunct therapies that protect mitochondrial health and improve long-term outcomes and quality of life for PLWH [58, 59].

1.2 Endogenous retroviruses

1.2.1 Overview

Transposable elements (TEs), commonly known as "jumping genes", are mobile DNA sequences capable of moving or copying themselves to different locations within the genome. These elements are ubiquitous across all forms of life and make up a substantial fraction of many genomes. In mammals, TEs account for nearly 50% of the genome, while in some plant species they can constitute up to 90% of the genetic material [60, 61]. In humans, about 48% of the genome is composed of TEs, highlighting their evolutionary and functional significance (Fig. 1.2) [62, 63]. TEs are broadly classified into two major categories based on their mode of transposition: DNA transposons and retrotransposons. DNA transposons move through a "cut and paste" mechanism and were once active during early primate evolution but lost mobility in the human genome around 37 million years ago [64]. In contrast, retrotransposons operate via a "copy and paste" mechanism involving an RNA intermediate that is reverse-transcribed into DNA

and inserted into new genomic locations. Retrotransposons are further divided into long terminal repeat (LTR) retrotransposons and non-LTR retrotransposons based on structural features [65]. Non-LTR retrotransposons are composed of LINEs (Long Interspersed Nuclear Elements) and SINEs (Short Interspersed Nuclear Elements).

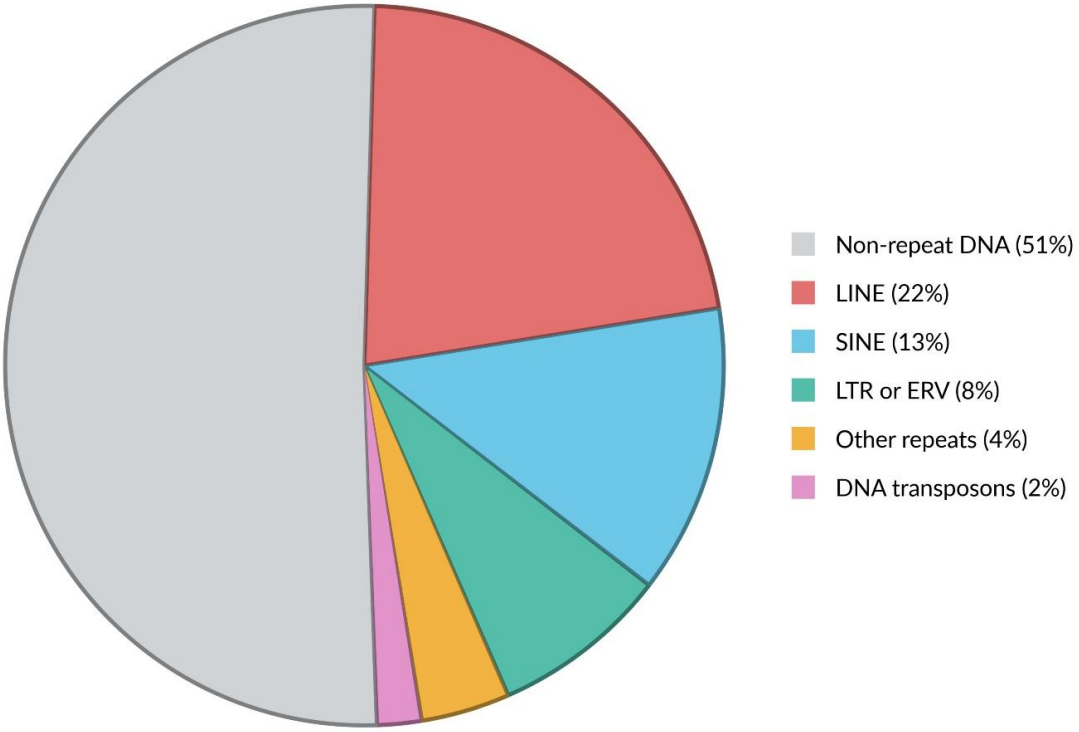

Figure 1.2: Transposable elements are key components of the human genome (Created with BioRender.com): This pie chart illustrates the composition of the human genome, revealing that around 50% is comprised of "jumping genes" known as transposable elements (TEs). Specifically, it breaks down these mobile genetic segments into approximately 22% LINEs (Long Interspersed Nuclear Elements), 13% SINEs (Short Interspersed Nuclear Elements), 8% HERVs (Human Endogenous Retroviruses), 2% DNA transposons, and 4% other repeats. The gray slice depicts the non-repeat DNA, including protein-coding sequences [66].

Among LTR retrotransposons, human endogenous retroviruses (HERVs) represent a significant component of the human genome. HERVs are remnants of ancient retroviral infections that became permanently integrated into the germline DNA of our ancestors [67]. While many HERV families are indeed ancient, some, such as the HERV-K (HML-2) family, are much younger, with evidence of integrations occurring as recently as a few million years ago, and even polymorphic insertions in modern humans [68]. These sequences, passed down through generations, now comprise approximately 8% of the

human genome [67, 69]. While all HERVs have lost their ability to produce infectious particles due to mutations and deletions, they are not biologically silent [70]. Some HERV elements have been co-opted for beneficial host functions such as immune regulation and placental development. For instance, syncytins, proteins encoded by ERV-derived envelope genes, play a vital role in the fusion of placental cells during pregnancy [71].

HERVs may also contribute to host defense by interfering with exogenous retroviral infections, acting as natural antiviral elements [3, 72]. However, when their expression becomes dysregulated due to aging, infection, inflammation, or epigenetic changes, HERVs can exert pathogenic effects. Aberrant HERV activity has been implicated in a range of diseases including cancers, autoimmune disorders, and neurodegenerative conditions such as multiple sclerosis and amyotrophic lateral sclerosis [73, 74].

The dual nature of HERVs as both genomic relics with functional utility and potential drivers of disease makes them an important subject of study. Understanding the mechanisms that regulate HERV activity, such as DNA methylation, histone modification, and small RNA pathways, is critical for unraveling their complex roles in human health and disease [75, 76].

1.2.2 Origin and evolution

HERVs (human endogenous retroviruses) are grouped into three main classes based on phylogenetic analysis of their pol genes, reflecting distinct origins and evolutionary paths [77, 78].

Class I includes elements related to gammaretroviruses and comprises families such as HERVW, HERVH, HERV-FRD, and HERVF [78]. These HERVs are some of the most studied due to their presence in key regulatory regions and their occasional expression in tissues such as the placenta and the brain [79].

Class II consists primarily of the HERV-K (HML-2) family, which remains among the most biologically active and evolutionarily recent HERV groups, with evidence of integrations occurring within the last few million years and even polymorphic insertions observed in modern human populations [80, 81]. Some HERV-K elements are transcriptionally active in human tissues and have been associated with diseases including cancer and neurodegeneration [80].

Class III includes more ancient elements such as HERVL and HSERVIII, which share similarities with spumaviruses (foamy viruses). These elements are thought to represent some of the earliest retroviral integrations in the human lineage [80, 81].

The origin of HERVs can be traced to exogenous retroviruses that infected the germline of primate ancestors, leading to their initial integration into the host genome [78]. Once integrated and fixed in the human genome, these sequences were inherited in a Mendelian fashion and gradually accumulated mutations, insertions, deletions, and recombination events. Many of these processes resulted in the loss of protein coding potential and the formation of solo-LTRs, remnants of full length HERVs left behind after internal sequence deletions (Fig. 1.3) [82].

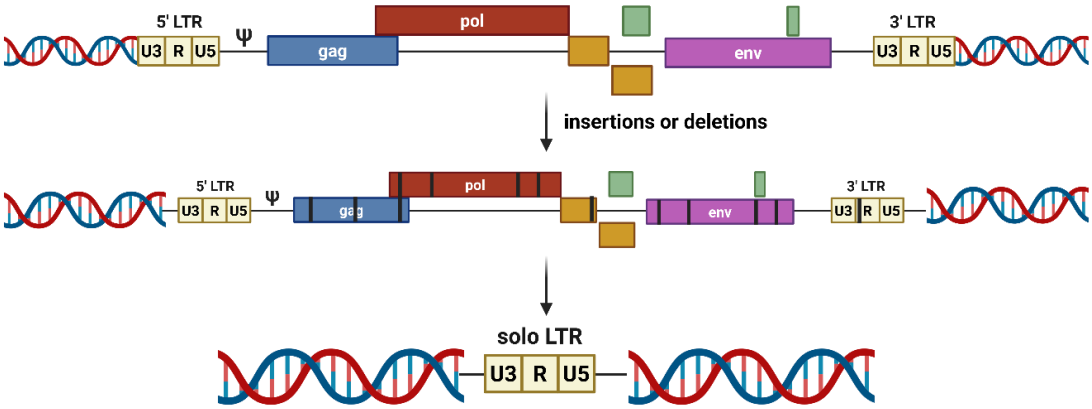

Figure 1.3: Evolution of human endogenous retroviruses (HERVs) and solo-LTR formation (Created with BioRender.com): HERVs are ancient retroviral remnants, comprising ~8% of the human genome, originating from germline integrations. Initially, full-length HERVs possessed LTRs (Long Terminal Repeats) flanking their *gag*, *pol*, and *env* genes, along with other viral sequences such as the packaging signal (Ψ). Each LTR is further subdivided into three regions: U3 (Unique 3'), R (Repeat), and U5 (Unique 5'). Over time, these sequences progressively accumulate mutations and deletions. As illustrated, internal gene loss often leads to the formation of "solo-LTRs," leaving only the flanking repeat sequences. While no longer infectious, these genomic fossils reflect significant evolutionary processes impacting host genome architecture.

Despite widespread inactivation, certain HERV elements have been co-opted by the host for beneficial functions, notably in placental development where syncytins, derived

from HERV *env* genes, are essential for cell fusion, and also in modulating immune responses or regulating nearby gene expression [83].

Among these, the ERV9/LTR12 family notable for its high copy (~5,000 LTR12 elements) and significant transcriptional activity across various human tissues [84]. These LTRs, particularly subtypes such as LTR12C, are frequently co-opted as *cis*-regulatory elements, acting as alternative promoters or enhancers for host genes [72, 85, 86]. LTR12 elements contain recurrent binding sites for various transcription factors, including NF-Y and GATA-2, which contribute to their tissue-specific expression patterns [85]. Furthermore, ERV9/LTR12 can initiate the transcription of long non-coding RNAs (lncRNAs) that act *in cis* to modulate the activity of downstream genes, including erythroid genes [87]. The epigenetic regulation of LTR12 activity is also a critical area of study, as their transcriptional states can be influenced by factors such as histone deacetylase inhibitors, highlighting their dynamic regulatory potential [88]. This widespread regulatory capacity underscores their importance in shaping human gene expression networks and their potential involvement in various physiological and pathological processes [89].

The evolutionary trajectory of HERVs reflects a dynamic interplay between retroviral invasion, host genomic defense mechanisms, and natural selection. Understanding the classification and evolutionary history of HERVs offers critical insight into how these once pathogenic elements have shaped and continue to influence human biology [90].

1.2.3 Co-option of HERVs as regulatory elements and their activation upon HIV-1 infection

Human endogenous retroviruses (HERVs) are typically silenced in the germline. However, during early embryonic development, particularly around the zygotic genome activation phase, there is a period of global epigenetic reprogramming where transposable elements, including some HERVs, are de-repressed, before being re-silenced in somatic lineages [91, 92]. This tight control is essential for preserving genomic stability and preventing harmful consequences of HERV activation in differentiated cells. Nevertheless, certain cellular stressors, such as infections by exogenous viruses, can disrupt this regulation and trigger HERV expression [93, 94].

Several viral infections, including those caused by human immunodeficiency virus type 1 (HIV-1), Influenza A virus (IAV), Dengue virus (DENV), Hepatitis B virus (HBV), SARS-

CoV-2 and Epstein-Barr virus (EBV), have been linked to the reactivation of endogenous retroviruses (ERVs), including families and subfamilies such as ERV-9 (LTR12C), HERV-K (ERV1, ERV3, ERVMER61), HERVW, LTR69_Dup69 [95-100]. However, it remains unclear whether this upregulation actively contributes to pathogenesis or if it is merely a secondary consequence of broader dysregulation.

In the context of HIV-1 infection, multiple mechanisms have been proposed to explain HERV activation, including direct transcriptional activation by viral proteins, modulation of immune signaling pathways, and epigenetic modifications [72, 101]. HIV-1 is particularly well studied for its ability to induce HERV expression [72, 102, 103]. HIV-1 infection has been shown to trigger both transcription and translation of HERV-K loci, the youngest and most transcriptionally active ERV family in the human genome [102, 104]. One mechanism behind this activation involves the HIV-1 Rev protein interacting with the HERV-K regulatory element RcRE, promoting the nuclear export of HERV-K transcripts [105].

Notably, HIV-1 infection directly impacts the expression of other HERV families, including the highly abundant ERV9/LTR12 elements [72]. Our research has demonstrated that HIV-1 infection specifically upregulates LTR12-driven transcription. For instance, RNA sequencing of *ex vivo* HIV-infected $CD4^+$ T cells revealed a significant upregulation of various transposable elements (TEs), including LINE1 elements and several hundred endogenous retrovirus (ERV) loci. Notably, members of the ERV9 lineage, such as LTR12C and LTR12D, exhibited elevated expression levels, indicating that HIV-1 infection broadly influences the transcriptional activity of TEs, irrespective of viral subtype [72]. This induction of LTR12 elements is particularly relevant given their widespread distribution in the human genome and their established roles as *cis*-regulatory elements influencing the expression of adjacent host genes [72]. Specific studies have detailed how LTR12 activation can lead to changes in gene expression profiles in HIV-1 infected cells, potentially contributing to altered cellular physiology or immune responses [84, 85].

One key epigenetic regulatory mechanism contributing to HERV silencing involves DNA methylation, which plays a fundamental role in maintaining proviral silencing. Both HIV-1 proviruses and HERV elements, including HERV-K (HML-2) and LTR12, are normally suppressed through CpG methylation, primarily maintained by DNA methyltransferase 1 (DNMT1) [106-108]. Loss of this methylation can lead to activation. However, whether

HIV-1 actively influences the methylation status of proviral DNA remains an open question [109-111]. If HIV-1 was capable of reducing methylation levels, this could lead to enhanced HERV expression in infected cells, potentially altering cellular physiology and immune responses. Additionally, more complex regulatory mechanisms such as transcriptional interference may also contribute to the control of HERV expression [109, 112].

Given the intricate interplay between host epigenetic regulation, immune responses, and viral infections, further research is needed to delineate the precise mechanisms governing HERV reactivation and its implications for disease progression. Understanding the factors influencing HERV expression in the context of viral infections could have significant implications for both basic virology and therapeutic interventions. Targeting pathways that regulate HERV activation may provide novel insights into viral pathogenesis and potential strategies for mitigating associated diseases. Specifically, the derepression of HERV elements, particularly solo-LTRs such as LTR12, can contribute to cellular stress, genomic instability, and chronic inflammation, all of which are hallmarks of cellular senescence and premature aging in the context of chronic infections with viruses such as HIV-1 [84, 93].

1.3 Cellular senescence

1.3.1 Definition

Cellular senescence is a complex stress-response program characterized by an irreversible cell cycle arrest, distinct morphological changes, and often the acquisition of a pro-inflammatory senescence-associated secretory phenotype (SASP). Senescence is triggered when cells encounter significant stressors such as DNA damage, oxidative stress, oncogenic signaling, or telomere attrition [113, 114]. As highlighted in the preceding section (1.2.3), the aberrant transcriptional activity originating from derepressed HERVs, including LTR12, can contribute to this cellular stress and chronic inflammatory environment, thereby acting as a significant inducer of senescence. While critical in processes such as embryonic development, wound healing, and tumor suppression, the persistent accumulation of senescent cells contribute to aging and age-related pathologies [114].

Cellular senescence is a fundamental biological process wherein cells permanently exit the cell cycle while maintaining metabolic activity [114]. Unlike temporary cell cycle

arrest, which can be reversed when conditions improve, senescence represents a stable and irreversible state. This mechanism evolved as a protective strategy to prevent the propagation of damaged or dysfunctional cells, particularly those with compromised genomic integrity. In doing so, senescence functions as an intrinsic barrier against uncontrolled cell proliferation and tumor formation [115]. While initially beneficial, the long-term accumulation of senescent cells can become detrimental, disrupting tissue homeostasis and contributing to age-associated diseases [116].

To appreciate how senescence unfolds, it is essential to understand the cell cycle. The cycle is divided into distinct phases: G1 (cell growth), S (DNA replication), G2 (preparation for division), and M (mitosis). Cells may also enter a resting state called G0, where they are quiescent but capable of re-entering the cycle if needed [117]. The progression through these phases is tightly regulated by cyclins, cyclin-dependent kinases (CDKs), and their inhibitors, with critical checkpoints at G1/S and G2/M ensuring that only cells with intact and properly replicated DNA proceed to divide [118].

Senescence is triggered when cells encounter significant stressors such as DNA damage, oxidative stress, oncogenic signaling, or telomere attrition [119]. These stress signals activate tumor suppressor pathways, most notably those governed by p53 and retinoblastoma protein (pRb). Upon DNA damage, p53 becomes stabilized and induces the expression of p21, a potent inhibitor of CDKs. The inhibition of CDKs prevents the phosphorylation of pRb, which in its hypophosphorylated form suppresses E2F transcription factors, thereby halting the transcription of genes essential for DNA synthesis and cell cycle progression [120, 121]. The outcome is a stable cell cycle arrest, primarily at the G1 phase, that cannot be reversed even in the presence of growth stimuli [122].

Although senescent cells no longer divide, they undergo significant phenotypic changes. They typically become enlarged and flattened, display increased lysosomal activity, and exhibit altered chromatin architecture [123]. A defining feature of senescent cells is the persistent activation of DNA damage responses, particularly at telomeres, which reinforces their arrested state [124]. Another crucial hallmark is the senescence-associated secretory phenotype (SASP), a complex mixture of cytokines, chemokines, proteases, and growth factors secreted by senescent cells. These secretions can influence the surrounding tissue environment and neighboring cells [115, 125, 126].

The SASP has both beneficial and harmful consequences. In the short term, it can promote wound healing, tissue regeneration, and the recruitment of immune cells to clear senescent cells [126]. However, when senescent cells accumulate and persist, particularly with age or in chronically inflamed tissues, the continuous release of SASP factors leads to sustained low-grade inflammation. This inflammatory milieu, often termed inflammaging, contributes to the progression of a wide range of pathologies including neurodegeneration, cardiovascular disease, osteoporosis, and certain cancers [127-130]. Thus, while the initial induction of senescence acts as a tumor-suppressive mechanism, its chronic presence may create a tissue environment that paradoxically promotes malignancy [131].

In conclusion, cellular senescence is a dynamic and multifaceted process rooted in cell cycle regulation and stress response. It plays a vital role in early life and tissue maintenance by preventing the division of damaged cells. However, the long-term accumulation of senescent cells, coupled with their pro-inflammatory secretory profile, can have deleterious effects on tissue function and organismal aging. Understanding the fine balance between the protective and pathological aspects of senescence is crucial, especially in the context of developing therapies aimed at promoting healthy aging and mitigating age-related diseases [132-135].

1.3.2 Senescence-Associated Secretory Phenotype (SASP)

As discussed earlier in section 1.3.1, the senescence-associated secretory phenotype (SASP) is a key hallmark of senescent cells. It involves the secretion of a wide range of bioactive molecules that allow these cells to interact with their surrounding microenvironment, thereby influencing numerous physiological and pathological processes. [125, 136, 137]

Transcriptional regulation plays a pivotal role in SASP expression, with transcription factors such as NF-κB and C/EBPβ serving as central regulators. NF-κB, in particular, governs the expression of key SASP components such as IL-1α, IL-6, and IL-8, establishing a positive feedback loop that amplifies its own activity [138]. The SASP composition is highly context-dependent, influenced by factors such as the nature of the senescence-inducing stimulus, cell type, and duration of senescence [139]. For instance, during oncogene-induced senescence, fluctuations in NOTCH1 signaling can shift the SASP from

an early TGF-β-rich immunosuppressive profile to a more pro-inflammatory state [140, 141].

Classical SASP factors include cytokines (e.g., IL-6, IL-8), chemokines (e.g., MCPs, GROs), and extracellular matrix (ECM) modulators (e.g., MMPs, TIMPs) [125]. These factors are secreted into the extracellular space, exerting autocrine and paracrine effects. Additionally, many SASP components are released via ectodomain shedding or packaged into extracellular vesicles such as microvesicles and exosomes, which deliver proteins, lipids, noncoding RNAs, and nucleotides to neighbouring cells [142, 143].

Identifying senescent cells is a key to understand the impact of the SASP on tissue microenvironments. Among various senescence markers, Senescence-Associated β-galactosidase (SA-β-gal) remains one of the most widely used. Unlike endogenous lysosomal β-galactosidase, which functions optimally at pH 4.0-4.5, SA-β-gal activity is detectable at pH 6.0-a feature linked to increased lysosomal content in senescent cells [144]. This pH-dependent distinction allows selective detection of senescent cells and has become a standard tool for studying SASP-producing populations in vitro and in vivo.

Functionally, the SASP has a dual role. Beneficially, it supports tissue repair, regeneration, and immune surveillance by recruiting immune cells such as NK cells, macrophages, and T cells to clear senescent cells [139, 145, 146]. During embryonic development and wound healing, the SASP contributes to tissue remodeling and stem cell activation [139]. Furthermore, the SASP reinforces senescence-associated growth arrest through autocrine signaling, supporting tumor suppression by creating an anti-proliferative microenvironment [147]. Conversely, chronic SASP production can be detrimental, particularly in aging tissues. Persistent SASP secretion leads to chronic low-grade inflammation, termed "inflammaging," contributing to age-related pathologies such as cancer, cardiovascular diseases, fibrosis, and neurodegeneration [148-150]. Certain SASP factors promote angiogenesis, tissue invasion, and epithelial-to-mesenchymal transition, facilitating tumor progression. Moreover, SASP-mediated paracrine signaling can induce secondary senescence in neighbouring cells via pathways like NOTCH1 and JAK2/STAT3, amplifying cellular dysfunction [151, 152].

Despite stable growth arrest, senescent cells evade apoptosis by activating senescent cell anti-apoptotic pathways (SCAPs), including BCL-2 family proteins, HSP90, PI3K/AKT, and HIF-1α [153]. These pathways protect senescent cells from the deleterious effects

of their own SASP factors. Given their role in senescent cell survival, SCAPs have emerged as therapeutic targets. Inhibiting SCAPs can selectively eliminate senescent cells while sparing healthy cells [154].

This understanding has led to the development of senotherapeutics, comprising senolytics and senomorphics. Senolytics, such as dasatinib combined with quercetin and navitoclax, target SCAPs to induce senescent cell apoptosis, reducing SASP output [155, 156]. Senomorphics, like the JAK1/2 inhibitor ruxolitinib, suppress SASP production without eliminating senescent cells, mitigating age-related disorders such as osteoporosis [157, 158].

In summary, the SASP is a central feature of cellular senescence, exerting significant influence on tissue homeostasis, aging, and disease. Its composition and effects are highly variable and temporally regulated, reflecting the complexity of senescent cell behaviour. Elucidating the regulation of the SASP and its interaction with survival pathways like SCAPs offers promising avenues for therapeutic interventions aimed at promoting healthy aging and combating chronic diseases.

1.3.3 p53/p21$^{WAF1/CIP1}$ and p16^{INK4A}/pRB

Cellular senescence is a critical mechanism for tumor suppression and tissue homeostasis, primarily driven by the p53/p21$^{WAF1/CIP1}$ and p16^{INK4A}/pRB pathways [159, 160]. These pathways are interconnected, contributing to the irreversible arrest of the cell cycle in response to various stress signals such as DNA damage, telomere shortening, and oxidative stress. The activation of p53 serves as one of the earliest and most important responses to cellular stress. Upon sensing DNA damage or oncogenic stress, p53 is stabilized and activated through various post-translational modifications, such as phosphorylation by ATM kinase [159]. Activated p53 induces the expression of several key target genes, including p21$^{WAF1/CIP1}$, which directly inhibits cyclin-dependent kinases (CDKs), halting the progression of the cell cycle at the G1 phase [161]. This cell cycle arrest is a critical first step in initiating senescence, ensuring that cells with damaged DNA do not proliferate. p53 can also induce apoptosis if the damage is irreparable, contributing to cell death under extreme stress conditions. Thus, p53 functions as a central hub, regulating both the induction of senescence and apoptosis depending on the severity of the damage and the cellular context [161].

$p21^{WAF1/CIP1}$, a downstream target of p53, is crucial for the initiation of senescence. It inhibits the kinase activity of CDK4/6 and prevents the phosphorylation of the retinoblastoma (pRB) protein, which is necessary for the transition from G1 to S phase [162]. By inhibiting CDK4/6, p21 ensures the maintenance of pRB in its active, unphosphorylated form, preventing the release of E2F transcription factors, which are necessary for cell cycle progression. While p21 plays a vital role in the initiation of senescence, its function is complex and context-dependent. At high levels, p21 acts as a potent cyclin-dependent kinase inhibitor (CDKI), enforcing cell cycle arrest and promoting senescence [163]. However, at lower levels, p21 can promote cell cycle progression by facilitating the assembly of cyclin D/CDK4/6 complexes, highlighting its dual role in regulating cell proliferation. Therefore, the precise level and location of p21 within the cell determine whether it functions as a cell cycle inhibitor or promoter, further complicating the regulation of senescence [162]. Interestingly, while p21 is essential for the initiation of senescence, its expression does not persist in senescent cells [164]. Instead, its role is primarily confined to the early stages of senescence induction, after which other pathways, such as $p16^{INK4A}$, play a more prominent role in maintaining the senescent state [165, 166].

Unlike p21, which is required for the initiation of senescence, p16 acts as a permanent cell cycle inhibitor, primarily by inhibiting CDK4/6. This leads to the stabilization of pRB and the formation of repressive complexes with E2F, ultimately ensuring persistence of the cell cycle arrest in the G1 phase (Fig. 1.4) [165, 167, 168]. p16 is often considered the key player in maintaining the senescent phenotype, especially in response to prolonged or chronic stress. The expression of p16 increases with age, and it is commonly associated with senescence in aged tissues and certain precancerous lesions [169]. In addition to its role in maintaining cell cycle arrest, $p16^{INK4A}$ and p21 have been implicated in regulating the senescence-associated secretory phenotype (SASP) that influence the local microenvironment and contribute to tissue remodeling, aging, and cancer progression. In this way, p16 (and p21) not only plays a role in sustaining the senescent state but also mediates the paracrine effects of senescence, further reinforcing the non-proliferative state of the affected cells [166].

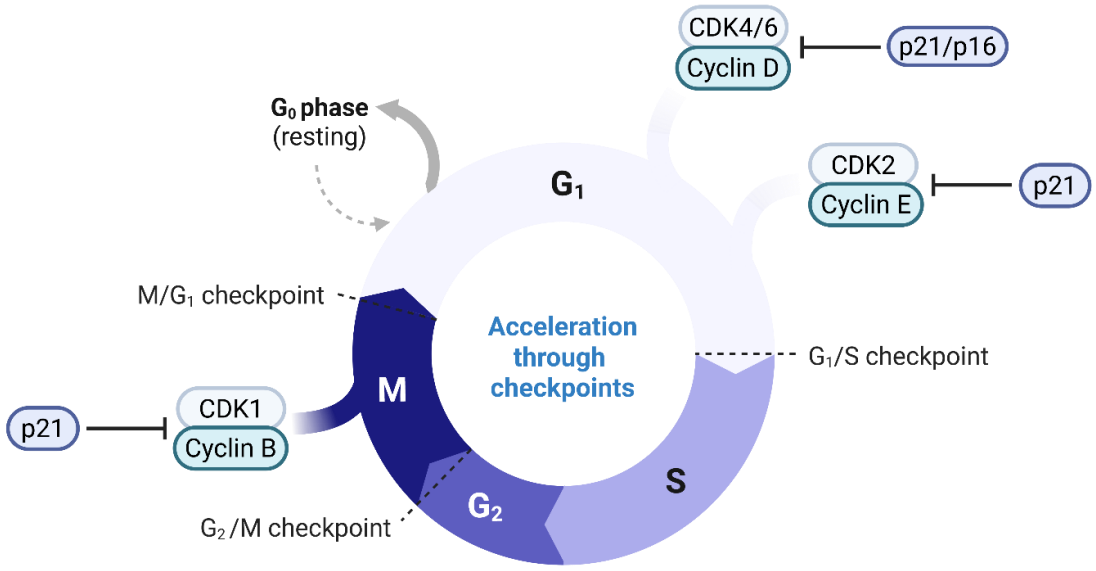

Figure 1.4: Cell cycle regulation and deregulation (**Created with BioRender.com):** This diagram illustrates the key regulatory points within the cell cycle and how specific proteins, such as p21 and p16, govern progression or arrest. Cell cycle transitions, particularly from G1 to S phase, are driven by cyclin-dependent kinase (CDK) complexes (e.g., CDK4/6-Cyclin D, CDK2-Cyclin E), but these can be inhibited by p21 and p16. P21, a protein induced by p53, is essential for initiating cell cycle arrest and triggering senescence by inhibiting CDKs. Concurrently, p16 acts as a specific inhibitor of CDK4/6, which is vital for maintaining a sustained G1 phase arrest and preserving the senescent state. If these crucial regulatory mechanisms are compromised, leading to an "acceleration through checkpoints", the result can be uncontrolled cell proliferation.

In addition to the p53/p21/p16 axis, other factors also contribute to the regulation of senescence. The mTOR pathway, for example, plays an important role in the regulation of senescence and the SASP. Inhibition of mTOR can suppress senescence and reduce the inflammatory secretome [170]. FOXO4, a member of the FOXO family of transcription factors, also plays a key role in regulating senescence by interacting with p53 and modulating its activity during cellular stress [171]. Sirtuins, a family of NAD+-dependent deacetylases, also influence the senescence process by modulating chromatin structure and DNA repair mechanisms [172]. The accumulation of reactive oxygen species (ROS) during mitochondrial dysfunction is another factor that reinforces the senescent state by promoting oxidative stress [173]. Together, these additional pathways form an integrated network that governs the onset, maintenance, and

eventual resolution of senescence, highlighting the multifaceted nature of this process in both aging and tumor suppression.

Thus, p53, p21, and p16 are integral to the regulation of senescence, each performing distinct but complementary roles in initiating, maintaining, and reinforcing cell cycle arrest, while additional pathways contribute to the overall dynamics of senescence, influencing both cellular behaviour and the surrounding microenvironment.

1.3.4 DHRS2

The intricate regulation of senescence, encompassing the initiation, maintenance, and reinforcement of cell cycle arrest by p53, p21, and p16, is further influenced by a network of additional upstream components. A particularly compelling example is Dehydrogenase/Reductase 2 (DHRS2), which functions as an integral upstream component of the canonical p53-p21 senescence pathway itself. DHRS2 exhibits unique subcellular dynamics, particularly its ability to translocate from the mitochondria to the nucleus in response to cellular stress [174]. Under oxidative stress or DNA damage conditions, DHRS2 migrates from its mitochondrial localization into the nucleus, where it interacts directly with MDM2, the principal E3 ubiquitin ligase responsible for regulating the stability of the tumor suppressor protein p53 [175]. MDM2 typically binds to p53 and targets it for ubiquitination and proteasomal degradation, thus maintaining low levels of p53 under normal conditions [176]. However, DHRS2 disrupts this interaction by binding to MDM2 and inhibiting its E3 ligase activity. This inhibition prevents MDM2 from targeting p53 for degradation, thereby stabilizing and activating p53 [176, 177].

Once stabilized, p53 accumulates in the nucleus and transactivates several downstream genes, including *CDKN1A*, which encodes the cyclin-dependent kinase inhibitor $p21^{WAF1/CIP1}$. Elevated p21 levels lead to the inhibition of CDK2 and CDK4/6 activity, resulting in the dephosphorylation and activation of the retinoblastoma protein (pRB), which in turn blocks E2F-mediated transcription and arrests the cell cycle at the G1 phase. This chain of events not only halts cellular proliferation but also sets the stage for the establishment of cellular senescence (Fig. 1.5) [162, 178].

The short-chain dehydrogenase/reductase (SDR) superfamily represents a large and diverse group of NAD(P)(H)-dependent oxidoreductases that play crucial roles in lipid metabolism, redox sensing, and cellular detoxification [179, 180]. Members of this

family function not only as oxidoreductases but also as lyases and isomerases, enabling them to catalyse a broad range of substrates such as steroids, retinoids, lipids, polyols, ribonucleotides, and xenobiotics [181]. By mediating the conversion between active and inactive states of these signaling molecules, SDR enzymes are central to maintaining cellular homeostasis and responding to metabolic and oxidative stress. One such member, Dehydrogenase/Reductase member 2 (DHRS2), also known as Hep27, is an NADH/NADPH-dependent SDR enzyme that has garnered increasing attention for its role in both metabolic regulation and tumor suppression [182-184].

In recent years, DHRS2 has emerged as a significant player in cancer biology. The gene encoding DHRS2 is located on chromosome 14q11.2, a region that is frequently deleted in a variety of malignancies, including esophageal, nasopharyngeal, and ovarian cancers [182, 185]. This chromosomal loss hints at a potential tumor-suppressive function of DHRS2. Indeed, numerous studies have demonstrated that DHRS2 expression is significantly downregulated in several types of tumors when compared to corresponding normal tissues. The loss or reduced expression of DHRS2 has been shown to correlate with increased cancer cell proliferation, invasion, migration, and resistance to chemotherapeutic agents [182]. For instance, in esophageal squamous cell carcinoma (ESCC), DHRS2 is consistently found to be under-expressed, with low levels negatively correlating with clinical parameters such as tumor invasion depth, lymph node metastasis, and overall disease stage [186]. Functionally, re-expression of DHRS2 in ESCC cells results in decreased cellular reactive oxygen species (ROS) levels and alters the NADP/NADPH redox balance, thereby suppressing activation of the p38 MAPK pathway and reducing matrix metalloproteinase 2 (MMP2) expression, factors essential for cancer cell motility and invasiveness [186].

In nasopharyngeal carcinoma, overexpression of DHRS2 has been reported to inhibit cell proliferation through the disruption of intracellular lipid homeostasis [177]. Additionally, in ovarian cancer, treatment with histone deacetylase inhibitors (HDACi) has been shown to induce *DHRS2* expression [187]. Interestingly, cancer cells with higher DHRS2 levels exhibited increased sensitivity to HDACi, suggesting that DHRS2 may act as a sensitizing factor in epigenetic therapy. Despite these findings, the precise molecular mechanisms by which DHRS2 exerts its tumor-suppressive effects have only recently begun to be elucidated.

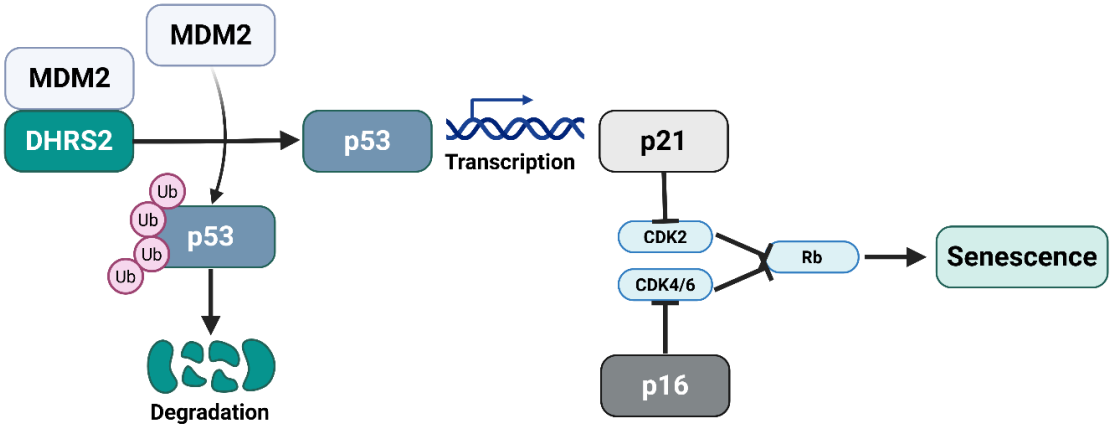

Figure 1.5: DHRS2-mediated p53 stabilization leading to senescence (Created with BioRender.com): This diagram illustrates how DHRS2 regulates the p53 pathway, culminating in cellular senescence. Under cellular stress, DHRS2 translocates into the nucleus, where it directly interacts with MDM2, the E3 ubiquitin ligase typically responsible for degrading the tumor suppressor p53. DHRS2 inhibits the activity of MDM2, thereby preventing p53 ubiquitination and degradation, leading to p53 stabilization and accumulation. This stabilized p53 then transactivates the gene encoding p21, which in turn inhibits cyclin-dependent kinases (CDK2 and CDK4/6). The inhibition of CDKs activates the retinoblastoma protein (Rb), ultimately blocking cell cycle progression and inducing senescence.

Furthermore, the regulation of redox homeostasis by DHRS2 adds another layer to its tumor-suppressive role. By reducing intracellular ROS and modulating the NADP+/NADPH ratio, DHRS2 may fine-tune redox-sensitive signaling pathways such as p38 MAPK and NF-κB, which are often aberrantly activated in cancer [188, 189]. In this way, DHRS2 coordinates both metabolic and cell cycle checkpoints to maintain cellular integrity under stress.

In conclusion, DHRS2 represents a multifaceted tumor suppressor whose functions span from redox regulation and lipid metabolism to the activation of nuclear senescence pathways via p53 stabilization. Its ability to translocate to the nucleus and inhibit MDM2 directly links mitochondrial redox sensing to nuclear cell fate decisions. The downregulation or loss of DHRS2 in multiple cancers underscores its importance in maintaining normal cellular physiology, and its modulation may hold therapeutic

promise for reactivating senescence programs in tumors where p53 remains wild-type but is functionally suppressed.

1.3.5 Different types of senescence

The type of senescence a cell undergoes largely depends on the nature, duration, and intensity of the inducing signal, as well as the cellular context. Stress-induced premature senescence (SIPS) occurs independently of telomere shortening and is initiated by a wide array of stimuli, including oxidative stress, endoplasmic reticulum (ER) stress, mitochondrial dysfunction, oncogene activation, and exposure to chemotherapeutic agents. These stressors can push cells into a stable, irreversible growth arrest characterized by a senescent phenotype [115, 190-194].

One of the most extensively studied inducers of senescence is oxidative stress. Reactive oxygen species (ROS), such as hydrogen peroxide (H_2O_2), inflict damage on cellular components including DNA, proteins, and lipids, thereby activating the DNA damage response (DDR) and triggering senescence [195-197]. *In vitro*, H_2O_2 is commonly used to model oxidative stress-induced senescence, particularly in fibroblasts. Prolonged oxidative stress not only damages nuclear DNA but also impairs mitochondrial function, resulting in a subtype known as mitochondrial dysfunction-associated senescence (MiDAS) [198, 199]. MiDAS is marked by disrupted NAD^+ metabolism, persistent activation of p53, and a distinct SASP that is less inflammatory and instead enriched in metabolic regulators [200].

Endoplasmic reticulum stress is another potent inducer of senescence. Pharmacological agents such as thapsigargin, which inhibits the ER calcium ATPase and disrupts calcium homeostasis, induce ER stress by causing accumulation of misfolded proteins [201, 202]. This stress activates the unfolded protein response (UPR), which, if unresolved, can trigger senescence through p53-p21 or p16-pRB pathways [203]. Similarly, treatment with staurosporine, a broad-spectrum kinase inhibitor known to induce apoptosis at high concentrations, can initiate a senescence-like state at sublethal doses, particularly through mitochondrial and ER stress pathways [204].

Nutlin-3a-induced senescence serves as a prominent and well-established model for p53-dependent senescence, functioning by stabilizing p53. Nutlin-3a acts as an MDM2 antagonist, which prevents the degradation of p53. This leads to the accumulation of p53 and the subsequent transcriptional activation of p21, a cyclin-dependent kinase

inhibitor [205, 206]. This p53-p21 axis halts the cell cycle at the G1 phase, and sustained activation leads to a senescent phenotype [207]. This model is especially valuable in cells with wild-type p53, such as primary human fibroblasts [208].

Oncogene-induced senescence (OIS) is another well-studied form of premature senescence. Activation of oncogenes such as $hRAS^{G12V}$ in normal primary or BJ fibroblast cells leads to a hyperproliferative burst followed by a strong DDR and stable cell cycle arrest [209, 210]. This mechanism serves as a safeguard against malignant transformation. OIS is characterized by robust activation of both $p16^{INK4a}$ and p53 pathways, as well as the formation of senescence-associated heterochromatin foci (SAHF), which contribute to the silencing of proliferation-promoting genes [211-213].

A unique and recently explored form of senescence is syncytia-mediated senescence, particularly observed in trophoblast cells [214]. Fusion of cells into multinucleated syncytia, as seen in BeWo choriocarcinoma cells or primary human trophoblasts, can trigger cellular senescence [215]. This type of senescence is relevant to placental biology, where controlled syncytialization is essential for normal placental function [216]. However, abnormal syncytium formation or stress during this process may lead to premature senescence, potentially contributing to pregnancy-related complications [217].

Therapy-induced senescence (TIS) is another category wherein genotoxic agents, ionizing radiation, or certain chemotherapeutic drugs trigger senescence in tumor cells as a defense mechanism. While TIS can suppress tumor growth temporarily, the persistence of senescent cancer cells and their SASP output can also promote relapse, therapy resistance, or inflammation in the tumor microenvironment [218].

In summary, senescence is not a one-size-fits-all process but rather a highly context-dependent cellular fate that can be induced by diverse signals, including oxidative stress, ER and mitochondrial dysfunction, DNA damage, oncogene activation, and cell fusion. These distinct triggers lead to overlapping yet unique molecular signatures of senescence, typically involving activation of the p53-p21 or p16-pRB pathways, DDR signaling, and the SASP. Understanding the nuanced pathways of these senescence types is critical for designing targeted interventions in aging, cancer, and regenerative medicine.

1.4 Preliminary data

Building upon the observation that HIV infection upregulates specific ERV9/LTR12 elements (as detailed in Section 1.2.3), preliminary investigations of my host laboratory have explored the functional consequences of this activation, particularly regarding one specific LTR12D element (hg38 chr14:23636315-23636374) and its potential role in cellular senescence. This LTR12D element drives the expression of the adjacent cellular gene, *DHRS2* (Dehydrogenase/Reductase member 2). As detailed in Section 1.3.4, DHRS2 is an enzyme involved in redox reactions [219] and has been implicated in activating the p53 pathway by stabilizing p53 via inhibition of MDM2 [176, 189], thereby promoting cellular senescence [174, 220].

RNA-seq data revealed that upon HIV-1 infection, transcripts containing LTR12D sequences fused to *DHRS2* were significantly increased (Fig. 1.6A, 1.6B). Subsequent experiments confirmed that the LTR element acts as a *bona fide* promoter driving *DHRS2* expression (Fig. 1.6C) [221]. Further validation using q-RTPCR and flow cytometry (Fig. 1.7A) demonstrated a concomitant increase in LTR12D-*DHRS2* transcript levels, accompanied by the upregulation of p53 and *CDKN1A* (p21) (Fig. 1.7B, 1.7C, 1.7D). Moreover, HIV-1-infected cells also showed hallmarks of senescence, including increased senescence-associated β-galactosidase activity (Fig. 1.7E) and elevated levels of key SASP components, such as pro-inflammatory cytokines and chemokines, including CCL5, CCL17, IL-6, IL-8, CXCL10 (IP-10), and TNF-α (Fig. 1.8A, 1.8B). These findings collectively support the activation of an LTR12D-DHRS2-p53-p21 pathway in HIV-1-induced cellular senescence.

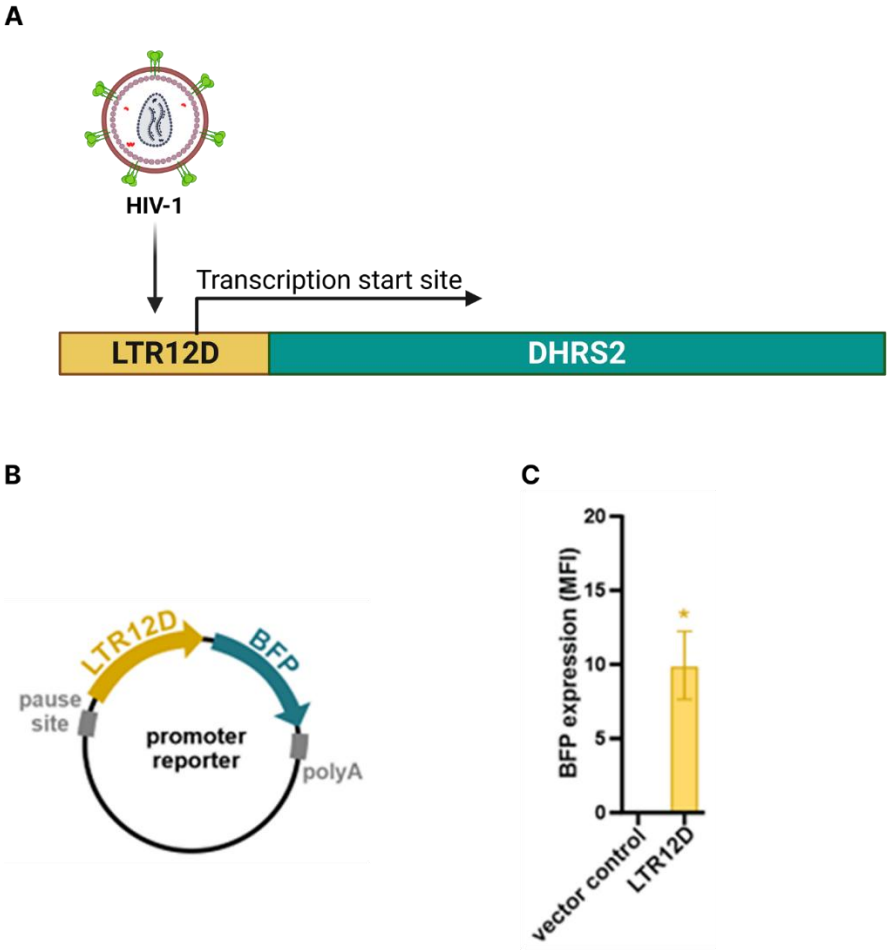

Figure 1.6: LTR12D-mediated *DHRS2* expression in response to HIV-1 infection. (A) Upon HIV-1 infection, transcripts containing LTR12D sequences fused to *DHRS2* are significantly increased, suggesting a link between infection and *DHRS2* regulation. **(B-C)** HEK293T cells were transfected with reporter plasmid expressing (B) blue fluorescent protein (BFP) under the control of the LTR12D repeat alone. Vectors lacking the LTR12D repeat served as negative control. Two days post transfection, cells were harvested, and (C) reporter gene expression was analyzed by flow cytometry. All data are presented as mean ± standard error of the mean (SEM) from three independent experiments. One-way ANOVA was used to determine statistical significance, with $p<0.05(*)$ indicating significant differences compared to mock-infected controls. (Dr. Smitha Srinivasachar Badarinarayan generated the plasmid shown in panel B and performed the experiment shown in panel C).

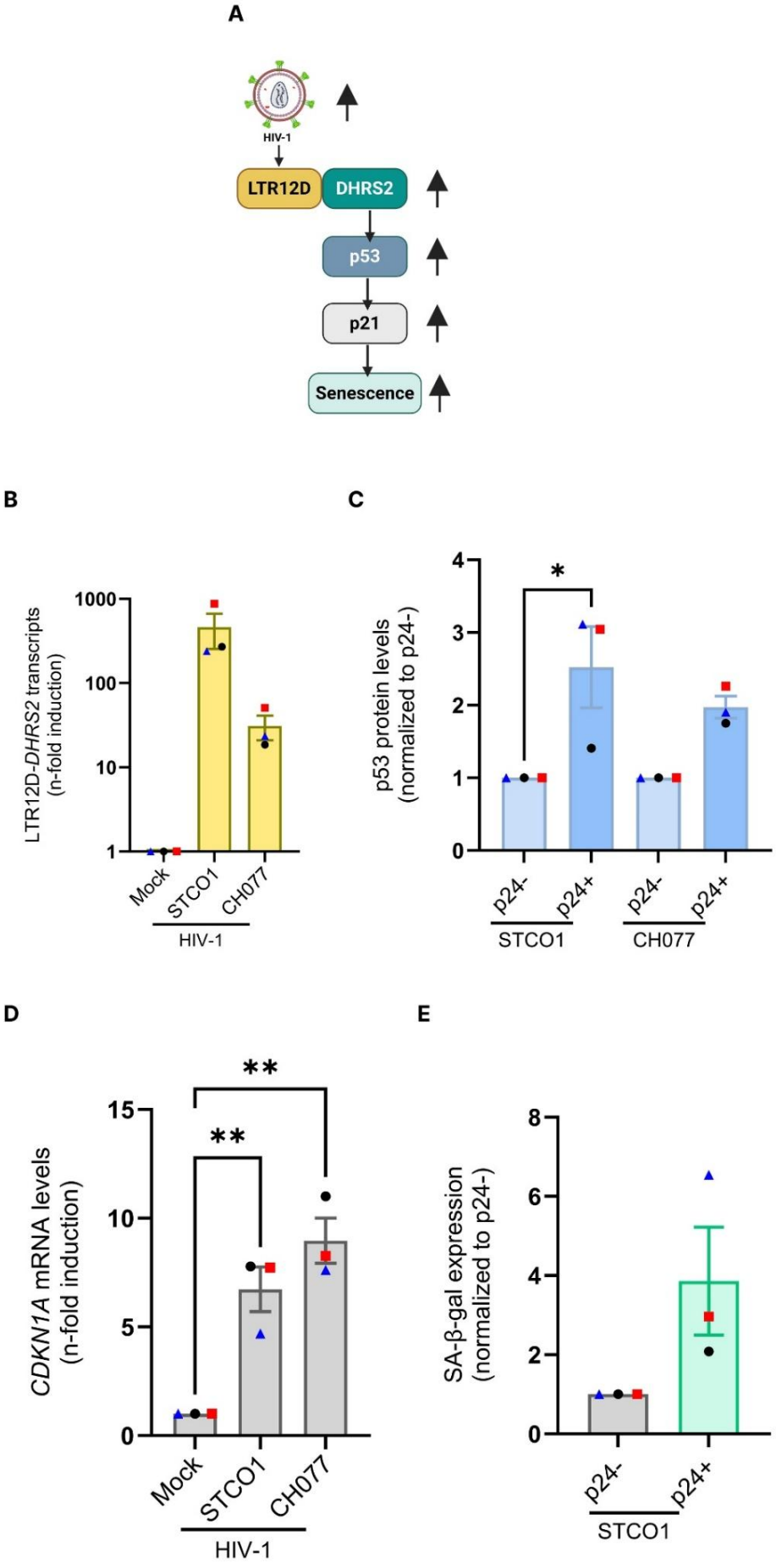
A
HIV-1
LTR12D
DHRS2
p53
p21
Senescence
B
LTR12D-DHRS2 transcripts (n-fold induction)
1000
100
10
1
Mock
STCO1
CH077
HIV-1
C
p53 protein levels (normalized to p24-)
4
3
2
1
0
*
p24-
p24+
p24-
p24+
STCO1
CH077
D
CDKN1A mRNA levels (n-fold induction)
15
10
5
0
**
**
Mock
STCO1
CH077
HIV-1
E
SA-β-gal expression (normalized to p24-)
8
6
4
2
0
p24-
p24+
STCO1

Figure 1.7: Activation of an LTR12D-DHRS2-p53-p21 pathway in HIV-1-induced cellular senescence. (**A)** Illustration of the proposed pathway: Upon HIV-1 infection, LTR12D_*DHRS2* is activated. DHRS2 then binds to MDM2, causing p53 stabilization, leading to increased *CDKN1A* transcription, an increase in senescence-associated β-galactosidase (SA-β-gal) activity, and ultimately cellular senescence. **(B-E)** To experimentally validate this pathway, primary $CD4^+$ T cells were infected with HIV-1 clones STCO1 or CH077. The levels of **(B)** LTR12D_*DHRS2* transcripts (n-fold induction), **(C)** p53 protein (normalized to p24- cells), and **(D)** *CDKN1A* mRNA (n-fold induction), which encodes p21, were determined by q-RTPCR and flow cytometry. **(E)** Senescence-associated β-galactosidase activity (normalized to p24- cells) was measured by flow cytometry. All data are presented as mean ± standard error of the mean (SEM) from three independent experiments. Statistical significance was determined using one-way ANOVA, with $p<0.05(*)$ and $p<0.01(**)$ indicating significant differences compared to mock-infected controls. (Experiments in B-E were conducted by Dr. Smitha Srinivasachar Badarinarayan.)

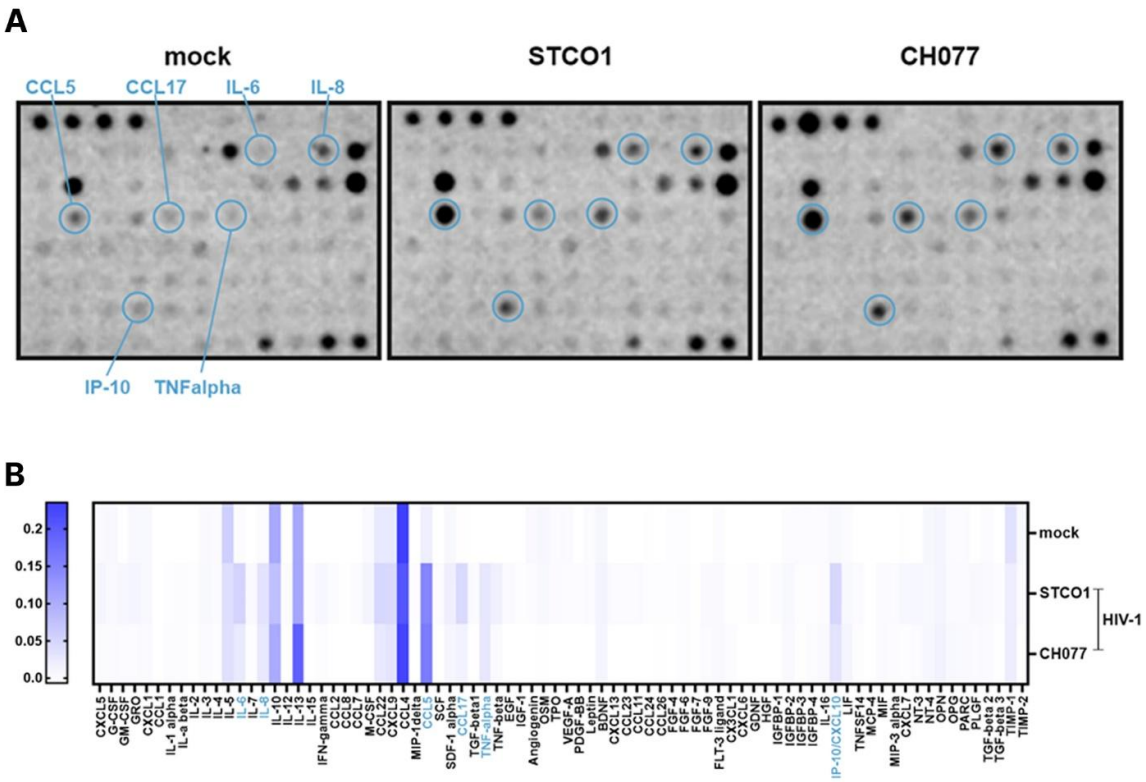

Figure 1.8: HIV-1-induced senescence and cytokine release. (A) Primary $CD4^+$ T cells were either mock-infected or infected with HIV-1 clones STCO1 and CH077. This panel displays representative semi-quantitative cytokine array blots from the supernatants,

showing the release of various cytokines and chemokines into the supernatant. Key pro-inflammatory cytokines and chemokines, such as CCL5, CCL17, IL-6, IL-8, CXCL10 (IP-10), and TNF-α, are highlighted, demonstrating their induction upon HIV-1 infection. **(B)** Heatmap illustrating the results obtained in (A). Numerous cytokines, particularly those associated with a SASP, appeared elevated in supernatants of HIV-1-infected cells compared to mock controls (observed visually). Elevated levels of IL-6 and TNF-α were observed. These factors are recognized components of the senescence-associated secretory phenotype (SASP).

This page is intentionally left blank

2 Scientific aims

Human endogenous retroviruses (HERVs), comprising ~8% of the human genome, are germline-integrated remnants of once infectious exogenous retroviruses. While many of them are often epigenetically silenced, some can be transcriptionally reactivated by various stimuli [222, 223]. Intriguingly, some HERV-derived LTRs exert important regulatory functions, acting as *cis*-regulatory elements for cellular genes [223, 224]. For instance, several MER41 LTRs contain STAT1 binding sites, and upregulate the expression of immune factors (e.g., *AIM2*, *IFI6*) in response to IFN-γ stimulation [225]. Similarly, the HERV-W LTR functions as a promoter for *HERVW-1*, a critical gene for human placental syncytiotrophoblast formation [79].

Exogenous viruses such as HIV-1 induce specific patterns of HERV activity, potentially contributing to chronic immune activation and cellular dysfunction [226]. Prior work of our research group revealed that HIV-1 infection activates a specific host response mediated by an endogenous retroviral LTR12D element located on chromosome 14 (hg38: chr14:23636315–23636374) [72]. In primary $CD4^+$ T cells, activation of this LTR12D element leads to upregulation of the adjacent *DHRS2* gene [72]. DHRS2 stabilizes p53 by preventing its degradation via MDM2, thereby enhancing p53-dependent transcription of *CDKN1A* and inducing cellular senescence [174, 186].

This project aims to precisely delineate how LTR12D-driven DHRS2-p53-p21 signaling contributes to cellular senescence in HIV infection and other cellular stress contexts.

Specifically, I aim to:

1. characterize the LTR12D-DHRS2-p53-p21 cascade in HIV infection: To this end, I will investigate its activation and downstream effects on primary cells such as $CD4^+$ T cells, macrophages, as well as immortalized cell lines such as SupT1 and Jurkat during HIV-1 and HIV-2 infection (Chapters 1-4).

2. delineate the role of DHRS2 in senescence: Using over-expression and depletion approaches, I will determine if DHRS2 is sufficient and/or required for the induction of cellular senescence (Chapters 5-7).

3. identify upstream regulators of the LTR12D-*DHRS2* cascade: I will uncover and characterize factors governing the activation of LTR12D and its impact on *DHRS2* expression (Chapters 8-9).

4. evaluate LTR12D-*DHRS2*-induced signaling in non-viral senescence: By comparing different stressors, I will assess the contribution of this cascade to senescence in the absence of viral infection (Chapter 10).

These investigations will advance our understanding of TE-driven gene regulation in cellular senescence, with implications for HIV-associated comorbidities and age-related pathologies.

3 Materials and methods

3.1 Material

3.1.1 Cell culture

3.1.1.1 Eukaryotic cell lines

Cell line	Description
HEK293T	Human embryonic kidney 293 large T antigen cells are based on a human renal epithelial cell line derived from a female fetus. Cells were transformed by human adenovirus type 5 and stably express the simian virus 40 (SV40) large T antigen [227]. The cell line was obtained via the ATCC (#CRL- 3216).
SupT1	This T lymphoblast cell line was derived from malignant cells collected from the malignant pleural effusion of an 8-year-old child with T-Cell Lymphoblastic Lymphoma. The cell line was obtained via the ATCC (#CRL-1942).
Jurkat	Jurkat, Clone E6-1 is a clone of the Jurkat-FHCRC cell line, a derivative of the Jurkat cell line, which was established from the peripheral blood of a 14-year-old, male, acute T-cell leukemia patient. This cell line can be used in immune system disorder research and immunology and immuno-oncology research and was obtained via the ATCC (#TIB-152).
BeWo	BeWo cells are a placental cell line that has been widely used as an *in vitro* model for the placenta. The cell line was obtained via the ATCC (#CCL-98).
Immortalized BJ hRAS^{G12V}	Immortalized BJ cells are derivatives of human primary BJ fibroblast cells, established through hTERT transgenesis and subsequently transformed by the stepwise expression of the oncogene hRAS^{G12V}.

3.1.1.2 Primary cells

Cells	Origin
CD4$^+$ T lymphocytes	Buffy coats of healthy donors were obtained from the German Red Cross Blood Donor Service Baden-Württemberg at the University Hospital Tübingen. CD4$^+$ T cells were negatively isolated using the RosetteSep^{TM} Human CD4$^+$ T Cell Enrichment Cocktail (STEMCELL

Cells	Origin
	Technologies #15061) and Pancoll Separating Solution (PAN Biotech #P04-69600).
Monocyte-derived macrophages	Buffy coats of healthy donors were obtained from the German Red Cross Blood Donor Service Baden Württemberg at Tübingen University Hospital. PBMCs were isolated from buffy coats by density gradient centrifugation using Pancoll separating solution (PAN Biotech #P04-69600). Monocytes were allowed to adhere to plastic for 3 days in macrophage differentiation medium.

3.1.1.3 Bacteria

Strain	Description	Source/company
***Escherichia coli* XL-2 blue**	endA1 supE44 thi-1 recA1 gyrA96 relA1 lac F´ proAB lacIqZΔM15 Tn10 (Tetr)	Agilent
***Escherichia coli* XL-2 blue MRF'**	endA1 supE44 thi-1 recA1 gyrA96 relA1 lac F´ proAB lacIqZΔM15 Tn10 (Tetr) McrA-, McrCB-, McrF-, Mrr-, HsdR	Agilent

3.1.2 Media

3.1.2.1 Eukaryotic cell culture

Medium	Manufacturer/composition	Source/company
DMEM	Dulbecco's Modified Eagle Medium	Gibco/Life Technologies
RPMI-1640	Roswell Park Memorial Institute Medium	Gibco/Life Technologies

3.1.2.2 Bacterial culture

Medium	Composition	Manufacture
LB medium	Lysogeny broth (LB) medium; 10 g/l Bacto Tryptone, 5 g/l Bacto Yeast Extract, 10 g/l NaCl in distilled water; supplemented with ampicillin (100 µg/ml) or kanamycin (50 µg/ml)	Sigma-Aldrich

Medium	Composition	Manufacture
LB agar	16 g/l Bacto Agar in LB medium; supplemented with ampicillin (100 µg/ml) or kanamycin (50 µg/ml)	Sigma-Aldrich
S.O.C. Medium	Super Optimal broth with Catabolite repression	Thermo Fisher Scientific

3.1.3 Nucleic acids

3.1.3.1 Expression vectors and proviral constructs

All plasmids used contain an ampicillin or kanamycin resistance gene for selection in bacteria.

Vector	Description
pCG_hum HSF1 C-HA IRES eGFP	Expression vector based on the human cytomegalovirus (CMV) immediate early (IE) promoter [228]. Unique XbaI and MluI restriction sites were used to insert the open reading frame (ORF) encoding C-terminally HA-tagged human HSF1. The unique restriction site BamHI was used to insert an internal ribosome entry site (IRES) together with the ORF encoding eGFP.
pHIT-G VSV-G	CMV promoter-based vector expressing the envelope glycoprotein of Vesicular stomatitis virus [229]
pBR322 STCOr1	Vector expressing the infectious molecular clone of HIV-1 M subtype B STCOr1 [230]
pCR-XL-Topo CH077_TF1	Vector expressing the infectious molecular clone of HIV-1 M subtype B CH077_TF1 [231]
pHIV-1 AD8	Vector expressing the infectious molecular clone of HIV-1 M subtype B AD8. [232]
pCR-XL TOPO-HIV1-YU2C	Vector expressing the infectious molecular clone of HIV-1 M subtype B YU2C [232-235]
HIV-2 ROD10	Vector expressing the infectious molecular clone of HIV-2 A ROD10 [236-238]

Vector	Description
SNAG (pblueskript_ HIV-2 AB 7312A)	Vector expressing the infectious molecular clone of HIV-2 CRF01_AB 7312A [239]
pUC19_HIV-2 A GH123	Vector expressing the infectious molecular clone of HIV-2 A GH123 [240]
pCSC-SP-PW-GFP (aka: pBOB-GFP)	pCSC-SP-PW-GFP, also known as pBOB-GFP, is a lentiviral expression plasmid that expresses Green Fluorescent Protein (GFP) in mammalian cells for visualization and tracking, and carries an ampicillin resistance gene for bacterial selection (Addgene #12337) [241]
psPAX2	2nd generation lentiviral packaging plasmid from the Trono lab expressing the HIV-1 *gag*, *pol*, *rev*, and *tat* genes. It can be used with 2nd or 3rd generation lentiviral vectors and an envelope expressing plasmid, such as pMD2.G (Addgene #12260) [242].
pMD2.G	CMV promoter-based vector expressing the envelope glycoprotein of HIV-1 (Addgene #12259) [242]
pRSV rev	3rd generation lentiviral packaging plasmid from the Trono lab containing the HIV-1 *rev* gene (Addgene #12253) [242]
pMDLg/pRRE	3rd generation lentiviral packaging plasmid from the Trono lab containing the HIV-1 *gag* and *pol* genes (Addgene #12251) [242]
pHAGE EF1α dCas9-VP64	Constitutive dCas9-VP64 lentiviral expression vector (Addgene #50918) [243]
pLKO.1-puro U6 gRNA BfuAI stuffer	U6-driven gRNA expression vector where guide sequences can be inserted between BfuAI sites; used as empty vector control (Addgene #50920) [244]
pLKO.1-puro U6 gRNA CAG	pLKO.1 plasmid with an oligonucleotide cloning site containing two *Bfu*AI sites for inserting guide sequences via 4-bp 5’ overhangs (ACCG and AAAC)

Vector	Description
	into the gRNA sequence (scaffold gRNA) (Addgene #50927) [243]
pLKO.1-puro U6 gRNA BfuAI DHRS2 gRNA1	U6-driven gRNA cloning vector where *DHRS2*-specific guide RNA sequence gRNA1 was inserted between BfuAI sites
pLKO.1-puro U6 gRNA BfuAI DHRS2 gRNA2	U6-driven gRNA cloning vector where *DHRS2*-specific guide RNA gRNA2 was inserted between BfuAI sites
pLKO.1-puro U6 gRNA BfuAI DHRS2 gRNA3	U6-driven gRNA cloning vector where *DHRS2*-specific guide RNA gRNA3 was inserted between BfuAI sites
pLKO.1-puro U6 gRNA BfuAI DHRS2 gRNA4	U6-driven gRNA cloning vector where *DHRS2*-specific guide RNA gRNA4 was inserted between BfuAI sites
pTAL-Firefly Luciferase	Control vector expressing firefly luciferase under the control of the TATA-like promoter (pTAL) region of the herpes simplex virus thymidine kinase promoter (Clontech #631909)
pGL4.32 Firefly luciferase (no promoter)	Derived from pGL4.32 [luc2P/NF-κB-RE/Hygro] vector (Promega # 9PIE849); base pairs 33 to 176, which contain the NF-κB response element and the minimal promoter region, were removed. A stop codon was introduced after the luciferase gene to terminate translation to ensure that luciferase expression is entirely dependent on the introduction of an external promoter by the user, making it ideal for promoter functional studies.
pGluc-MiniTK2 LTR12D (*DHRS2*)	LTR12D (Hg38 chr14:23635627-23636652) was inserted via KpnI and BamHI restriction sites into pGluc-MiniTK2 [72].
pGluc-MiniTK2 + LTR12C (*GBP2*)	LTR12C (Hg38 chr1:89127019-89128609) was inserted via XhoI and HindIII restriction sites into pGluc-MiniTK2 [72].

Vector	Description
LentiCRISPRV2	This 3rd generation lentiviral transfer vector from the Zhang lab is used to deliver Cas9 and a gRNA of interest into mammalian cells [245].
LentiCRISPRV2_NT gRNA	U6-driven gRNA transfer vector expressing Cas9 where non-targeting guide sequence NT gRNA was inserted between BsmBI sites.
LentiCRISPRV2_gRNA DHRS2 ko	U6-driven gRNA transfer vector expressing Cas9 where *DHRS2*-targeting guide sequence *DHRS2* gRNA was inserted between BsmBI sites.

3.1.3.2 Primers used for cloning and qPCR

Primers used for Cloning	Primer name	Primer sequence (5'-3')
pCG_HSF-1_C-HA tag	fwd	CCTCTAGAGCCACCATGGATCTGCCCGTGGGCCCCGG
	rev	GGACGCGTTTAAGCGTAATCTGGAACATCGTATGGGTAGGAGACAGTGGGGTCCT
***DHRS2* CRISPRa gRNA1**	upper	ACCGGAACTTGCATCCTGCAGAC
	lower	AAACGTCTGCAGGATGCAAGTTC
***DHRS2* CRISPRa gRNA2**	upper	ACCGGTGAGTGCCCTGTACAGTG
	lower	AAACCACTGTACAGGGCACTCAC
***DHRS2* CRISPRa gRNA3**	upper	ACCGCACACACTGCAGGACTTTG
	lower	AAACCAAAGTCCTGCAGTGTGTG
***DHRS2* CRISPRa gRNA4**	upper	ACCGTGGGCCGGCCGGTGCCAGC
	lower	AAACGCTGGCACCGGCCGGCCCA
***DHRS2* ko gRNA (electroporation)**		CCGGCTGCTGATGACCACGT

Primers used for Cloning	Primer name	Primer sequence (5’-3’)
Non-targeting gRNA (electroporation)		ACGGAGGCTAAGCGTCGCAA
LentiCRISPRv2	fwd	GGTACCGAGGGCCTATTTCCC
	rev	ATGTCCAGGCCGATGCTGTACTTC
LentiCRISPRv2_DHRS2 ko gRNA	upper	CACCGCCGGCTGCTGATGACCACGT
	lower	AAACACGTGGTCATCAGCAGCCGGC
LentiCRISPRv2_non-targeting gRNA	upper	CACCGCCCCAAACCCGGGGGGTTTT
	lower	AAACAAAACCCCCCGGGTTTGGGGC

Primers used for qPCR	Fwd/rev	Primer sequence (5´-3´)
DHRS2	fwd	CACCAAGCGGTGAGACTATCAC
	rev	CGGGCAACTGCTGACAGCATAG
GAPDH	fwd	TGCACCACCAACTGCTTAGC
	rev	GGCATGGACTGTGGTCATGAG
	lower	AAACGCTGGCACCGGCCGGCCCA
dCAS9	fwd	TCGGATCTGCTACCTGCAGGAGATCTTT AG
	rev	CAGCCTTATCAGTACTGTCTACCAGCT TCT
p53	fwd	GCCCCTCCTCAGCATCTTATC
	rev	TGATGATGGTGAGGATGGGC
MDM2	fwd	GTATCAGGCAGGGGAGAGTG
	rev	GAAGCCAATTCTCACGAAGG
IL6	fwd	CTGTTCTGGAGGTACTCTAGGT
	rev	CAAAGATGGCTGAAAAAGATGGA
CCL5	fwd	CCTGCTGCTTTGCCTACATTGC
	rev	ACACACTTGGCGGTTCTTTCGG
CXCL10	fwd	GGTGAGAAGAGATGTCTGAATCC

Primers used for qPCR	Fwd/rev	Primer sequence (5´-3´)
	rev	GTCCATCCTTGGAAGCACTGCA
TNF	fwd	CTCTTCTGCCTGCTGCACTTTG
	rev	ATGGGCTACAGGCTTGTCACTC
CCL17	fwd	TTCTCTGCAGCACATCCACGCA
	rev	CTGGAGCAGTCCTCAGATGTCT
TIMP-1	fwd	GGAGAGTGTCTGCGGATACTTC
	rev	GCAGGTAGTGATGTGCAAGAGTC
TIMP-2	fwd	ACCCTCTGTGACTTCATCGTGC
	rev	GGAGATGTAGCACGGGATCATG

3.1.3.3 TaqMan qPCR primer probes

Target	Species	Dye	Quencher	Manufacturer	Unique Identifier
GAPDH	Human	VIC	MGB	Thermo Fisher Scientific	4448489 # Hs02786624_g1
CDKN1A	Human	FAM	MGB	Thermo Fisher Scientific	4453320 # Hs00355782_m1
CDKN2A	Human	FAM	MGB	Thermo Fisher Scientific	4331182 # Hs00923894_m1

3.1.4 Kits and reagents

Kit	Manufacturer
DNA-free DNA Removal Kit	Thermo Fisher
DNA Ligation Kit Ver 2.1	Takara Bio Inc.
laboratories FIX&PERM Cell Fixation and Permeabilization Kit	Nordic-MUbio
Human T Cell Nucleofector™ Kit	Lonza
Luciferase Assay System 10-pack	Promega
Mini DNA Preparation Kit	Qiagen

Kit	Manufacturer
Monarch® DNA Gel Extraction Kit	New England BioLabs
Phire High-Fidelity DNA Polymerase	New England BioLabs
RNeasy Plus Mini Kit	Qiagen
PrimeScript RT Reagent Kit	TAKARA
TaqMan™ Fast Universal PCR Master Mix	ThermoFisher
SuperScript III Reverse Transcriptase Kit	Invitrogen/Life Technologies
QIAGEN Plasmid Midi Kit	Qiagen
Wizard Plus Midi DNA Preparation Kit	Promega Corporation
Cellular Senescence Detection Kit - SPiDER-βGal	Dojindo
Human Cytokine Array C5	RayBiotech

Reagent	Manufacturer
1,4-diazabicyclo-(2,2,2)-octane (DABCO)	Carl Roth GmbH & Co. KG
4-(2-hydroxyethyl)-1-piperazine-ethanesulfonic acid (HEPES)	Sigma-Aldrich
Accutase	Sigma-Aldrich
Agarose	Sigma-Aldrich
Ampicillin	Ratiopharm
Bacto Tryptone	BD Biosciences
Bacto Yeast Extract	BD Biosciences
BlueStar Prestained Protein Marker	Nippon genetics Co. Ltd.
Bovine serum albumin (BSA)	KPL
Calcium chloride ($CaCl_2$) dihydrate	Sigma-Aldrich
Coelenterazine	pjk
Complete ULTRA Tablets, Mini EDTA-free	Roche
Diethylaminoethyl (DEAE)-dextran	Sigma-Aldrich
Disodium phosphate (Na_2HPO_4)	AppliChem GmbH

Reagent	Manufacturer
Dulbecco's phosphate buffered saline (DPBS)[-]$CaCl_2$ [-]$MgCl_2$	Gibco/Life Technologies
Ethanol	Dispensary
Ethidium bromide	AppliChem GmbH
Ethylendiaminetetraacetate (EDTA)	Biochrom GmbH
FACS Flow Solution	BD Biosciences
FACS Shutdown Solution	BD Biosciences
Fetal calf serum (FCS)	Gibco/Life Technologies
Fluorescence-activated Cell Sorting (FACS) Clean Solution	BD Biosciences
Glucose	Carl Roth GmbH & Co. KG
Glycerol	Sigma-Aldrich
Glycine	AppliChem GmbH
Human Interferon-α 2a (IFN-α 2a)	PBL Assay Science
Human Interferon-γ (IFN-γ)	Sigma-Aldrich
Human Interleukin-2 (IL-2)	Miltenyi Biotec GmbH
Human Serum	Sigma-Aldrich
Isopropanol	Dispensary
Kanamycin	Invitrogen/Life Technologies
L-glutamine	Gibco/Life Technologies PAN-Biotech
Loading dye	Carl Roth GmbH & Co. KG
Luciferase Assay System	Promega
Luciferase Cell Culture Lysis 5x Reagent	Promega
Methanol	Sigma-Aldrich
Molecular weight size marker '1KB plus DNA ladder'	Invitrogen/Life Technologies
NEBuffers	New England BioLabs Inc.
Non-Essential Amino Acids (NEAA) Solution	Thermo Fisher

Reagent	Manufacturer
Nonidet P-40	USB
NuPAGE MES SDS Running Buffer (20x)	Invitrogen/Life Technologies
Nutlin-3a	Selleckchem
Pancoll Separating Solution	Biochrom GmbH
Paraformaldehyde (PFA)	Merck Millipore
Penicillin-Streptomycin	Gibco/Life Technologies PAN-Biotech
Polyethylenimine	Polysciences
Poly-L-lysine (PLL)	Sigma-Aldrich
Potassium chloride (KCl)	AppliChem GmbH
Potassium dihydrogenphosphate (KH_2PO_4)	AppliChem GmbH
Protein Loading Buffer (4x)	LI-COR
RosetteSep Human $CD4^+$ T Cell Enrichment Cocktail	STEMCELL Technologies
Skimmed milk powder	Fluka
Sodium chloride (NaCl)	Fluka
Sodium dodecyl sulfate (SDS)	Fluka
Sodium pyruvate ($C_3H_3NaO_3$)	Thermo Fisher
Staurosporine	Sigma-Aldrich
Sucrose	Sigma-Aldrich
Sulfuric acid (H_2SO_4) 0.5 M	Sigma-Aldrich
Thapsigargin	Sigma-Aldrich
Tris	AppliChem GmbH
Tris-acetate-EDTA (TAE) buffer (50x)	Carl Roth GmbH & Co. KG
Triton X-100	Sigma-Aldrich
Tween-20	Sigma-Aldrich
β-mercaptoethanol	Sigma-Aldrich

3.1.5 Enzymes

Enzyme	Manufacturer
Restriction endonucleases	New England BioLabs Inc.
Trypsin/EDTA	PAN-Biotech
Trypsin/EDTA (10x)	Gibco/Life Technologies

3.1.6 Solutions and buffers

Solution/buffer	Composition
HEPES buffered saline (HBS) (2x)	5.94% HEPES (w/v), 8.18% NaCl (w/v), 0.25% Na_2HPO_4 x $2H_2O$ (w/v) in distilled water for 10x HBS; for 2x HBS, the 10x stock was diluted in distilled water, pH 7.12, sterilized by filtration
2 M $CaCl_2$ solution	2 M $CaCl_2$ in distilled water, sterilized by filtration
FACS buffer	1% FCS (v/v) in DPBS
FACS fixing solution	2% PFA (v/v) in DPBS
FACS permeabilizing agent	Ice chilled 90% methanol
Western Blot running buffer	1x NuPAGE MES SDS Running Buffer in distilled water
Western Blot transfer buffer	47.9 mM Tris, 38.6 mM glycine, 1.3 mM SDS, 20% methanol (v/v) in distilled water, pH 8.3
Western Blot blocking buffer	5% skimmed milk powder (w/v) in PBS
Western Blot antibody buffer	1% skimmed milk powder (w/v), 0.2% Tween-20 (v/v) in PBS or Hikari solution A/B (primary/secondary antibody)
Western Blot washing buffer	0.2% Tween-20 (v/v) in PBS
5x PBS	140 mM NaCl, 8.1 mM Na_2HPO_4, 2.7 mM KCl, 1.5 mM KH_2PO_4 in distilled water, pH 7
10x Poly-L-lysine (PLL) stock	0.1 mg/ml (w/v) in DPBS

3.1.7 Antibodies

Antibody and final concentration	Manufacturer
For Western Blot	
Mouse monoclonal anti-HA tag, 1µg/ml	Abcam (#ab18181)
Rat monoclonal anti-GAPDH, 0.5 µg/ml	BioLegend (#607902)
IRDye 680RD Goat anti-Mouse IgG (H + L), 25 ng/ml	LI-COR (#926-68070)
IRDye 680RD Goat anti-Rat IgG (H + L), 25 ng/ml	LI-COR (#926-68076)
IRDye 800CW Goat anti-Mouse IgG (H + L), 25 ng/ml	LI-COR (#926-32210)
IRDye 800RD Goat anti-Rat IgG (H + L), 25 ng/ml	LI-COR (#925-32219)
For flow cytometry	
Rabbit monoclonal anti-β-catenin, PE-conjugated, 40 µg/ml	Cell signaling technology (#14903)
Mouse monoclonal anti-DHRS2, 0.1 mg/ml	Santa Cruz (#sc-517054)
Mouse monoclonal anti-HSF1, Alexa Fluor 647-conjugated, 4 µg/ml	Santa Cruz (#sc-13516)
Rabbit monoclonal Anti-HSF1 (phospho S303 + S307) antibody, 17.44 µg/ml	Abcam (#ab81281)
Mouse monoclonal HIV-1 core antigen-RD1, KC57, 1 µg/ml	Beckman coulter (#6604667)
Mouse monoclonal HIV-1 core antigen-FITC, KC57, 1 µg/ml	Beckman coulter (#6604665)
Mouse mAb IgG2a κ isotype control	BioLegend (#400220)
Mouse mAb IgG1 isotype control, Alexa Fluor 647 conjugated	Santa Cruz (#sc-24636)
Rabbit mAb IgG XP® Isotype Control, PE-conjugated	Cell signaling technology (#5742)
Goat anti-Rabbit IgG (H+L) cross-adsorbed secondary antibody, Alexa Fluor 555	Thermo Fisher Scientific (#A-21428)
Rabbit mAb IgG isotype control	Abcam (#ab37415)

3.1.8 Consumables

Consumable	Manufacturer
C-Chip Disposable Hemocytometer, Neubauer Improved	Nano EnTek Inc
Cell culture flasks	Sarstedt AG & Co. KG
Cell culture plates	Sarstedt AG & Co. KG
Combitips plus/advanced	Eppendorf AG
96-well Multiply fast PCR plate	Sarstedt AG & Co. KG
Filter tips (10, 1000 µl)	Nerbe plus GmbH
Filter tips (20, 200 µl)	Sarstedt AG & Co. KG
Filtropur V50 0.45 µm Vacuum Filter	Sarstedt AG & Co. KG
Gel loading tips	Santa Cruz Biotechnology, Inc.
Immobilon-FL Transfer Membrane	Merck Millipore
Nunc Cell-Culture Treated Multidishes	VWR
Nunc white polystyrene 96-well Microwell plates	Nunclon/Thermo Scientific
NuPAGE Novex Bis-Tris gels	Invitrogen/Life Technologies
Polystyrene 5 ml round-bottom tubes	Falcon/Corning, Inc.
Reaction tubes (0.25, 1.5, 2 ml)	Sarstedt AG & Co. KG
Sealing tape	Thermo Scientific
Serological pipettes (5, 10, 25 ml)	Sarstedt AG & Co. KG
Stericup & Steritop 0.45 µm	Merck Millipore
Tubes (15, 50 ml)	Sarstedt AG & Co. KG
Whatman chromatography paper 2 mm CHR	GE Healthcare

3.1.9 Equipment

Equipment	Manufacturer
Bacteria incubator BD 720	BINDER
Bacteria incubator Certomat IS	Sartorius AG

Equipment	Manufacturer
Bacteria incubator RS 422	BINDER
Centrifuge 5417C	Eppendorf AG
Centrifuge 5417R	Eppendorf AG
Centrifuge 5427R	Eppendorf AG
Centrifuge 5430	Eppendorf AG
Centrifuge 5810R	Eppendorf AG
CO_2 incubator HERAcell 240	Heraeus
CO_2 incubator Steri-Cult 3311	Thermo Scientific
Flow cytometer	Miltenyi biotec MACSQuant
Flex cycler	Analytik Jena AG
Fluorescence Microscope DM IL LED Fluo	Leica Camera AG
Gel Doc XR+	Bio-Rad Laboratories GmbH
LI-COR Odyssey Imager	LI-COR Biosciences GmbH
Model 200/2.0 Power Supply	Bio-Rad Laboratories GmbH
NanoDrop 2000	Thermo Scientific
Nucleofector I	Amaxa Biosystems
Orbital shaker	GFL
Power Pac HC	Bio-Rad Laboratories GmbH
Rotary Tube Mixer RSM7	Ratek Instruments Pty Ltd
StepOnePlus Real-Time PCR System	Applied Biosystems
Stuart tube roller mixer SRT6D	Sigma-Aldrich
Thermomixer compact/comfort	Eppendorf AG
Trans-Blot SD Semi-Dry Transfer Cell	Bio-Rad Laboratories GmbH
XCell SureLock Electrophoresis cell	Thermo Scientific
XCell4 SureLock Midi-Cell	Thermo Scientific

3.1.10 Software

Software	Provider
Benchling	https://benchling.com
FlowLogic	Inivai technologies
Extended Nucleic Acid Sequence Massager	https://biomodel.uah.es/en/lab/cybertory/analysis/massager.htm
CorelDRAW 2017	Corel Corporation
GraphPad Prism 8.4.2	GraphPad Software, Inc.
Image Lab 5.2.1	Bio-Rad Laboratories GmbH
Image Studio Lite Ver 4.0	LI-COR Biosciences GmbH
Microsoft Office 2016	Microsoft Corporation
Multalin	http://multalin.toulouse.inra.fr [246]
NEBaseChanger® v. 1.2.9	https://nebasechanger.neb.com/
Nanodrop 2000	Thermo Scientific
Odyssey Image Studio	LI-COR Biosciences GmbH
LightCycler Software 3.5	Informer technologies

3.1.11 External facilities

Company	Services provided
Metabion	DNA oligo synthesis
Metabion	DNA sequencing
Microsynth AG SeqLab	DNA sequencing

3.2 Methods

3.2.1 Identification of promoter regions and genomic features

3.2.1.1 UCSC genome browser

The UCSC Genome Browser (https://genome.ucsc.edu) was used to visualize genomic loci and identify promoter regions associated with target genes. The human genome assembly GRCh38/hg38 was used as the reference. Genomic coordinates of interest were located using gene names or precise chromosomal positions. To identify potential

promoter elements derived from transposable elements, including long terminal repeats (LTRs), the RepeatMasker track was enabled. This track shows the annotation of repetitive elements and allowed detection of specific LTR subfamilies (e.g., LTR12C or LTR12D) overlapping with transcription start sites (TSSs). The RefSeq Genes and GENCODE tracks were used to determine the location of gene exons and annotated TSSs. By comparing the position of LTR elements with the TSS, candidate LTR-driven promoters were identified. Additional features such as conservation scores and regulatory marks (e.g., DNase hypersensitivity, histone modifications) were optionally inspected to support functional relevance of the identified LTRs.

3.2.1.2 WashU epigenome browser

Epigenomic datasets were visualized using the WashU Epigenome Browser (https://epigenomegateway.wustl.edu/), an interactive web-based platform that enables exploration and comparison of genomic and epigenomic annotations. Genomic coordinates of interest were uploaded in BED format, and relevant public datasets, including histone modifications, transcription factor binding sites, and chromatin accessibility profiles, were integrated from ENCODE and other available repositories. The browser's track configuration features were employed to overlay and align multiple data tracks for comparative analysis. Screenshots were generated for representative regions to highlight specific epigenetic features.

3.2.2 Transcription factor binding site analysis

3.2.2.1 Cistrome toolkit:

To investigate transcription factor (TF) binding at specific genomic loci and promoter regions, we utilized the Cistrome Data Browser Toolkit (http://dbtoolkit.cistrome.org), which integrates public ChIP-seq datasets to provide experimentally determined TF-DNA interactions.

a) Promoter-Associated Transcription Factor Profiling: To identify potential regulatory transcription factors for a specific gene, we used the "What factors regulate your gene of interest?" query option in the Cistrome Toolkit. The gene name was entered along with a defined search window (±10 kb) surrounding the TSS to capture promoter and nearby regulatory elements. Output included a ranked list of transcription factors based on regulatory potential scores derived from ChIP-seq signal intensity and peak proximity

to the TSS. Results were visualized both as tables and figures, and source-specific datasets (cell lines or tissue types) were selectively included for context-specific analysis.

b) Binding Site Analysis in Genomic Intervals: To assess TF binding at defined genomic intervals, we used the “What factors bind in your interval?” function. The genomic region of interest was input in the format *chr: start-end*, based on genomic coordinates from the human reference genome (GRCh38/hg38). Upon submission, the toolkit generated results in both tabular and graphical formats, listing transcription factors with ChIP-seq peaks overlapping the queried region. The results were filtered based on specific transcription factors and cell types relevant to the study. Data visualization and further inspection of ChIP-seq peaks were carried out using the WashU Epigenome Browser interface, which allowed high-resolution exploration of TF occupancy and overlap with regulatory features, including transcription start sites (TSS).

This approach enabled the identification of candidate transcription factors with experimental evidence of binding to either transposable element-derived regulatory regions or canonical gene promoters, supporting downstream functional hypotheses.

3.2.2.2 JASPAR database

Transcription factor binding motif analysis was performed using the JASPAR database (https://jaspar.genereg.net), which provides curated, non-redundant transcription factor binding profiles derived from experimental data. Transcription factors of interest were selected based on prior knowledge or complementary experimental datasets. Corresponding position frequency matrices (PFMs) were added to the analysis workspace. DNA sequences of interest, typically from regulatory regions such as long terminal repeats (LTRs) or gene promoters, were entered in FASTA format. Using the "Scan" function, input sequences were searched for potential transcription factor binding sites based on motif similarity. The output included predicted binding sites with associated scores and positions within the input sequence, facilitating comparison with experimental binding data and enabling identification of candidate regulatory interactions.

3.2.2.3 HOCOMOCO database

To identify putative transcription factor binding sites (TFBS) within the LTR12D element and its upstream region (~1 kb), we used the MoLoTool (Motif Locator Tool), a web-

based sequence scanning tool integrated with the HOmo sapiens COmprehensive MOdel COllection (HOCOMOCO) v11. HOCOMOCO v11 provides curated transcription factor (TF) binding models for 680 human and 453 mouse TFs, including both mononucleotide and dinucleotide position weight matrices (PWMs), which are derived from ChIP-Seq datasets. All PWMs were generated using the ChIPMunk and diChIPMunk motif discovery tools and benchmarked through cross-validation. The underlying ChIP-Seq data were obtained from the Gene Transcription Regulation Database (GTRD) on the BioUML platform. The HOCOMOCO v11 database and tools are publicly available at https://hocomoco11.autosome.org/.

Sequence analysis was performed using the MoLoTool with a default P-value threshold of 1e-4 to identify statistically significant TFBS hits. Following motif identification, the predicted binding sites were further validated using SPRY-SARUS, a command-line motif scanner included in the HOCOMOCO toolkit. SPRY-SARUS applies the PWMs to a given sequence set to efficiently and accurately map motif occurrences. This two-step approach ensured robust prediction and validation of TF binding motifs in our sequences of interest.

3.2.3 Cloning

3.2.3.1 Polymerase chain reaction

Polymerase chain reaction (PCR) was carried out using either the Phire™ Hot Start II DNA Polymerase (Thermo Fisher Scientific), according to the manufacturer's instructions. A total of 35 thermal cycles per PCR were performed in a VeritiTM 96-Well Thermal Cycler (Applied Biosystems) in a total volume of 50 µl. To validate the reaction, 20 µl of the PCR product were separated in agarose gels (1% agarose (w/v) in 1x TAE buffer) with the addition of ethidium bromide (0.2 µg/ml). After 50 minutes of electrophoresis at 110 V, DNA bands were visualized using the Gel Doc XR+ (Bio-Rad Laboratories GmbH) detection system.

3.2.3.2 Restriction digest

DNA digestion was performed using NEB enzymes and buffers according to the manufacturer's instructions.

3.2.3.3 DNA purification from agarose gels

DNA fragments were separated by gel electrophoresis in agarose gels (1% w/v, containing 0.2 µg/ml ethidium bromide) together with 1 kb plus ladder and visualized

on a UV screen (366 nm) or the Gel Doc XR+ (Bio-Rad Laboratories). Bands of the desired length were cut out and the DNA was purified from the gel using the Monarch® DNA Gel Extraction Kit (New England BioLabs) according to the manufacturer's instructions.

3.2.3.4 Ligation

Vector and insert DNA were mixed at a volume ratio of 1:4 and ligated for 1 h at 16°C or overnight at 4°C using the DNA Ligation Kit 2.1 (Takara Bio Inc.).

3.2.3.5 Transformation

XL-2 Blue *E. coli* were transformed with stable expression constructs. For recombination-prone proviral constructs, XL-2 Blue MRF' *E. coli* were used for transformation. In both cases, the ligation mix was incubated on ice with 13 µl of the respective *E. coli* strain for 20 minutes. After a heat-shock at 42 °C for 30 s (XL-2 blue) or 37°C for 30 s (XL-2 blue MRF'), bacteria were incubated on ice for 2.5 min. Following the addition of 200 µl S.O.C medium, the transformed cells were incubated at either 37 °C for 60 min (XL-2 blue) or at 30 °C for 90 min (XL-2 blue MRF') on a shaker and plated on LB agar plates containing the appropriate antibiotic (ampicillin or kanamycin) and overnight incubation was performed at 37°C (XL-2 blue) and 30°C (XL-2 blue MRF'). Single colonies were picked the next day.

3.2.3.6 Mini preparation

To isolate plasmid DNA for cloning and sequencing, single colonies were picked from agar plates and grown in 5 ml LB medium supplemented with ampicillin (100 mg/l) or kanamycin (50 mg/l) at 37°C overnight on a shaker. Plasmid DNA was prepared with the Qiagen Miniprep Kit according to the manufacturer's instructions.

3.2.3.7 DNA sequencing

Plasmid DNA was sent to Microsynth Seqlab GmbH for nucleotide sequencing. Sequencing reaction mixtures were prepared according to the provider's instructions.

3.2.3.8 Midi preparation

Plasmid DNA for transfection was prepared with Qiagen Plasmids Midi Kit according to the manufacturer's instructions. Concentration and quality of the purified DNA were determined using the NanoDrop 2000 spectrophotometer (Thermo Fischer Scientific).

3.2.4 Cell culture

3.2.4.1 Cell line culture

Human embryonic kidney 293T (HEK293T) cells were maintained in Dulbecco's modified Eagle medium (DMEM) supplemented with 10% heat-inactivated fetal calf serum (FCS), 0.05 mg/ml penicillin, and 0.05 mg/ml streptomycin. These cells were routinely tested for mycoplasma contamination every few months, and only mycoplasma-negative cultures were utilized.

Jurkat and SupT1 cells were cultured in RPMI1640 supplemented with 5% FCS, 0.05 mg/ml penicillin, and 0.05 mg/ml streptomycin at 37°C in a 5% CO_2 atmosphere.

3.2.4.2 Isolation and culture of human $CD4^+$ T cells

Human $CD4^+$ T cells were isolated from lymphocyte concentrates (buffy coats) obtained from the German Red Cross Blood Donor Service, Baden-Württemberg, at the University Hospital Tübingen. Buffy coats were diluted 1:1 with phosphate-buffered saline (PBS) and carefully layered over an equal volume of Pancoll separating solution (PAN Biotech) in 50 ml conical tubes. Density gradient centrifugation was performed at 1200 × *g* for 20 minutes at room temperature with the brake turned off. The mononuclear cell layer at the interface was collected, and $CD4^+$ T cells were subsequently enriched by negative selection using the RosetteSep™ Human $CD4^+$ T Cell Enrichment Cocktail (STEMCELL Technologies), according to the manufacturer's instructions.

Isolated $CD4^+$ T cells were cultured at a density of 1.5×10^6 cells/ml in RPMI-1640 medium supplemented with 2 mM L-glutamine, 100 µg/ml streptomycin, 100 U/ml penicillin, and 10% (v/v) heat-inactivated fetal calf serum (FCS) for 3 days. Cells were either left untreated or activated with 1 µg/ml phytohaemagglutinin (PHA) and stimulated with 10 ng/ml interleukin-2 (IL-2).

3.2.4.3 Isolation and differentiation of monocyte-derived macrophages (MDMs)

Peripheral blood mononuclear cells (PBMCs) were isolated from buffy coats by density gradient centrifugation using Pancoll separating solution (PAN Biotech). Monocytes were allowed to adhere to plastic for 3 days in macrophage differentiation medium consisting of RPMI-1640 supplemented with 4% human AB serum, 2 mM L-glutamine, 100 µg/ml penicillin-streptomycin, 1 mM sodium pyruvate, 1× non-essential amino acids, and 0.4× MEM vitamins. Non-adherent cells were removed by washing with PBS,

and the adherent monocytes were further differentiated for an additional 4 days in fresh macrophage medium.

For downstream applications, differentiated macrophages were detached using Accutase® (Sigma-Aldrich) by incubation for 45 minutes at 37°C.

3.2.5 Virus production and infection of primary CD4⁺ T cells

3.2.5.1 Virus production

HEK293T cells were seeded in 6-well plates and cultured to approximately 70–80% confluency. Cells were co-transfected using the calcium phosphate method. Briefly, 1 µg of VSV-G expression plasmid and 5 µg of proviral plasmid (HIV-1 CH077, STCO1, or HIV-2 molecular clones) were mixed with 2M $CaCl_2$ and combined dropwise with an equal volume of 2× HEPES-buffered saline (HBS). After incubation for 20 minutes at room temperature, the transfection mix was added to the cells. A mock transfection (transfection mix without DNA) served as negative control. After 48 hours, supernatants containing virus particles were harvested, centrifuged at 300 × g for 10 minutes to remove debris and the supernatant (virus stock) was used for the infection.

3.2.5.2 Spinoculation of CD4⁺ T Cells

CD4⁺ T cells were activated with phytohemagglutinin (PHA; 1–2 µg/mL) and interleukin-2 (IL-2; 20–100 U/mL) for 72 hours prior to infection. Post-stimulation, cells were harvested by centrifugation at 1400 rpm for 4 minutes at room temperature. The supernatant was discarded, and the pellet was gently loosened by tapping or scratching the tube wall. Cells were resuspended in 2 mL RPMI 1640 medium supplemented with 10% fetal bovine serum (FBS) and penicillin/streptomycin (referred to as RPMIxxx), and thoroughly mixed by pipetting. A 1:100 dilution was prepared in PBS for cell counting using a hemocytometer.

A total of 1.5×10^6 cells were seeded in 100 µL RPMIxxx per well of a 96-well U-bottom plate. The plate centrifuge in the biosafety level 3 (S3) laboratory was pre-warmed to 37 °C. For spinoculation, 120 µL of viral supernatant was added to each well. The plate was sealed with adhesive plastic foil to prevent aerosol formation during centrifugation and balanced with a second plate containing an equal volume of PBS. Plates were centrifuged at 1200 × g for 2 hours at 37 °C. After centrifugation, the foil was carefully removed, and cells were gently resuspended by pipetting up and down 2–3 times. The entire content of each well was then transferred into a 6-well plate containing 2 mL of

pre-warmed RPMIxxx supplemented with IL-2 (1:1000 final dilution). Cells were subsequently cultured under standard conditions (37 °C, 5% CO_2) until further analysis.

3.2.5.3 Infection of $CD4^+$ T cells

Primary $CD4^+$ T cells were isolated from buffy coats of healthy donors using the RosetteSep™ Human $CD4^+$ T Cell Enrichment Cocktail (STEMCELL Technologies) according to the manufacturer's instructions. Isolated cells were stimulated for 2-3 days using phytohemagglutinin (PHA) in the presence of interleukin-2 (IL-2) to promote cell proliferation. Following activation, $CD4^+$ T cells were infected in triplicate with virus-containing supernatants derived from HEK293T cells transfected with HIV-1, HIV-2, or mock constructs. Spinoculation was used. Cells were incubated with the virus for at least 2 hours at 37 °C, then cultured in fresh RPMI medium supplemented with IL-2. At 3 days post-infection (d.p.i.), cells were harvested for downstream analyses such as RNA extraction, protein analysis, or flow cytometry.

3.2.6 Transfection and transduction

3.2.6.1 Calcium-phosphate transfection

One day prior to transfection, $6x10^5$ or $3x10^4$ HEK293T cells were seeded per well of a 6-well in 2 ml medium or 96-well plate in 100 µl, respectively. 96-well plates were coated with poly-L-lysine for 1 h at 37 °C before seeding. Cell culture medium was changed before transfection. The appropriate amount of DNA and 13 µl of 2 M $CaCl_2$ were mixed and filled up to a volume of 100 µl with distilled water. For 96-wells, only a 10 µl of the mixture in triplicates was added. 100 µl 2x HBS was added dropwise to the DNA mixture. A similar mixture without DNA served as negative control/mock. After mixing via pipetting, the mixture was added dropwise to the cells (10% of the cell culture medium). Cells were incubated for 14-16 h before medium was replaced by fresh medium. 48 h post transfection, cells were used for further analysis.

3.2.6.2 CRISPR/dCas9-mediated activation

To activate *DHRS2* from its endogenous locus, a CRISPR activation (CRISPRa) strategy was employed using a catalytically inactive dCas9 fused to the VP64 transcriptional activator. The LTR12D element upstream of *DHRS2* was selected as the target regulatory region. A multiple sequence alignment of all human LTR12D elements was performed to identify sequences unique to the *DHRS2*-associated LTR12D, which served as the basis for designing four guide RNAs (gRNA1-4) (Table 3.1.3.2; *DHRS2* CRISPRa gRNAs) targeting distinct regions within this locus.

Each gRNA was individually cloned into a pLKO1 lentiviral expression vector under the control of the U6 promoter. Lentiviral particles were generated in HEK293T cells by co-transfecting the cells with selected combinations of gRNA plasmids (gRNA1+2, gRNA1+3, gRNA1+4, gRNA2+3, and gRNA1+2+3+4), dCas9-VP64 and third-generation packaging constructs. Control conditions included a vector-only construct expressing GFP (pBob) and a non-targeting gRNA. Transfections were performed using the calcium phosphate method. Viral supernatants were collected 48 hours post-transfection and concentrated by ultracentrifugation. This was carried out in a Beckman Coulter Optima XE using a SW 28 rotor at 25,000g for 1.5 hours at 4°C. Following ultracentrifugation, the viral pellets were carefully resuspended in 50 µl of complete RPMI medium.

Human $CD4^+$ T cells, pre-activated with PHA and IL-2, were transduced with the concentrated viral lentiviral particles via spinoculation to enhance delivery efficiency. Transduction was monitored by flow cytometry, and only samples exhibiting >35% efficiency were included in the further analysis.

3.2.6.3 CRISPR/Cas9 knockout via electroporation

A specific guide RNA (gRNA), designed to target the *DHRS2* gene, was developed using the IDTDNA design tool (Fig. 3.1A) [247]. The design was optimized to ensure maximal on-target efficiency at the *DHRS2* locus while minimizing potential off-target effects throughout the genome. *In silico* analysis of this particular gRNA (sequence: CCGGCTGCTGATGACCACGT) predicted that its activity would induce frameshift mutations within the coding sequence of the *DHRS2* gene. Such mutations are anticipated to lead to the formation of a premature stop codon, consequently causing loss of functional DHRS2 protein production due to truncated or unstable transcripts/polypeptides (Fig. 3.1B). This experiment was performed in the laboratory of Prof. Frank Kirchhoff at Ulm University.

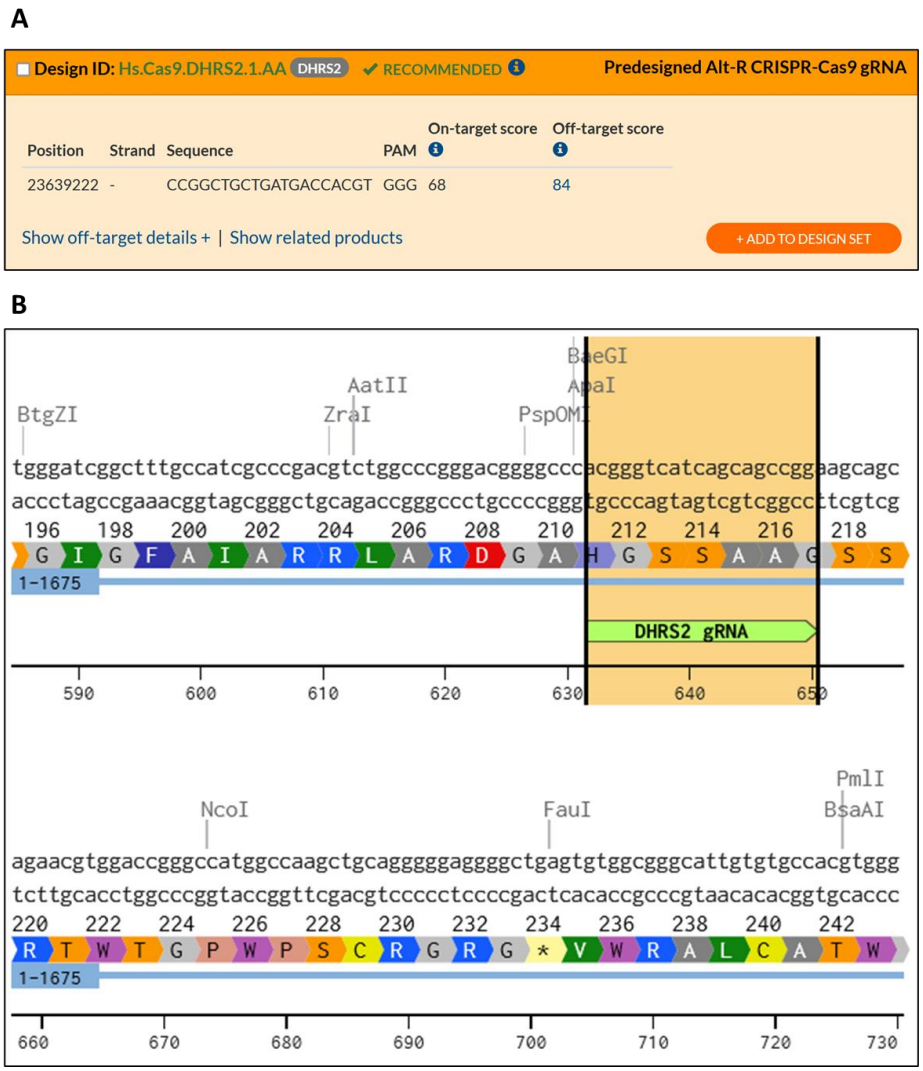

Figure 3.1: Design and predicted functional impact of *DHRS2*-targeting gRNA. (A) A specific gRNA was designed using the IDTDNA design tool, tailored to target the *DHRS2* gene. **(B)** *In silico* analysis of this particular gRNA (sequence: CCGGCTGCTGATGACCACGT) predicted that its activity would induce frameshift mutations within the *DHRS2* coding sequence. These mutations are anticipated to lead to the formation of a premature stop codon, consequently causing a loss of functional DHRS2 protein production.

$CD4^+$ T cells were isolated from two healthy donors and stimulated with CD3/CD28 beads and IL-2 for three days. After stimulation, cells were electroporated with either a non-targeting (NT) Cas9/gRNA complex or a *DHRS2*-specific Cas9/gRNA complex. Following electroporation, the cells were cultured for an additional four days.

At 96 hours post-electroporation, cells were infected using spinoculation with 60 µl of virus-containing supernatants. These supernatants had been concentrated tenfold using Amicon tubes before infection. The infection was performed in technical duplicates.

Post-infection, cells were washed three times with RPMI medium and seeded into 12-well plates at a density of 1 million cells per milliliter.

At 3 days post-infection (d.p.i.), supernatants were collected and frozen. Separately, one million cells per sample were lysed in RLT buffer supplemented with 1% β-mercaptoethanol for downstream qPCR analysis. At 3 d.p.i., DHRS2 and p24 protein levels were assessed via flow cytometry.

3.2.6.4 lentiCRISPRv2/Cas9-mediated knockout

Second-generation lentiviral particles were produced by transient transfection of HEK293T cells using a three-plasmid system. Cells were co-transfected with the transfer vector encoding either the *DHRS2*-targeting gRNA, a non-targeting control gRNA, or an empty vector control, together with the packaging plasmid psPAX2 and the envelope plasmid pMD2.G (VSV-G). The ratio of envelope vector to transfer vector to packaging plasmid (psPAX2) was maintained at 1:4:3. Transfection was performed using the calcium phosphate method, and the culture medium was replaced the following day to remove transfection reagents. Viral supernatants were harvested 48 hours post-transfection, concentrated by ultracentrifugation through a 20% sucrose cushion at 20,000g for 2-4 hours at 4°C, and resuspended in complete RPMI medium.

Primary $CD4^+$ T cells were isolated from healthy donor peripheral blood mononuclear cells (PBMCs) by negative selection and activated using anti-CD3/CD28-coated beads in the presence of IL-2. Activated T cells were transduced with the concentrated lentiviral particles by spinoculation. After transduction, puromycin was added at a final concentration of 1 µg/ml to select successfully transduced cells. Mock-transduced cells were used as controls and cultured in parallel to verify selection efficiency. Cells transduced with the pBob plasmid (expressing GFP) were used as transfection and transduction controls.

Following puromycin selection, surviving $CD4^+$ T cells were infected with HIV-1 (CH077 clone) by spinoculation. Infected cells were maintained in RPMI medium supplemented with IL-2. At 3 days post infection, cells were harvested and processed for downstream analyses, including flow cytometry and qPCR.

3.2.7 Dual luciferase reporter assay

To investigate the effect of HSF1, LEF1, TCF1, and β-catenin on *DHRS2* gene activity, HEK293T cells were transfected with varying amounts of expression plasmids for each of the proteins. Co-transfection was performed with either an empty vector or reporter constructs (LTR12C_*GBP2* or LTR12D_*DHRS2*) expressing *Gaussia* luciferase under the control of a minimal herpes simplex virus (HSV) thymidine kinase promoter and under the control of LTR12. The firefly luciferase reporter plasmid (pTAL) was used for normalization. The ratio of reporter to control vector was 20:1. 40 hours post-transfection, 20 µl of cell culture supernatant was transferred to a Nunc™ white polystyrene 96-well Microwell™ plate, and *Gaussia* luciferase activity was measured by coelenterazine turnover using a luminometer. For cell lysate analysis, transfected cells were lysed in 40 µl of 1x Luciferase Cell Culture Lysis Reagent (Promega) for 10 minutes at room temperature. Subsequently, 30 µl of either undiluted or 1:30 diluted lysate was transferred into a 96-well plate, and 50 µl of Luciferase Assay System (Promega) was added for firefly luciferase activity measurement using an Orion II microplate luminometer. The *Gaussia* luciferase signal was then normalized to the firefly luciferase signal for each sample to correct for transfection efficiency and cell viability.

3.2.8 Western blot

Unless stated differently, cells harvested from one well of either a 6-well plate were lysed in 100 µl of Co-IP lysis buffer. Lysates were incubated on ice for 20 min and centrifuged at 14,000 rpm for 20 min at 4 °C. Afterwards, lysates were mixed with Protein Sample Loading Buffer (LI-COR) (22.5% (v/v)) and β-mercaptoethanol (2.5% (v/v)) and boiled at 95 °C for 5 min. Equal amounts of lysates were separated in 4-12% NuPAGE Novex Bis-Tris precast polyacrylamide gels (Invitrogen). Immobilion-FL Transfer PVDF Membranes (Merck Millipore) were soaked in 100% methanol for 1 min and then in distilled H_2O for 1 min, before incubating them in transfer buffer for 20 min. Separated proteins were blotted onto activated membranes with the Trans-Blot SD Semi-Dry Transfer Cell (Bio-Rad Laboratories GmbH). Membranes were blocked in blocking buffer and stained using primary antibodies directed against GAPDH (BioLegend), HA-tag (abcam) and β-catenin (Cell Signaling Technology), followed by an incubation with Infrared Dye labeled secondary antibodies (LI-COR). Proteins were detected with a LI-COR Odyssey Imager (LI-COR Biosciences), and band intensities were quantified using Image Studio Lite Version 5.0 (LI-COR Biosciences).

3.2.9 Flow cytometry

Flow cytometry was performed to assess the expression of β-catenin, p24 (HIV-1 capsid), p27 (HIV-2 capsid), DHRS2, HSF1, and phosphorylated HSF1 (Ser303/307) in infected CD4+ T cells. At 3 days post-infection (d.p.i.), cells were harvested, washed twice with cold FACS buffer (PBS supplemented with 1% FBS), and fixed with 2% paraformaldehyde (PFA) for 10 minutes at room temperature (RT). After fixation, cells were washed once with FACS buffer and permeabilized by incubation in ice-chilled 90% methanol for 20 minutes on ice.

Following permeabilization, cells were washed and incubated with fluorochrome-conjugated primary antibodies specific to target proteins or, in the case of non-conjugated primary antibodies, stained sequentially with appropriate fluorochrome-conjugated secondary antibodies. Antibody incubations were carried out for 30 minutes at 4 °C in the dark. After staining, cells were washed and resuspended in FACS buffer for acquisition.

Samples were acquired using the MACSQuant Analyzer (Miltenyi Biotec). For intracellular protein detection within the infected population, GFP or FITC signal was used to gate on transduced/fluorescently labeled cells. The mean fluorescence intensity (MFI) of the fluorophore associated with the protein of interest (e.g., PE) was quantified within the GFP+/FITC+ population. In addition, the percentage of PE-positive cells within the GFP+/FITC+ population was determined to assess relative protein expression levels across conditions.

Flow cytometry data were analyzed using *FlowLogic* software (Inivai Technologies). Proper fluorescence compensation, gating strategies, and isotype controls were applied to ensure specificity and accuracy of the measurements.

3.2.10 Quantitative real-time reverse transcription PCR (qRT-PCR)

Quantitative real-time reverse transcription PCR (qRT-PCR) was performed to assess the expression levels of LTR12D_*DHRS2*, *CDKN2A*, *CDKN1A*, *IL-6*, *TNF*, *CXCL10*, *CCL5*, *CCL17* and the housekeeping gene *GAPDH* in primary CD4+ T cells infected with HIV-1 CH077, STCO1, or mock-infected cells. At 3 days post-infection (d.p.i.), cells were harvested and washed twice with Dulbecco's phosphate-buffered saline (DPBS). Total RNA was extracted from the cells using 350 µL of RLT Plus buffer (Qiagen) supplemented with 1% (v/v) β-mercaptoethanol to ensure RNase inactivation and cell lysis. Lysates were

immediately placed on ice and RNA isolation was performed using the RNeasy Plus Mini Kit (Qiagen) in accordance with the manufacturer's protocol.

To eliminate any residual genomic DNA contamination, especially important given the non-exon-spanning nature of the primers and probes, samples were treated with the DNA-free™ DNA Removal Kit (Thermo Fisher Scientific) following the manufacturer's instructions. RNA concentration and purity were measured using a NanoDrop 2000 spectrophotometer (Thermo Fisher Scientific). Equal amounts of total RNA were used for cDNA synthesis across all samples to avoid quantification bias.

First-strand cDNA was synthesized using the PrimeScript RT Reagent Kit (Takara Bio) with both random hexamer and oligo(dT) primers in a Veriti™ 96-Well Thermal Cycler (Applied Biosystems). Reactions were prepared according to the manufacturer's guidelines. No-RT controls (without reverse transcriptase) were included to confirm the complete removal of genomic DNA.

qRT-PCR was carried out using the TaqMan™ Fast Universal PCR Master Mix (Thermo Fisher Scientific) in a StepOnePlus™ Real-Time PCR System (Applied Biosystems). Reactions were performed in technical duplicates or triplicates. TaqMan primer and probe sets specific for LTR12D_*DHRS2*, *CDKN2A*, *CDKN1A*, and *GAPDH* were used. *GAPDH* served as the internal reference gene to normalize expression levels.

Quantification of gene expression was performed using the comparative Ct method (ΔΔCt). The Ct values of target genes were normalized to *GAPDH*, and the relative expression levels were calculated as fold change compared to mock-infected controls. Detailed sequences of primers and probes used in these assays are listed in Section 3.1.3.3.

3.2.11 Statistical analyses

Statistical analyses were performed using GraphPad Prism version 8.4.2. Depending on the experimental design, data were analyzed using one-way ANOVA, paired or unpaired Student's *t*-test. Differences were considered statistically significant if $p \leq 0.05$. Significance levels are indicated as follows: $p \leq 0.05$ (*), $p < 0.01$ (**), $p < 0.001$ (***), and $p < 0.0001$ (****).

3.2.12 Ethics statement

Ethical approval for the utilization of human peripheral blood cells was obtained from the Ethics Committee of Tübingen University Medical Center (project# 127/2022BO2).

4 Results

4.1 *CDKN2A* induction: limited consistency in HIV-1 infection

CDKN2A (p16) is a key senescence marker that induces cell cycle arrest by inhibiting CDK4/6 [248, 249]. Since we observed activation of the p53-p21 pathway during HIV-1 infection, I next investigated whether the p16 pathway also contributes to HIV-1-induced senescence. I measured *CDKN2A* mRNA levels in primary CD4⁺ T cells infected with two HIV-1 clones, STCO1 and CH077. These clones represent primary isolates from different stages of infection [230, 231] and belong to HIV-1 group M, subtype B. Both are dual-tropic viruses capable of using CCR5 and CXCR4 as co-receptors. Mock-infected cells served as negative control. Three days post-infection (d.p.i.), CD4⁺ T cells were harvested, and infection rates were determined by flow cytometry (Fig. 4.1A). *CDKN2A* mRNA levels were quantified using qPCR (Fig. 4.1B). We observed that infection with the HIV-1 clone STCO1 did not significantly change *CDKN2A* expression. In contrast, infection with CH077 led to a significant, approximately two-fold increase in *CDKN2A* mRNA levels compared to mock-infected cells. These findings suggest that *CDKN2A* induction is not a consistent feature of HIV-1 infection, as only one of the two tested strains led to its induction. This implies that HIV-1-mediated senescence may not strictly require *CDKN2A* induction and could instead rely on other pathways, such as the p53-p21 pathway.

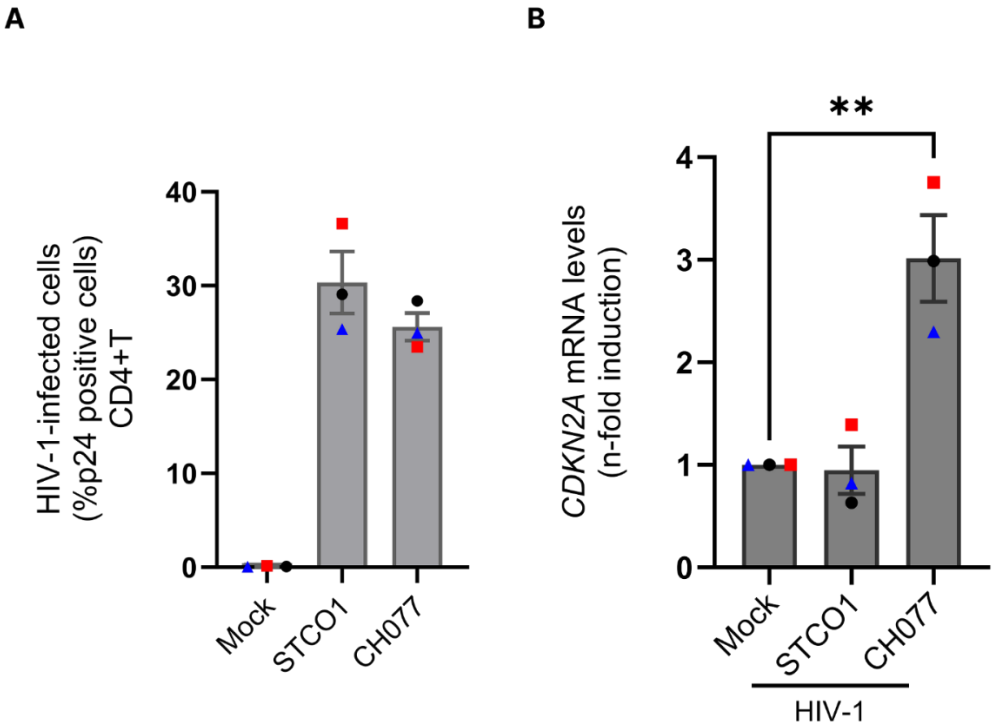

Figure 4.1: *CDKN2A* induction is not a universal feature of HIV-1 infection. (A) Infection rates were measured in primary $CD4^+$ T cells infected with HIV-1 clones STCO1 and CH077 at 3 d.p.i. Infection rates for both strains were assessed by quantifying the percentage of p24-positive cells via flow cytometry. **(B)** *CDKN2A* (p16) mRNA levels in the cells shown in (A) were quantified using qPCR. Expression values were normalized to a housekeeping gene (*GAPDH*), and fold changes were calculated relative to mock-infected control cells. Data represent the mean ± standard error of the mean (SEM) from three independent experiments. Statistical significance was determined using one-way ANOVA: (** $p < 0.01$), indicating significant differences compared to mock-infected controls.

4.2 HIV-1 induces LTR12D_*DHRS2* transcription in SupT1 and Jurkat cells.

In order to further investigate the activation of the LTR12D-DHRS2-p53-p21 cascade, two immortalized T cell lines, SupT1 [250] and Jurkat [251], were chosen due to their reproducibility, ease of handling, and ability to maintain experimental consistency. These cell lines provide a controlled environment for studying HIV-1 infection and senescence pathways, overcoming the challenges posed by primary T cells, such as donor variability and short lifespan [252].

SupT1 and Jurkat cells were infected with the HIV-1 clones STCO1, NL4-3, and CH077. HIV-1 NL4-3, a well-characterized, replication-competent laboratory strain, is widely used as a standardized model for studying HIV-1 biology and testing antiviral strategies [253]. At 3 d.p.i., both SupT1 and Jurkat cells were harvested, and infection rates were assessed by quantifying the percentage of p24 cells via flow cytometry. Fig. 4.2A, 4.2B, and 4.2E display representative primary FACS data showing infection rates, while Fig. 4.2C, 4.2F, and 4.2D, 4.2G present LTR12D_*DHRS2* and *CDKN1A* mRNA transcript levels, respectively.

The results consistently showed a 5- to 20-fold increase in LTR12D_*DHRS2* transcript levels and a 2- to 3-fold increase in *CDKN1A* mRNA levels in HIV-1-infected samples compared to mock-infected samples.

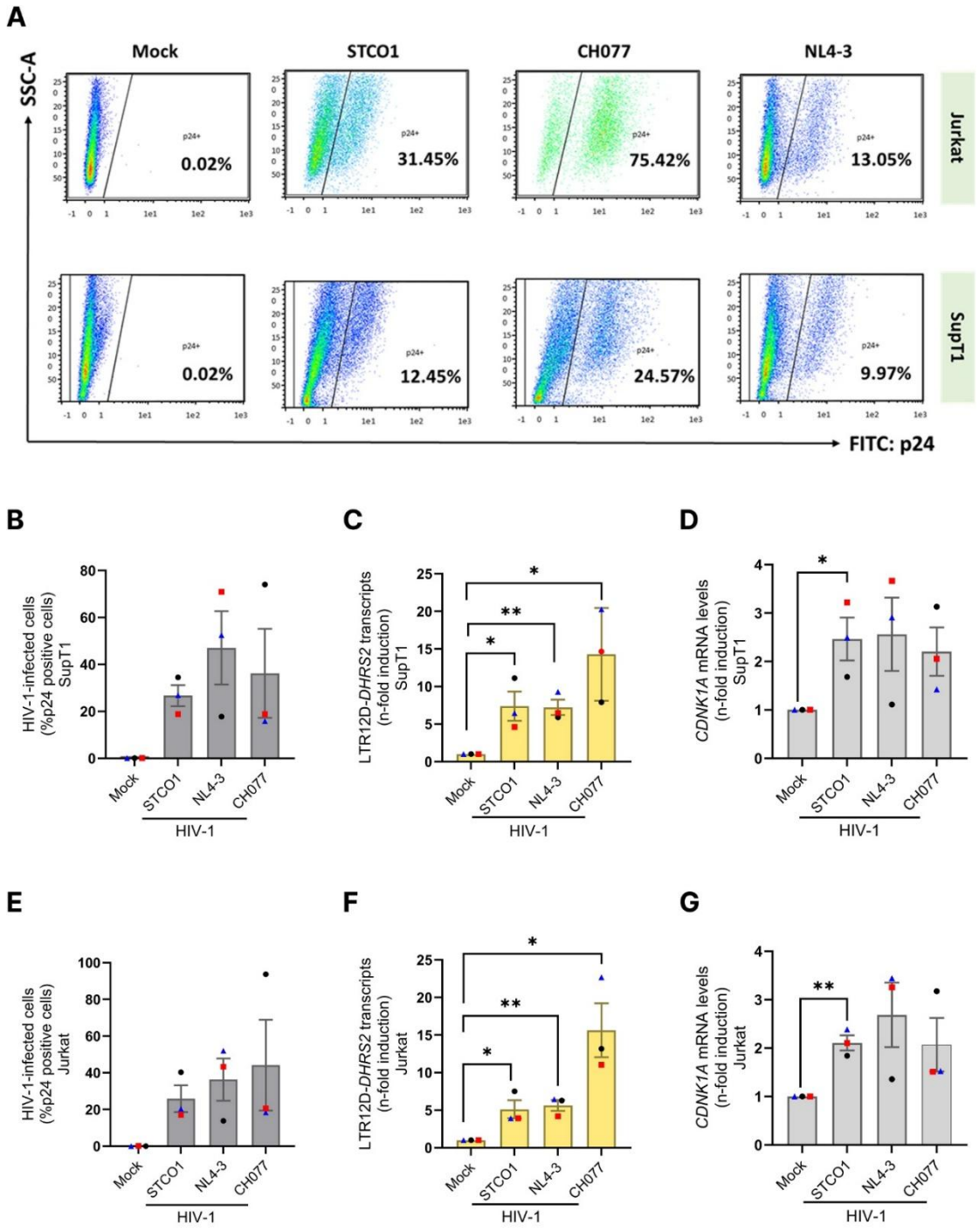

Figure 4.2: Induction of LTR12D_*DHRS2* and *CDKN1A* transcription in SupT1 and Jurkat cells infected with HIV-1. (A, B and E) (A) Primary FACS plots for both Jurkat and SupT1 cells infected with HIV-1 CH077 are shown. HIV-1 infection rates in (B) SupT1 and (E) Jurkat cells were quantified by measuring intracellular p24 protein levels using flow cytometry at 3 days post-infection. **(C, F)** LTR12D_*DHRS2* transcript levels of the samples shown in (B) and (E) were assessed using quantitative-RTPCR (q-RTPCR) in infected (C) SupT1 and (F) Jurkat cells. Expression levels were normalized to *GAPDH* (housekeeping

gene), and fold changes were calculated relative to mock-infected controls. **(D, G)** *CDKN1A* (p21) mRNA expression of the samples shown in (B) and (E) was measured in the same experimental conditions using qPCR. All data are presented as mean ± standard error of the mean (SEM) from three independent experiments. Statistical significance was determined using one-way ANOVA: (* $p < 0.05$, ** $p < 0.01$), indicating significant differences compared to mock-infected controls.

4.3 HIV-2 increases DHRS2 protein levels in SupT1, Jurkat and primary CD4⁺ T cells.

Given that HIV-2 is associated with slower disease progression and a different pattern of immune system involvement [254], it typically results in significantly lower viral loads (often below 10,000 copies/ml) and a more gradual decline in $CD4^+$ T cell counts [255]. This leads to a longer asymptomatic phase and delayed progression to AIDS. Therefore, it is essential to validate the LTR12D-DHRS2-p53-p21 cascade in HIV-2 infection to understand how the unique viral properties of HIV-2 influence cellular aging and senescence.

To assess how HIV-2 infection activates the LTR12D-DHRS2-p53-p21 cascade, Jurkat, SupT1, and primary $CD4^+$ T cells were infected with different HIV-2 clones. The 7312A clone, representing a primary HIV-2 isolate, was used to capture the physiological relevance of viral behavior in a near-native context, closely mimicking *in vivo* infection [256]. Additionally, ROD10 [257] and GH-1 [258], both well-characterized cell culture-adapted strains, were used to ensure reproducibility. 3 d.p.i., infection rates were analyzed by monitoring p27 via flow cytometry (Fig. 4.3A, 4.3B, 4.3C). Infection rates ranged from 2.5-28% in Jurkat cells, 2-20% in SupT1 cells, and 0.5-3.5% in primary $CD4^+$ T cells (Fig. 4.4A, 4.4B, 4.4C). Flow cytometry analysis revealed an increase in DHRS2 protein levels in both infected and bystander cells compared to mock-infected cells, across all tested models (Fig. 4.4D, 4.4E, 4.4F). Notably, Jurkat cells infected with the HIV-2 7312A strain, which achieved higher infection rates as compared to SupT1 and $CD4^+$ T cells infected with 7312A in two replicates, were further analyzed using q-RTPCR and exhibited a two-fold increase in *CDKN1A* mRNA levels compared to mock-infected cells (Fig. 4.4G).

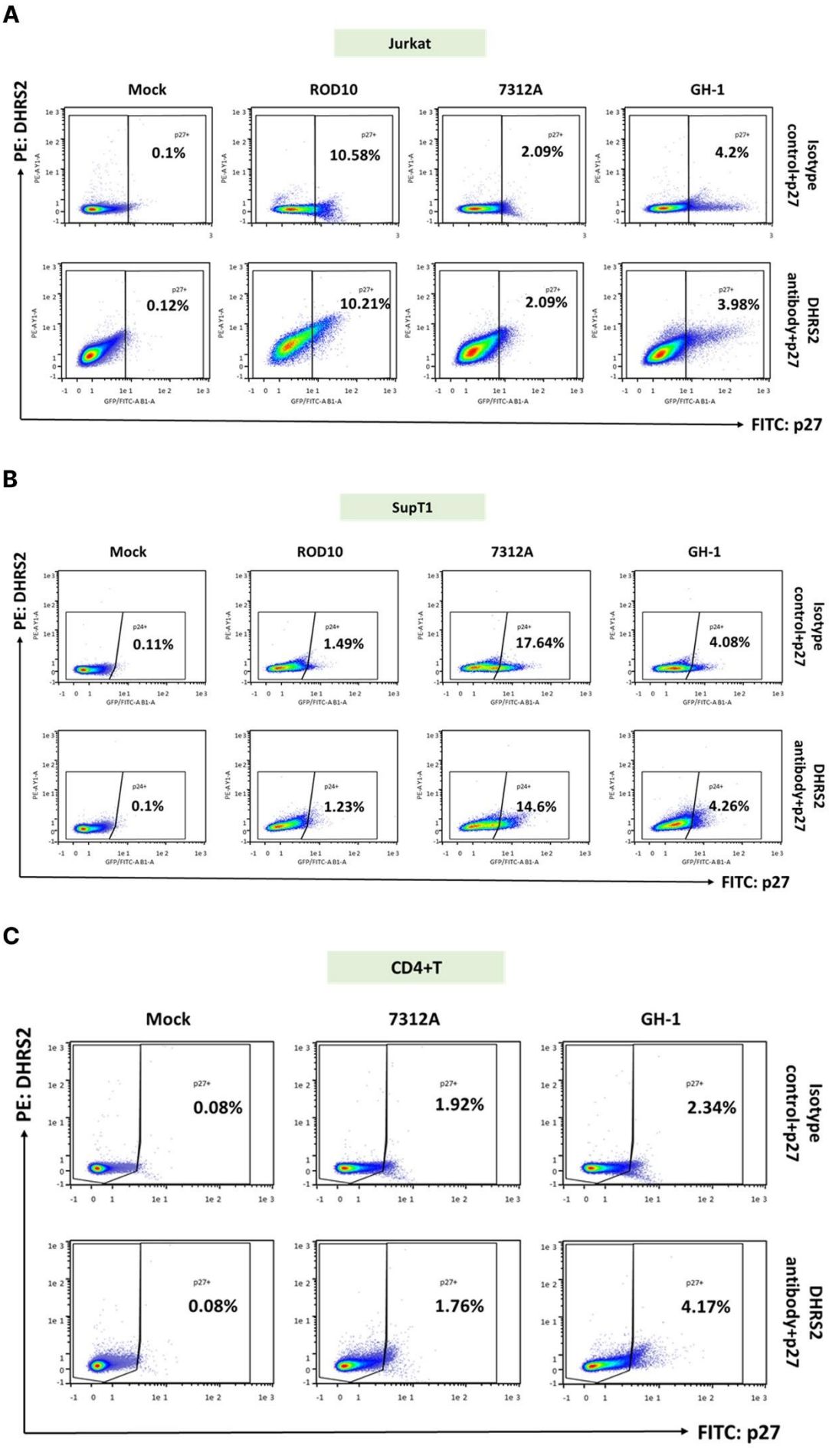
A
Jurkat
Mock
ROD10
7312A
GH-1
PE: DHRS2
FITC: p27
Isotype control+p27
DHRS2 antibody+p27
0.1%
10.58%
2.09%
4.2%
0.12%
10.21%
2.09%
3.98%
B
SupT1
Mock
ROD10
7312A
GH-1
PE: DHRS2
FITC: p27
Isotype control+p27
DHRS2 antibody+p27
0.11%
1.49%
17.64%
4.08%
0.1%
1.23%
14.6%
4.26%
C
CD4+T
Mock
7312A
GH-1
PE: DHRS2
FITC: p27
Isotype control+p27
DHRS2 antibody+p27
0.08%
1.92%
2.34%
0.08%
1.76%
4.17%

Figure 4.3: HIV-2 infection of Jurkat, SupT1 and CD4$^+$ T cells. **(A-C)** (A) Jurkat, (B) SupT1, and (C) primary CD4$^+$ T cells were infected with HIV-2 clones ROD10, 7312A, or GH-1. Infection rates were determined by assessing p27 protein levels using flow cytometry at 3 d.p.i. Representative FACS data from a single replicate are shown for each cell type (Jurkat, SupT1, and CD4$^+$ T cells). P27-: uninfected; shown on left side of the gating (100 - p27+) %, p27+: HIV-2-infected.

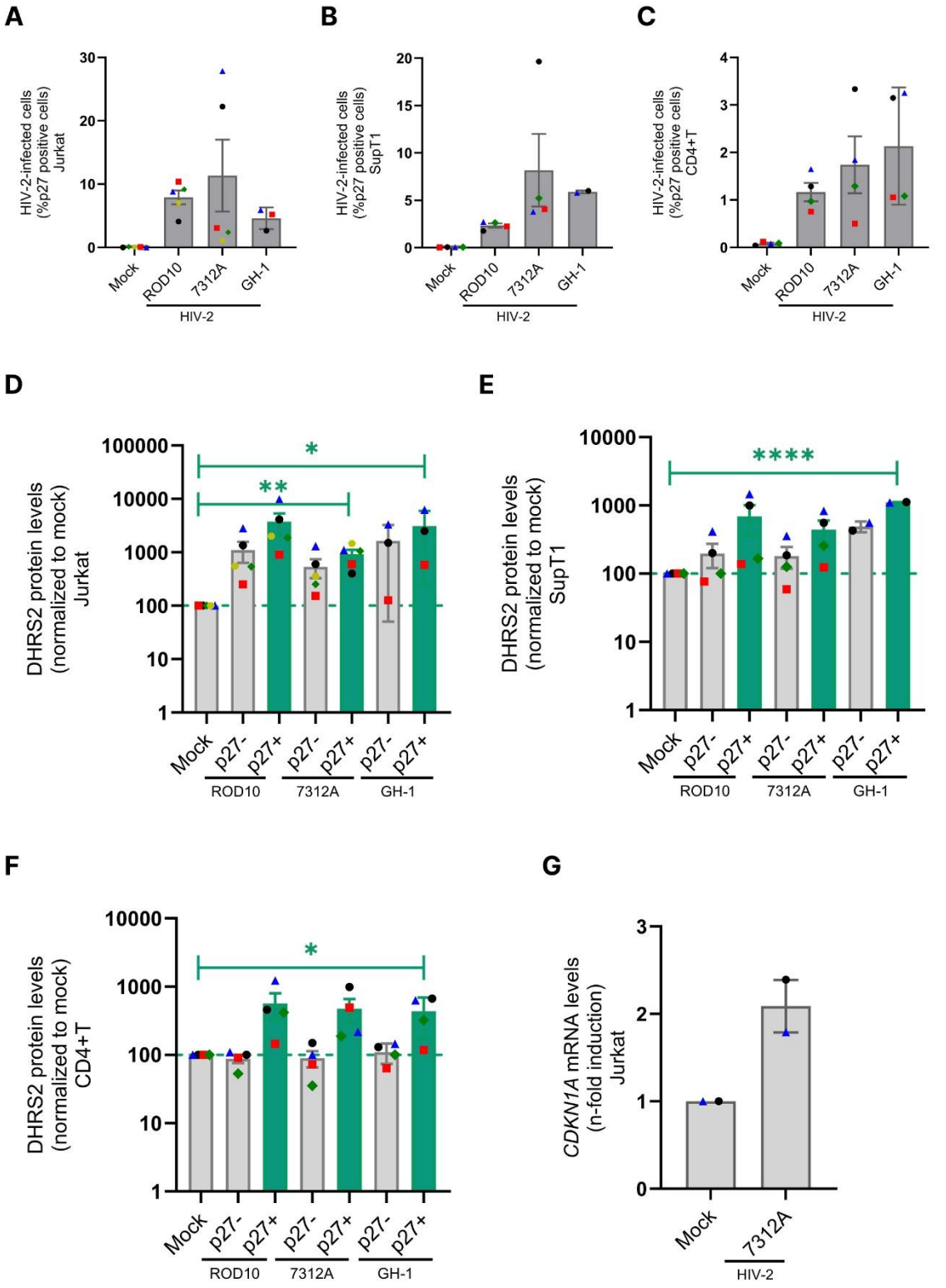

Figure 4.4: HIV-2 infection increases DHRS2 protein levels. **(A-F)** (A, D) Jurkat cells, (B, E) SupT1 cells, and (C, F) primary CD4⁺ T cells were infected with HIV-2 clones ROD10, 7312A, or GH-1. Infection rates were determined by assessing p27 protein levels using flow cytometry at 3 d.p.i. **(D-F)** DHRS2 protein levels were assessed using flow cytometry in infected (D) Jurkat, (E) SupT1 and (F) primary CD4⁺ T cells. The results in D-F were

obtained using the cells shown in A-C. DHRS2 protein levels were assessed in two to five independent experiments and are shown relative to mock-infected controls. **(G)** *CDKN1A* (p21) mRNA levels were measured in cells infected with the HIV-2 strain 7312A using q-RTPCR. *CDKN1A* expression was assessed in two independent experiments and is shown relative to mock-infected controls. Mean values ± standard error of the mean (SEM) are shown, with two to five independent experiments performed for each measurement. Statistical significance was determined using one-way ANOVA (* $p < 0.05$, ** $p < 0.01$, **** $p < 0.0001$), comparing HIV-2-infected cells to mock controls. P27-: uninfected, P27+: HIV-2 infected

4.4 HIV-1 infection increases DHRS2 protein levels in primary macrophages.

Primary macrophages, which are key targets and reservoirs of HIV [259], play a critical role in HIV pathogenesis [260]. To investigate how HIV contributes to cellular aging and immune dysfunction, we examined the involvement of the DHRS2 pathway in these cells. To evaluate this, primary monocyte-derived macrophages were infected with HIV-1 CH077 or a modified variant of HIV-1 NL4-3 harboring mutations in the V3 loop that render this clone CCR5-tropic and facilitate macrophage entry [261]. The modified CXCR4-tropic strain NL4-3 is a well-characterized and widely used HIV-1 clone that enables reproducible and standardized mechanistic studies in macrophages [262]. Furthermore, to enhance infection efficiency in primary macrophages, which are known for their resistance to HIV-1 due to the antiviral restriction factor SAMHD1, we employed Vpx-mediated SAMHD1 degradation [263]. This strategy effectively increased viral replication, achieving high infection rates and enabling the study of post-entry host responses under conditions of robust infection. At 8 d.p.i., infection rates (Fig. 4.5A, 4.5B) and LTR12D_*DHRS2* transcript levels (Fig. 4.5C) were quantified using flow cytometry and qPCR, respectively. Infection rates ranged from 8% to 85% for NL4-3, and from 2% to 6% for CH077. However, no significant differences in LTR12D_*DHRS2* transcript levels between HIV-1-infected and mock-infected cells were observed, suggesting that HIV-1 infection did not activate the DHRS2 pathway in macrophages under these conditions.

Although the modified NL4-3 strain combined with Vpx-mediated SAMHD1 degradation enabled efficient macrophage infection, I did not observe induction of the

LTR12D_*DHRS2* pathway under these conditions. Therefore, I extended our analysis to naturally macrophage-tropic (M-tropic) CCR5-tropic strains YU2 and AD8 [264]. These strains infect macrophages efficiently without SAMHD1 depletion [265], providing a more physiological infection model to validate DHRS2 pathway activation. Primary monocyte-derived macrophages were infected with these strains, and at 8 d.p.i., infection rates (Fig. 4.6A, 4.6B) and DHRS2 protein levels (Fig. 4.6C) were measured using flow cytometry. Infection rates ranged from 5% to 12% for YU2 and from 20% to 40% for AD8. Notably, an increase in DHRS2 protein levels was detected in infected macrophages, indicating that HIV-1 infection activates the DHRS2 pathway in macrophages infected with M-tropic viruses.

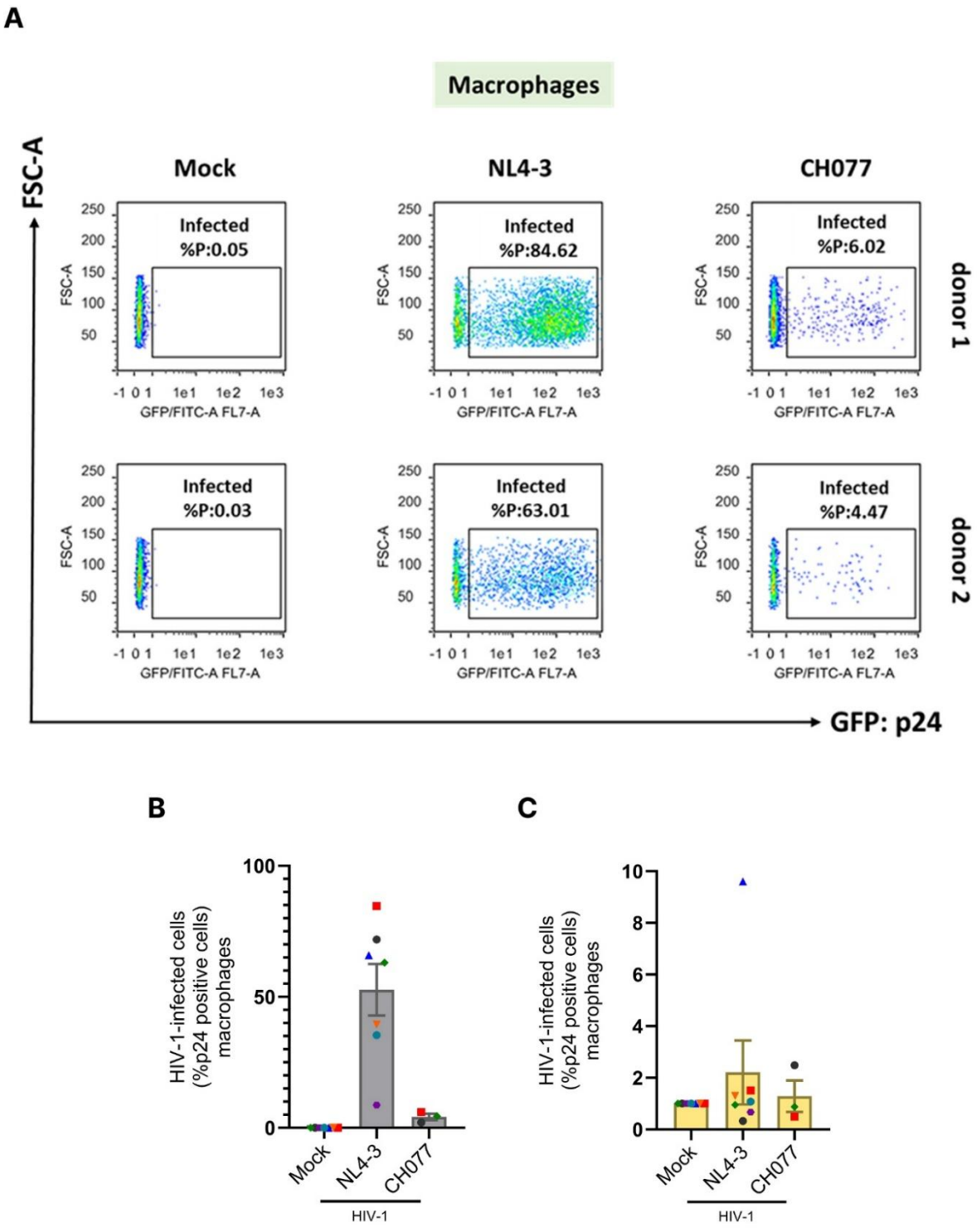

Figure 4.5: Modified T-tropic HIV-1 strain is not able to increase LTR12D_*DHRS2* transcript levels in macrophages (A, B) (A) Representative FACS data from two donors are shown. Infection rates were assessed by measuring the percentage of p24-positive cells among primary monocyte-derived macrophages infected with HIV-1 CH077 or a modified CXCR4-tropic HIV-1 NL4-3 at 8 d.p.i. (B) Infection rates for seven independent donors are shown. **(C)** LTR12D_*DHRS2* transcript levels were measured using qPCR at 8

d.p.i. No significant increase in transcript levels was observed across three to seven independent experiments. Mean values ± standard error of the mean (SEM) from three to seven independent experiments are shown in panel (C). The monocyte-derived macrophages were cultured, and some infection experiments (n=3; NL4-3) were performed by Dr. Martin Müller and MD student Ms. Lea Meckes in our Institute at Tübingen University.

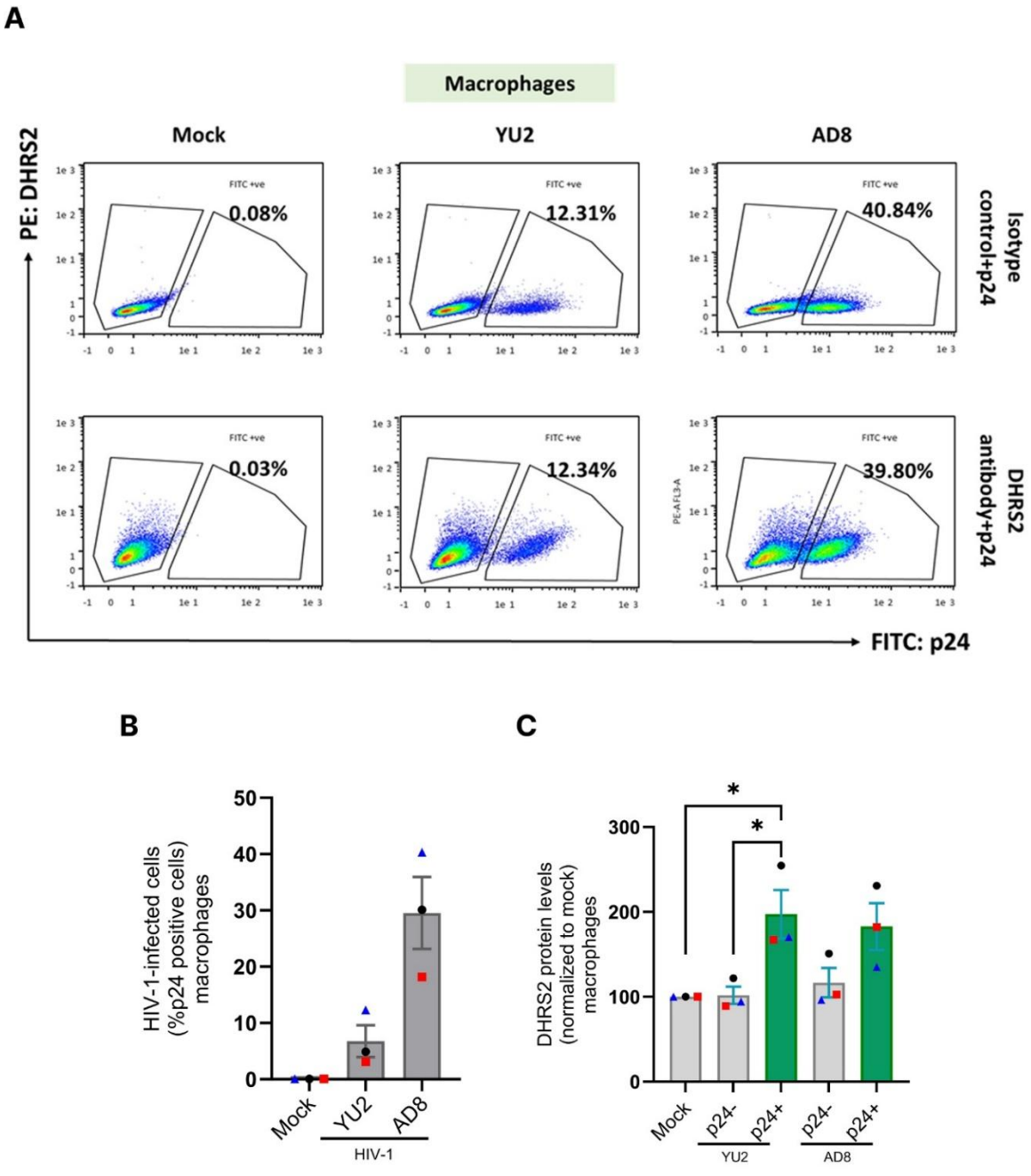

Figure 4.6: DHRS2 protein levels are upregulated in monocyte-derived macrophages infected with M-tropic strains (A, B) (A) Representative FACS data from a single replicate are shown. Infection rates were measured in primary monocyte-derived macrophages infected with M-tropic strains YU2 and AD8 at 8 d.p.i. Infection rates for both strains were assessed by monitoring p24 via FACS. (B) Infection rates for three independent donors are shown. **(C)** DHRS2 protein levels were measured in YU2- and AD8-infected macrophages at 8 d.p.i. DHRS2 protein levels were significantly higher in both HIV-1-infected macrophages as compared to mock-infected controls. Mean values ± standard error of the mean (SEM) from three independent experiments are shown in panels (B) and (C). Statistical significance was determined using one-way ANOVA: (* $p < 0.05$). P24-: uninfected; shown on left side of the gating (100 - p24+) %, p24+: HIV-1 p24 infected.

4.5 *DHRS2* knockout reduces HIV-1 infection and alters SASP profiles.

Building on our earlier observation that *DHRS2* is induced in M-tropic infected macrophages and potentially linked to strain-specific immune responses, we sought to functionally probe its role in $CD4^+$ T cell senescence. To investigate the functional role of DHRS2, we performed CRISPR/Cas9-mediated knockout [266] where $CD4^+$ T cells were electroporated using *DHRS2* specific guide RNA and non-targeting control. Following genetic manipulation, cells were infected with HIV-1, and the resulting senescence-associated secretory phenotype (SASP) markers were analyzed. Based on our hypothesis, we anticipated that the absence of *DHRS2* would lead to a reduction in the induction of both *CDKN1A* and various SASP factors, given their established roles in cellular senescence pathways.

This experiment was partly conducted by our collaborators in Prof. Frank Kirchhoff's laboratory at Ulm University. The experimental setup is shown in (Fig. 4.7). *DHRS2* knockout led to a ~40% reduction in DHRS2 protein levels in primary $CD4^+$ T cells transduced with *DHRS2*-specific gRNA compared to non-targeting gRNA controls, likely due to a mixed population of electroporated and non-electroporated cells (Fig. 4.8A). *DHRS2* knockout also resulted in reduced HIV-1 infection rates (Fig. 4.8B).

We previously showed that HIV-1 infection increases *CDKN1A* mRNA levels; however, *DHRS2* knockout did not alter *CDKN1A* expression. (Fig. 4.8C). HIV-1 infection also

triggered the secretion of senescence-associated cytokines, including IL-1α, TIMP-2, IGF-1, CXCL10, and angiogenin [125]. Upon *DHRS2* knockout, a marked reduction in these cytokines was observed compared to control cells expressing non-targeting gRNA (Fig. 4.8D). Conversely, cytokines whose expression or release is typically decreased during senescence, including LIF, TIMP-1, and EGF [125], showed increased levels upon *DHRS2* knockout (Fig. 4.8E). Cytokines that are normally unaffected during senescence remained stable in the *DHRS2* knockout cells (Fig. 4.8F).

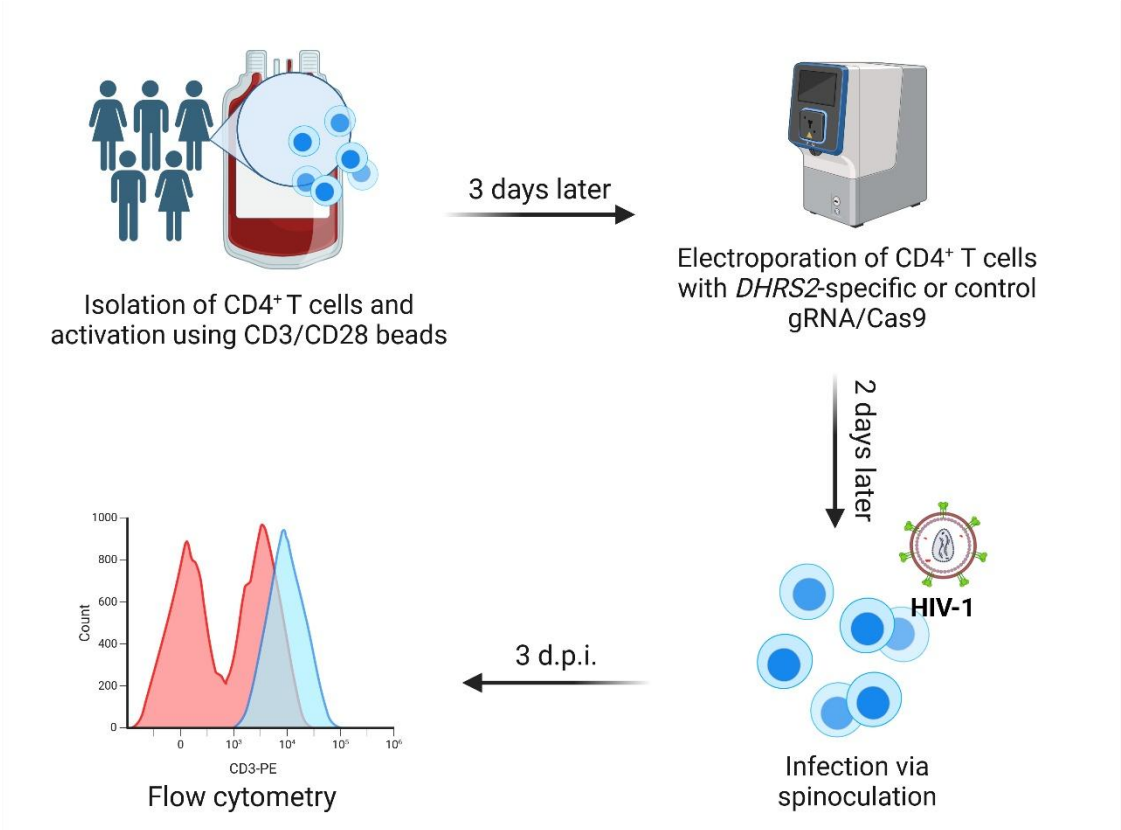

Figure 4.7: *DHRS2* knockout experimental setup (Created with BioRender.com). Primary human CD4⁺ T cells were activated, electroporated with *DHRS2*-specific or control gRNA/Cas9, infected with HIV-1, and analyzed by FACS to assess the role of *DHRS2* in T cell senescence.

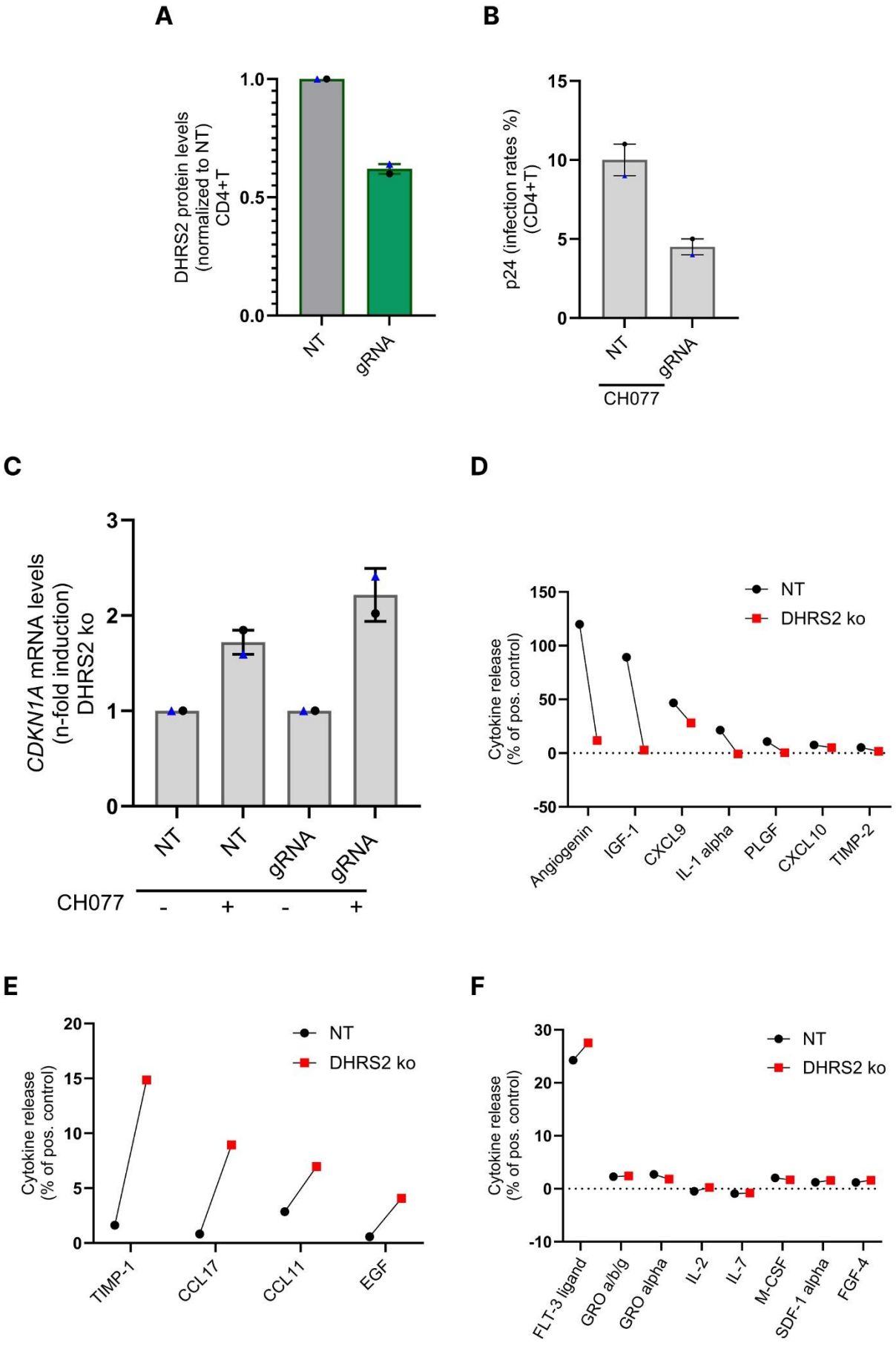
A
DHRS2 protein levels (normalized to NT) CD4+T
1.0
0.5
0.0
NT
gRNA
B
p24 (infection rates %) (CD4+T)
15
10
5
0
NT
gRNA
CH077
C
CDKN1A mRNA levels (n-fold induction) DHRS2 ko
3
2
1
0
NT
NT
gRNA
gRNA
CH077
-
+
-
+
D
Cytokine release (% of pos. control)
150
100
50
0
-50
NT
DHRS2 ko
Angiogenin
IGF-1
CXCL9
IL-1 alpha
PLGF
CXCL10
TIMP-2
E
Cytokine release (% of pos. control)
20
15
10
5
0
NT
DHRS2 ko
TIMP-1
CCL17
CCL11
EGF
F
Cytokine release (% of pos. control)
30
20
10
0
-10
NT
DHRS2 ko
FLT-3 ligand
GRO a/b/g
GRO alpha
IL-2
IL-7
M-CSF
SDF-1 alpha
FGF-4

Figure 4.8: *DHRS2* knockout may prevent the induction of senescence upon HIV-1 infection. (A) DHRS2 protein levels in CD4⁺ T cells were assessed by flow cytometry following CRISPR-Cas9-mediated knockout using *DHRS2*-specific guide RNA. Cells transduced with non-targeting (NT) guide RNA served as controls. Knockout resulted in a significant ~40% reduction in DHRS2 protein levels. **(B)** Primary CD4⁺ T cells with either *DHRS2* knockout or non-targeting (NT) gRNA control were infected with HIV-1 CH077 or mock-infected. Three d.p.i., infection rates were determined by flow cytometry. **(A-B)** Experiments were performed by our collaborator, Dr. Caterina Prelli Bozzo in Prof. Frank Kirchhoff's laboratory at Ulm University. **(C)** CD4⁺ T cells, either subjected to *DHRS2* knockout or treated with a non-targeting (NT) gRNA control, were subsequently infected with HIV-1 CH077 or mock-infected. *CDKN1A* mRNA levels in these cells were then measured by qPCR in two independent experiments, with expression shown relative to mock-infected controls. **(D-F)** A membrane-based semi-quantitative cytokine array was used to monitor cytokine release and a potential influence of DHRS2 and HIV-1 infection on senescence. For this assay, samples from both donors previously shown were pooled. (D) Cytokines that are known to be released to a higher extent from senescent cells showed decreased release upon *DHRS2* knockout. (E) Cytokines that are known to be released to a lower extent from senescent cells showed increased release upon *DHRS2* knockout. (F) Cytokines that remain unchanged upon transition to senescence remained unaffected by *DHRS2* knockout. Mean values ± standard error of the mean (SEM) from two independent experiments are shown in panels (A-F). NT: non-targeting control gRNA, gRNA: *DHRS2*-specific gRNA, pos. control: positive control.

4.6 *DHRS2* is essential for HIV-1-induced senescence.

In the previous experiment, it remained unclear whether DHRS2 is essential for HIV-1-induced senescence, as the results showed variability in infection rates, no change in *CDKN1A* mRNA levels, and a reduction in SASP profiles in *DHRS2* knockout CD4⁺ T cells. To investigate this further, I employed a different strategy to knock out *DHRS2* in CD4⁺ T cells and used the lentiCRISPRv2 system, which expresses Cas9. I cloned either *DHRS2*-specific gRNA or a non-targeting control gRNA into the vector; the experimental layout is shown in (Fig. 4.9). To investigate the impact of DHRS2 depletion on HIV-1-induced-senescence, cells were transduced with a *DHRS2*-specific guide RNA (gRNA) to target and reduce *DHRS2* expression. As controls, CD4⁺ T cells were transduced with a non-targeting (NT) gRNA or left mock-transduced, with all three groups subsequently

infected with HIV-1 CH077. Additionally, a separate mock-transduced sample was used as a 'kill control' for puromycin selection. FACS analysis revealed a significant reduction of approximately 40% in DHRS2 protein levels in *DHRS2* knockout cells compared to controls, confirming knockout of the target protein (Fig. 4.10B, 4.10C). Importantly, HIV-1 CH077 infection rates differed between donors, but were similar across the different conditions tested (specific guide-RNA, NT and mock) (Fig. 4.10A, 4.10D), indicating that *DHRS2* knockout does not significantly impact HIV-1 infection. This conclusion is supported by testing three donors (n=3), which is an increase from the two donors (n=2) used in the earlier *DHRS2* knockout electroporation experiment; however, additional experiments would be required to draw any definite conclusions.

Interestingly, *DHRS2* knockout led to a reduction in *CDKN1A* expression (Fig. 4.11A). Since our earlier data showed that HIV-1 infection induces several senescence-associated cytokines, including IL-6, TNF-α, CXCL10, CCL5, and CCL17 [125], I examined whether *DHRS2* influences their expression. Knockout of *DHRS2* reduced *IL6* (Fig. 4.11B), *TNF* (Fig. 4.11C), *CCL17* (Fig. 4.11E) and *CCL5* (Fig. 4.11F) mRNA levels compared to non-targeting and mock controls. However, *CXCL10* levels remained unchanged (Fig. 4.11D).

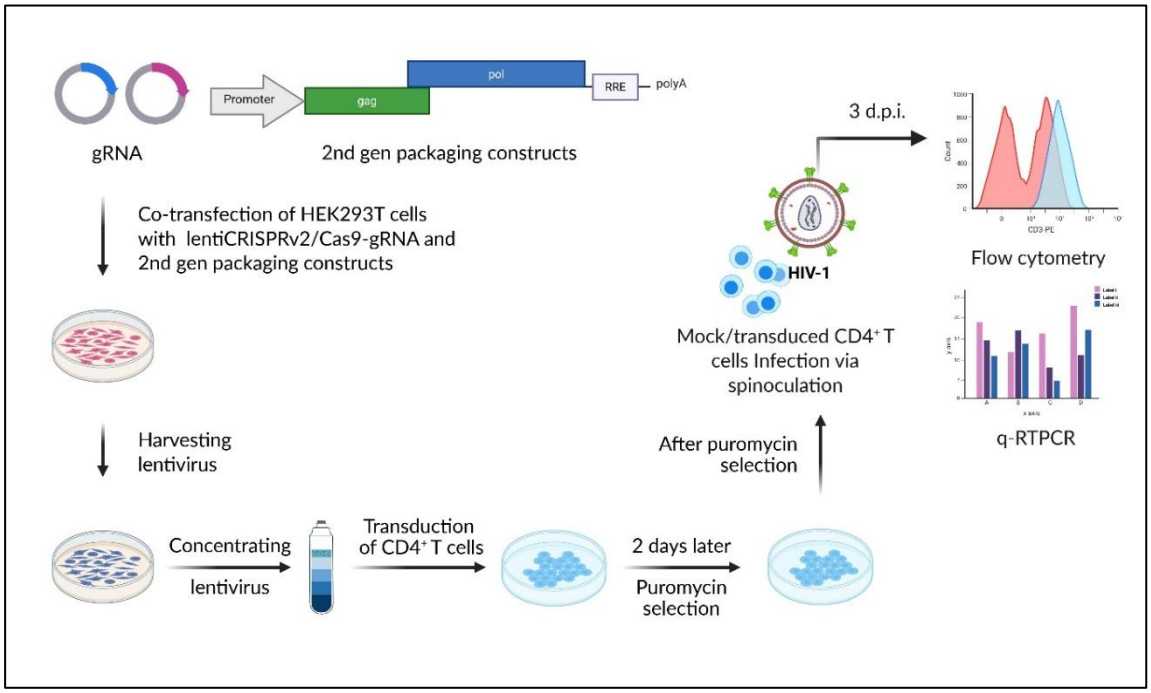

Figure 4.9: Experimental setup including *DHRS2* knockout using the lentiCRISPRv2 approach and subsequent HIV-1 infection (Created with BioRender.com). Lentiviral particles (LVPs), produced in HEK293T cells, encoded either *DHRS2*-specific or non-targeting (NT) gRNAs and were used to transduce primary CD4⁺ T cells from healthy

donors following 48 hours of PHA stimulation. Two days post-transduction, puromycin selection was applied to both NT and *DHRS2*-targeting populations and continued until mock-transduced cells were eliminated. Puromycin-resistant cells were then infected with HIV-1 CH077, and 72 hours post-infection, DHRS2 and p24 protein levels were assessed by flow cytometry, and *CDKN1A* mRNA levels and SASP factors were analyzed using q-RTPCR. 2nd gen: psPAX2 (HIV-1 *gag*+*pol*+*rev*) +pMD2.G (HIV-1 *env*).

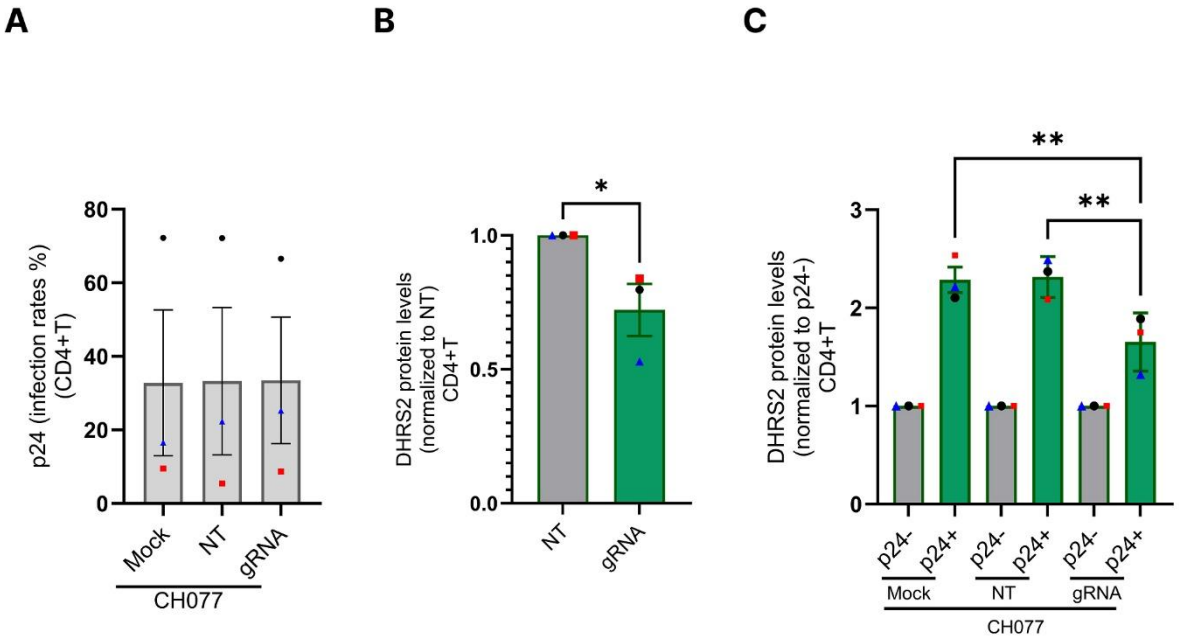
A
B
C
p24 (infection rates %) (CD4+T)
80
60
40
20
0
Mock
NT
gRNA
CH077
DHRS2 protein levels (normalized to NT) CD4+T
1.0
0.5
0.0
*
NT
gRNA
DHRS2 protein levels (normalized to p24-) CD4+T
3
2
1
0
**
**
p24-
p24+
p24-
p24+
p24-
p24+
Mock
NT
gRNA
CH077

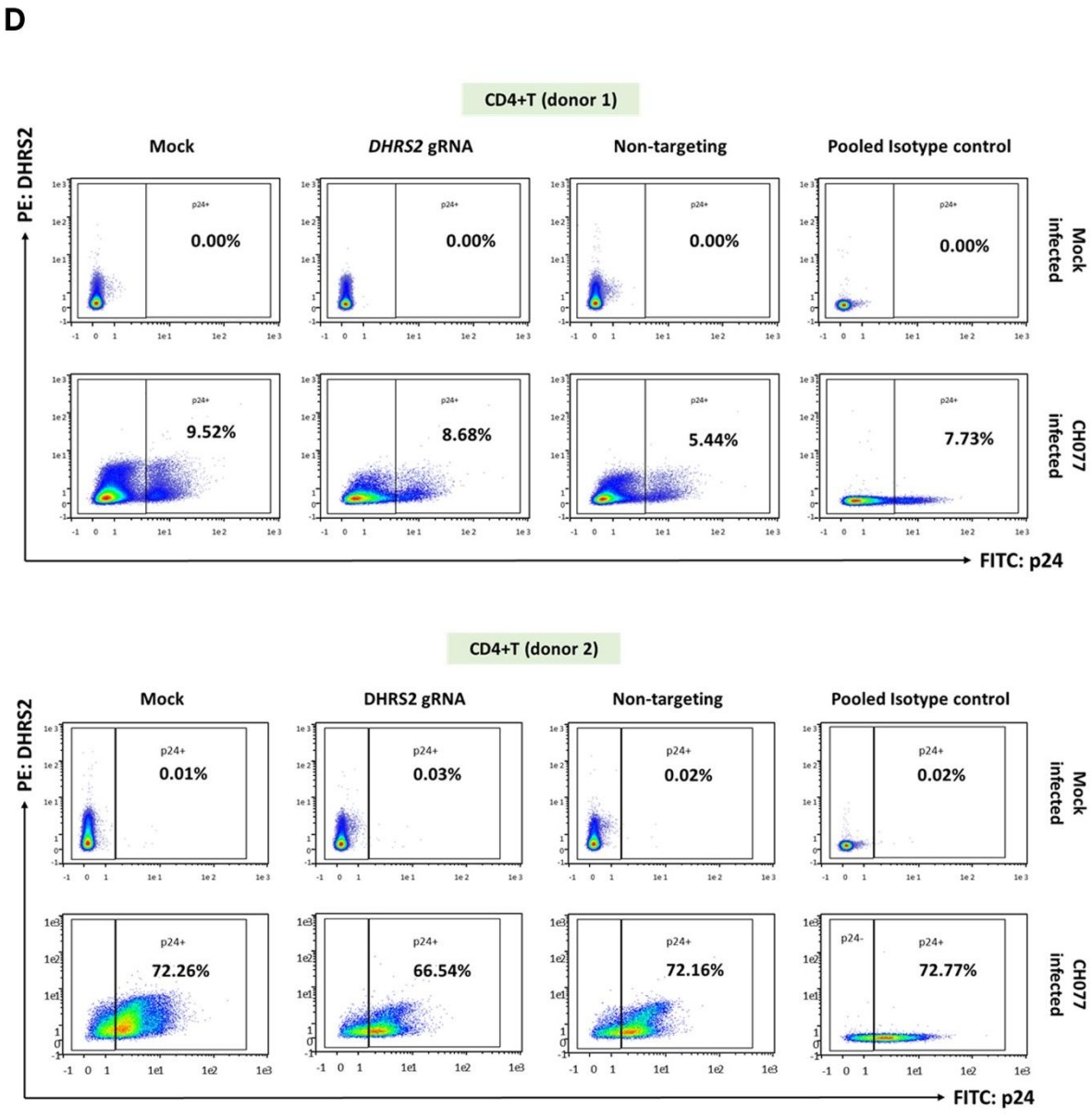
D
CD4+T (donor 1)
Mock
DHRS2 gRNA
Non-targeting
Pooled Isotype control
PE: DHRS2
FITC: p24
Mock infected
CH077 infected
0.00%
0.00%
0.00%
0.00%
9.52%
8.68%
5.44%
7.73%
CD4+T (donor 2)
Mock
DHRS2 gRNA
Non-targeting
Pooled Isotype control
PE: DHRS2
FITC: p24
Mock infected
CH077 infected
0.01%
0.03%
0.02%
0.02%
72.26%
66.54%
72.16%
72.77%

Figure 4.10: *DHRS2* knockout reduces DHRS2 protein levels in CD4⁺ T cells without altering HIV-1 CH077 infection rates. (A) Infection rates were assessed by measuring the percentage of p24-positive cells among primary CD4⁺ T cells that had been treated with either mock, *DHRS2*-knockout, or non-targeting (NT) gRNA control, and then infected with HIV-1 CH077. Three d.p.i., infection rates were determined by flow cytometry. Infection rates for three independent donors are shown. **(B)** DHRS2 protein levels in CD4⁺ T cells transduced with non-targeting (NT) gRNA, serving as a negative control, compared to *DHRS2* knockout cells infected with HIV-1 CH077. This panel highlights the significant ~40% reduction in DHRS2 protein levels achieved through knockout. **(C)** Comparison of DHRS2 protein levels in HIV-1 CH077-infected CD4⁺ T cells across different conditions: non-targeting (NT) gRNA transduced cells versus mock-transduced cells. This panel further illustrates the specificity of the ~40% DHRS2 protein reduction observed upon knockout. **(D)** Representative flow cytometry data from two independent primary donors are shown. Mean values ± standard error of the mean (SEM) from three independent experiments are shown. Statistical significance was determined using one-way ANOVA: (* $p < 0.05$, ** $p < 0.01$) indicating significant differences compared to mock-infected controls. NT: non-targeting gRNA control; P24-: uninfected; shown on left side of the gating (100 - p24+) %, p24+: HIV-1-infected.

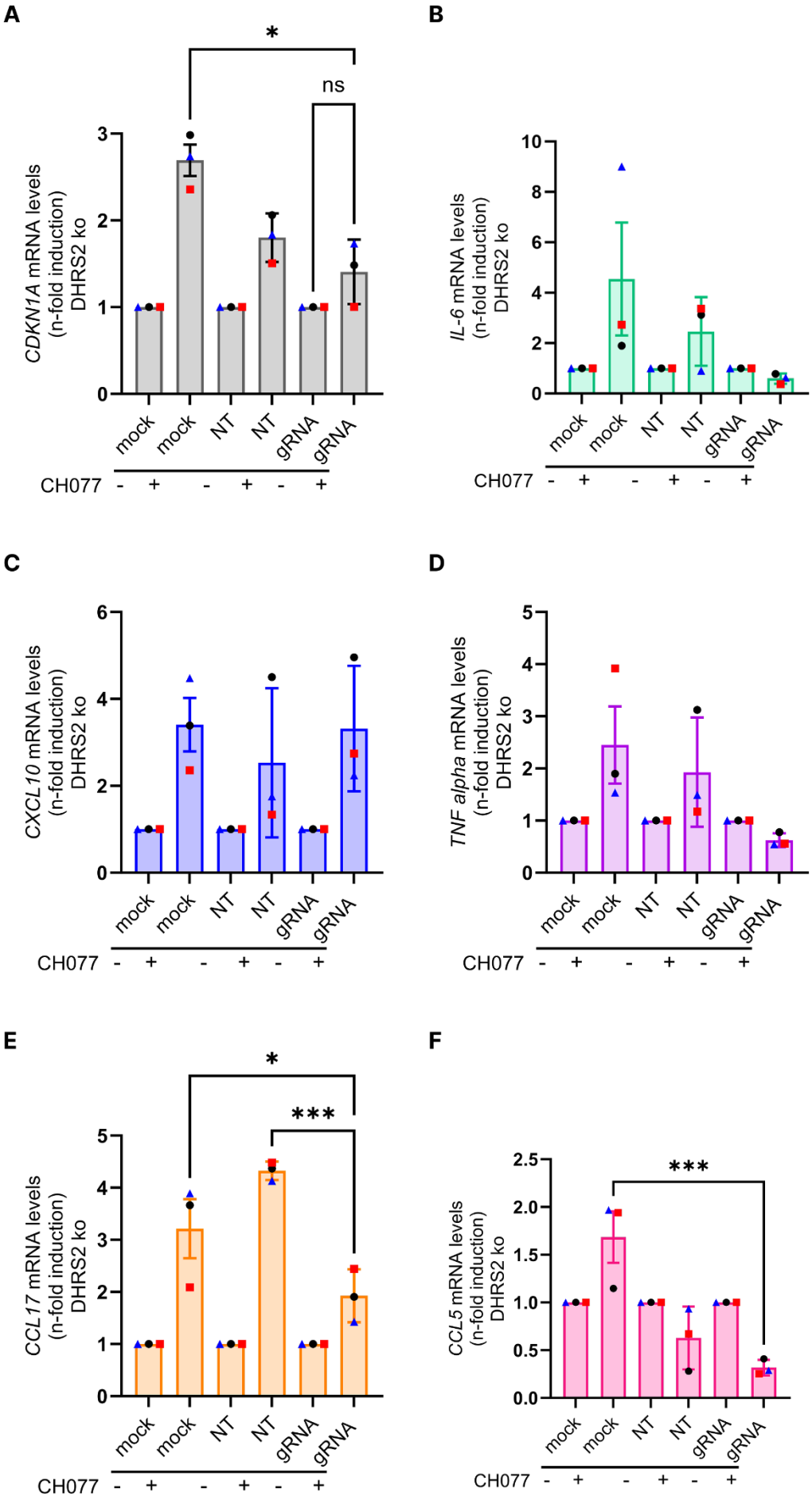
A
B
C
D
E
F
*
ns
***
CDKN1A mRNA levels (n-fold induction) DHRS2 ko
IL-6 mRNA levels (n-fold induction) DHRS2 ko
CXCL10 mRNA levels (n-fold induction) DHRS2 ko
TNF alpha mRNA levels (n-fold induction) DHRS2 ko
CCL17 mRNA levels (n-fold induction) DHRS2 ko
CCL5 mRNA levels (n-fold induction) DHRS2 ko
mock
NT
gRNA
CH077

Figure 4.11: DHRS2 is essential for HIV-1-induced senescence. (A–F) The samples analyzed in these panels are identical to those shown in (Figure 4.10)**.** $CD4^+$ T cells were transduced with either *DHRS2*-specific gRNA, non-targeting (NT) gRNA, or mock-treated, and subsequently infected with HIV-1 CH077 or mock-infected. (A) *CDKN1A* (p21) mRNA levels were measured by qPCR in three independent experiments and are shown relative to mock-infected controls. (B–E) mRNA levels of proinflammatory cytokines (B) *IL6*, (C) *TNF*, (D) *CXCL10,* (E) *CCL17* and (F) *CCL5* were quantified by qPCR in the same experimental setup. Expression values were normalized to the housekeeping gene *GAPDH*, and fold changes were calculated relative to mock-infected control cells. Data represent mean ± standard error of the mean (SEM) from three independent experiments. Statistical significance was determined using one-way ANOVA: (* $p < 0.05$, *** $p < 0.001$, ns: non-significant) compared to mock-infected controls.

4.7 Modest *DHRS2* induction via CRISPRa fails to significantly upregulate *CDKN1A* expression.

To determine whether DHRS2 is sufficient to induce senescence, we utilized the CRISPR/dCas9 gene activation technology [267] to upregulate *DHRS2* expression in primary $CD4^+$ T cells. The experimental setup is shown in Fig. 4.12A.

I first performed a multiple sequence alignment of all human LTR12D loci to identify unique regions within the LTR12D element upstream of *DHRS2* (human reference genome GRCh38/hg38, chromosome 14: 23,635,627–23,636,652). Based on predicted on-target and off-target scores, I selected four distinct guide RNAs (gRNAs 1-4) targeting this region. These gRNAs were designed to be located 300 to 600 bp upstream of the transcription start site (TSS) within the LTR12D element upstream of *DHRS2*. These gRNAs were synthesized and tested in various combinations (Fig. 4.12B).

$CD4^+$ T cells were transduced with lentiviral particles encoding both *DHRS2*-specific gRNAs and dCas9-VP64 [268] to enable targeted transcriptional activation of *DHRS2*. Cells transduced with a non-targeting gRNA served as negative controls. Puromycin was used for selection. Transduction efficiency was assessed by flow cytometry using a GFP-expressing lentiviral construct (pBob) as a control. Only $CD4^+$ T cells with transduction efficiencies above 35% were selected for further analysis (Fig. 4.12C). HIV-1-infected

$CD4^+$ T cells (strains STCO1 and CH077) served as positive controls in this experiment (Fig. 4.12C and 4.13B).

LTR12D_*DHRS2* transcript levels were measured following CRISPRa using guide RNA (gRNA) combinations 1+2, 1+3, 1+4, 2+3, and 1+2+3+4. Empty vector and non-targeting (NT) gRNA were used as negative controls (Fig. 4.13A). Notably, the gRNA combinations 1+2 and 1+2+3+4 resulted in a modest, approximately two-fold induction of LTR12D_*DHRS2* expression compared to the negative controls.

I also measured *CDKN1A* (p21) mRNA levels by qRT-PCR in the same samples. While the HIV-1-infected positive controls did cause a significant increase in *CDKN1A* expression (Fig. 4.13C, 4.13D), none of the gRNA combinations designed to upregulate *DHRS2* resulted in a significant increase in *CDKN1A* expression (Fig. 4.13B, 4.13D).

A

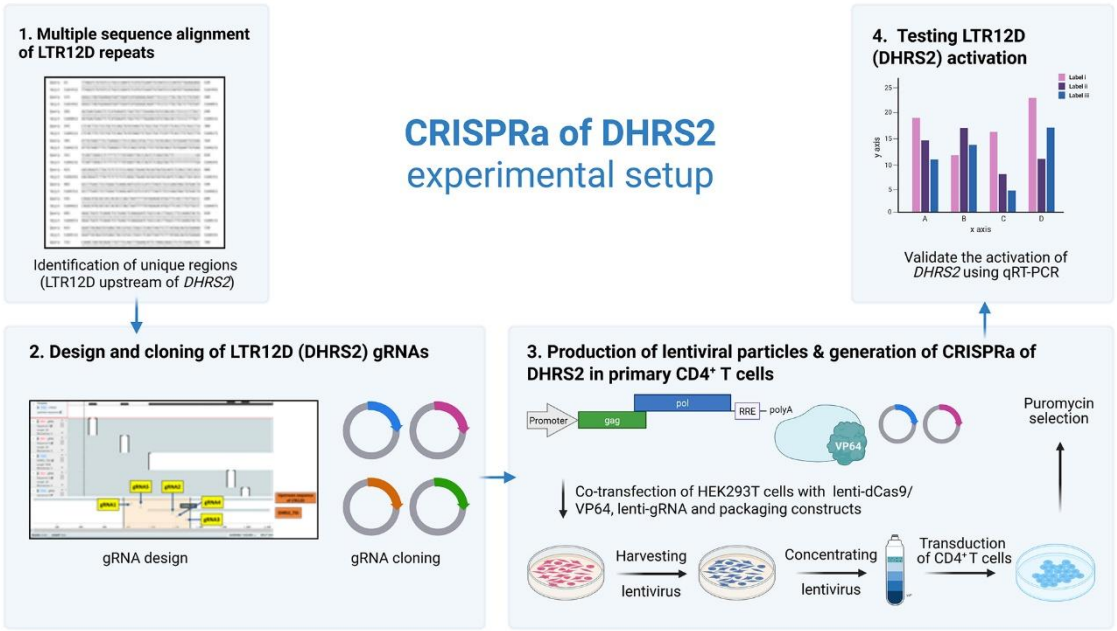
1. Multiple sequence alignment of LTR12D repeats
Identification of unique regions (LTR12D upstream of DHRS2)
CRISPRa of DHRS2
experimental setup
4. Testing LTR12D (DHRS2) activation
Validate the activation of DHRS2 using qRT-PCR
2. Design and cloning of LTR12D (DHRS2) gRNAs
gRNA design
gRNA cloning
3. Production of lentiviral particles & generation of CRISPRa of DHRS2 in primary CD4⁺ T cells
Promoter
gag
pol
RRE
polyA
VP64
Puromycin selection
Co-transfection of HEK293T cells with lenti-dCas9/ VP64, lenti-gRNA and packaging constructs
Harvesting
lentivirus
Concentrating
lentivirus
Transduction of CD4⁺ T cells

B

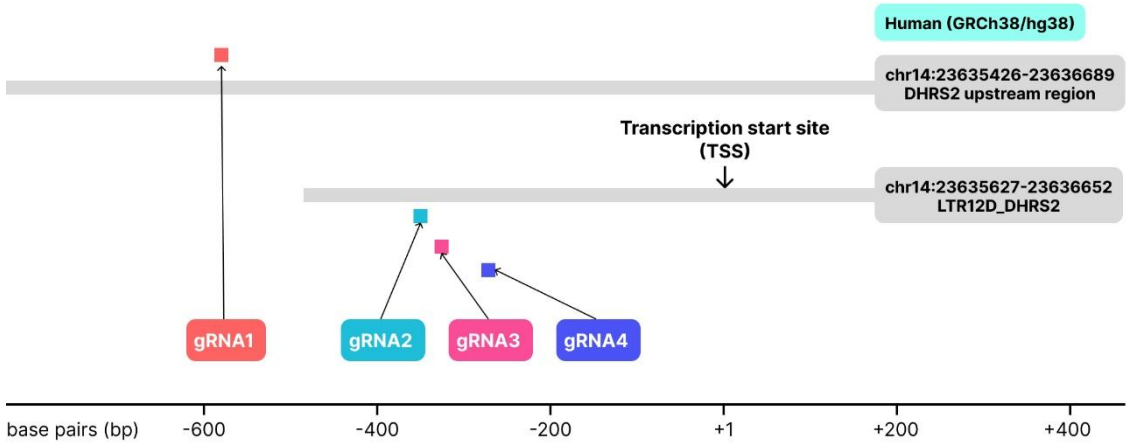
Human (GRCh38/hg38)
chr14:23635426-23636689
DHRS2 upstream region
Transcription start site (TSS)
chr14:23635627-23636652
LTR12D_DHRS2
gRNA1
gRNA2
gRNA3
gRNA4
base pairs (bp)
-600
-400
-200
+1
+200
+400

C

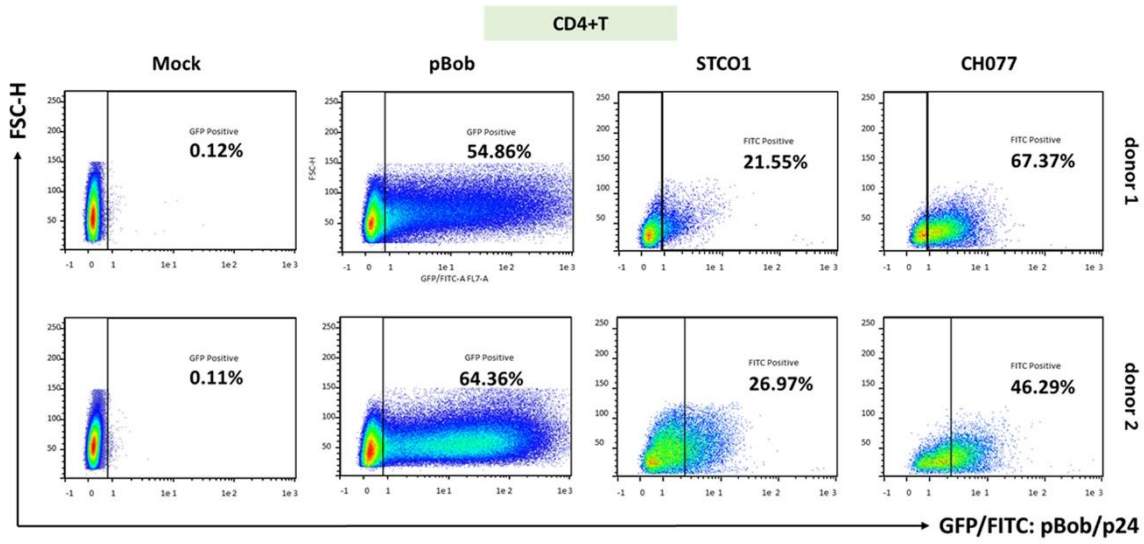
CD4+T
Mock
pBob
STCO1
CH077
FSC-H
GFP Positive
0.12%
54.86%
FITC Positive
21.55%
67.37%
donor 1
0.11%
64.36%
26.97%
46.29%
donor 2
GFP/FITC: pBob/p24

Figure 4.12: *DHRS2*-targeting guide RNA design and experimental setup. (A) Experimental setup of CRISPRa-mediated *DHRS2* induction: gRNAs specifically targeting *DHRS2* were designed and cloned into a pLKO.1 lentiviral vector. Five distinct gRNA pairs/combinations, namely gRNAs1+2, gRNAs1+3, gRNAs1+4, and gRNAs2+3, gRNAs1+2+3+4 were used. Lentiviral particles (LVPs) were produced, and primary human $CD4^+$ T cells were transduced. Transduced cells were selected by puromycin treatment. $CD4^+$ T cells with a transduction rate above 35% were further analyzed for LTR12D_*DHRS2* and *CDKN1A* mRNA levels using quantitative polymerase chain reaction (q-RTPCR). **(B)** Four guide RNAs, termed gRNA1, gRNA2, gRNA3, and gRNA4, were designed for the LTR12D locus located directly upstream of *DHRS2*. **(C)** A total of four donors were analyzed. The transduction rates for two donors, which exceeded 50%, are shown here. For the remaining two donors, transduction rates ranged between 35% and 50%, as determined by the use of pBob (a GFP-expressing lentiviral vector) as a transduction control. $CD4^+$ T cells infected with STCO1 and CH077 strains were used as positive controls, GFP negative: untransduced; shown on left side of the gating (100 - GFP+)%, GFP positive: transduced, FITC negative: uninfected; shown on left side of the gating (100 - FITC positive)%, FITC positive: HIV-1 p24-infected.

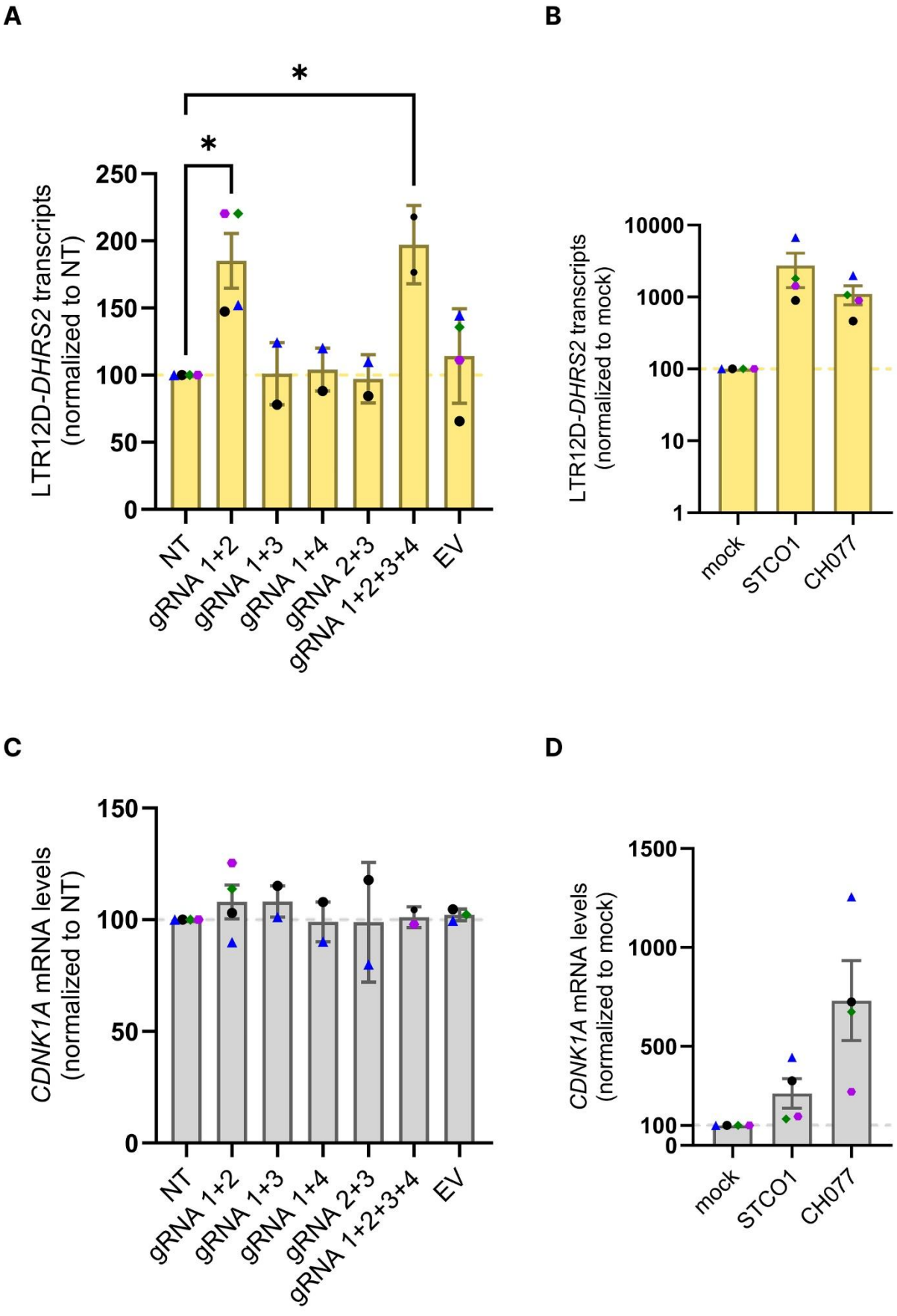
A
B
C
D
LTR12D-DHRS2 transcripts (normalized to NT)
LTR12D-DHRS2 transcripts (normalized to mock)
CDNK1A mRNA levels (normalized to NT)
CDNK1A mRNA levels (normalized to mock)
NT
gRNA 1+2
gRNA 1+3
gRNA 1+4
gRNA 2+3
gRNA 1+2+3+4
EV
mock
STCO1
CH077
*
*

Figure 4.13: gRNAs 1+2 and gRNAs 1+2+3+4 induce *DHSR2* and but not *CDKN1A*. Here, we tested whether CRISPRa-mediated induction of the *DHRS2* gene also results in the expression of *CDKN1A*. **(A-B)** qRT-PCR was used to measure and compare LTR12D_*DHRS2* transcript levels in (A) primary $CD4^+$ T cells transduced with gRNAs 1+2, 1+3, 1+4, 2+3, and 1+2+3+4 relative to empty vector and non-targeting (NT) gRNA controls, which served as negative controls, and (B) primary $CD4^+$ T cells infected with HIV-1 STCO1 and CH077, which served as positive controls. Data represent the means ± standard error of the mean (SEM) from two to four independent experiments (**Created with BioRender.com)**. **(C-D)** *CDKN1A* mRNA levels were assessed by qRT-PCR in the same experimental groups. Data represent the means ± standard error of the mean (SEM) from two to four independent experiments. Statistical significance was determined using one-way ANOVA (* $p < 0.05$), comparing targeting gRNA-transduced cells to non-targeting gRNA-transduced cells and mock controls.

4.8 HSF1 reduces LTR12D_*DHSR2* activity, and HIV-1 infection increases HSF1 protein levels.

To identify upstream regulators of *DHRS2* in the context of HIV-1 infection, we performed a comprehensive literature review and used the JASPAR database [269] to predict transcription factors with potential binding sites in the *DHRS2* promoter region. To validate and extend these predictions, we used the Cistrome database [270] for experimentally supported transcription factor binding events near the *DHRS2* locus. This analysis revealed binding of HSF1, LEF1, and TCF1 within the LTR12D element upstream of the *DHRS2* gene.

We began by focusing on HSF1 as a potential regulator of DHRS2 based on both computational predictions and prior biological evidence. Specifically, JASPAR analysis (Fig. 4.14A) identified a high-confidence HSF1 binding site within the LTR12D promoter upstream of *DHRS2*, with a relative binding score of ~78%. This prediction was further supported by experimental data from the Cistrome database (Fig. 4.14B), which confirmed HSF1 binding at this region. Additionally, prior work by Oda *et al*. [220] showed that HSF1 depletion in human diploid fibroblasts led to increased *DHRS2* expression and activation of the MDM2-p53-p21 pathway, ultimately driving cellular senescence. Taken together, the combination of strong computational predictions, existing experimental support, and biological relevance provided a clear rationale to

prioritize HSF1 as our starting point for detailed investigation into its potential direct regulatory role on *DHRS2*.

To validate our hypothesis that HSF1 directly regulates *DHRS2* expression through the LTR12D promoter, I performed overexpression experiments using an LTR12D luciferase reporter assay in conjunction with western blot analysis. Titration experiments revealed that HSF1 negatively regulates LTR12D_*DHRS2* activity in a dose-dependent manner (Fig. 4.14C). These findings provide strong evidence that HSF1 serves as a regulatory factor capable of suppressing *DHRS2* expression, potentially influencing cellular responses in HIV-1-infected cells.

To further investigate the role of HSF1 in HIV-1-infected cells, we infected primary $CD4^+$ T cells with T-tropic HIV-1 STCO1 and CH077 (Fig. 4.15A, 4.15C), while macrophages were infected with the M-tropic strains AD8 and YU2 (Fig. 4.15B, 4.15D). Infection rates were assessed by flow cytometry, measuring the percentage of p24-positive cells among primary $CD4^+$ T cells and monocyte-derived macrophages infected with HIV-1 strains. We observed a similar elevation in total HSF1 protein levels in both primary $CD4^+$ T cells and macrophages following infection (Fig. 4.16A, 4.16B). However, the activation of HSF1 is not solely dependent on its total protein levels. Instead, it is influenced by multiple factors, including its oligomeric state (trimeric or monomeric) [9], its subcellular localization (cytoplasm versus nucleus), and its phosphorylation status at key regulatory sites such as serine 230, 320, and 326 [271, 272] or serine 303 and 307. Among these, phosphorylation at serine 303/307 is particularly significant, as it is associated with HSF1 inactivation [273, 274]. When phosphorylated at these sites, HSF1 loses its transcriptional activity, highlighting the importance of post-translational modifications in its regulation.

To assess the impact of HIV-1 infection on HSF1 activation, I therefore measured the protein levels of HSF1 phosphorylated at serine 303/307 in HIV-1-infected $CD4^+$ T cells and compared them with mock-infected controls using flow cytometry. I observed an increase in the levels of HSF1 phosphorylated at serine 303/307 following HIV-1 infection (Fig. 4.16C). Next, I analyzed the ratio of serine 303/307 phosphorylated HSF1 to total HSF1 in $CD4^+$ T cells. I observed a consistent percentage of serine 303/307-phosphorylated (i.e., inactive) HSF1 in HIV-1-infected cells, similar to the levels observed in mock-infected controls (Fig. 4.16D). This suggests that while HIV-1 infection leads to

an overall increase in HSF1 protein levels, it does not significantly alter the relative ratio of HSF1 phosphorylated at serine 303/307 to total HSF1.

A

Predicted binding sites	Relative score
TTGGAGAACTTTT	0.7829688572812381 +
CTGCTAGCATATTGT	0.7739208341230702 –
TGCTAGCATATTG	0.7517185355327529 –
GCTGTGGAAGCTTTG	0.731167518037803 +
CTTGGAGAACTTTTG	0.7213268940488311 –
CTTCATGATAAATCT	0.7152161006994088 +

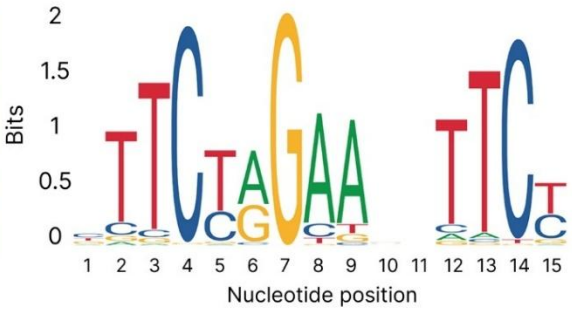

B

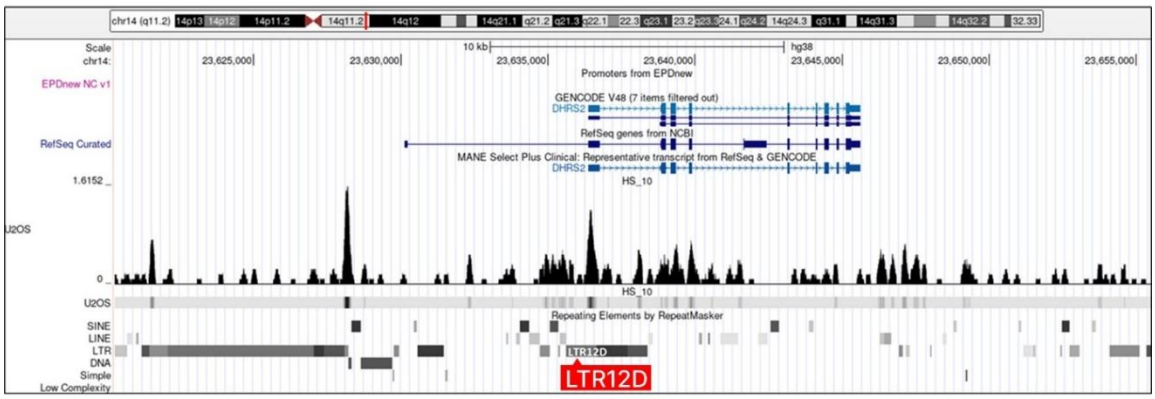

C

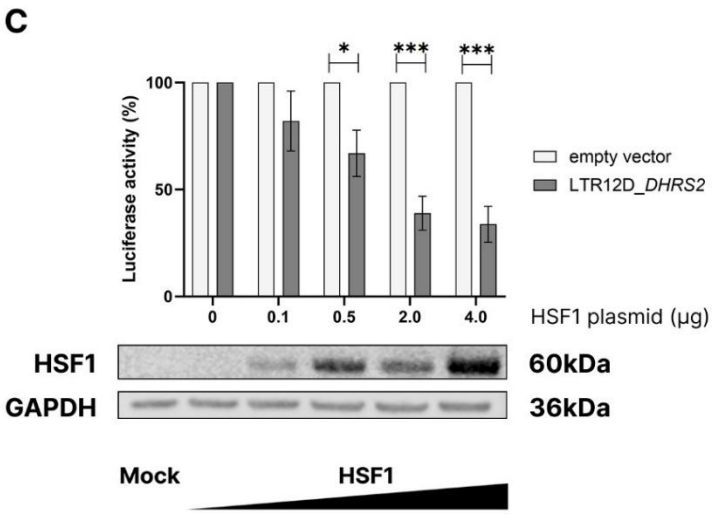

Figure 4.14: HSF1 reduces LTR12D_*DHSR2* activity. (A) On the left-hand side, a table presents the top six predicted Heat Shock Factor 1 (HSF1) binding sites within the LTR12D promoter region, identified using the JASPAR database, with relative binding scores of 70% or above and a maximum of 78%. On the right-hand side, the sequence logo (JASPAR Matrix ID: MA0486.1) illustrates the frequency matrix for the human HSF1

transcription factor, where the height of each nucleotide within a stack is proportional to its frequency, and the overall stack height indicates sequence conservation at that position. **(B)** The Cistrome database revealed an experimentally validated HSF1 binding site within the LTR12D promoter upstream of *DHRS2* in U2OS bone cells, suggesting a potential regulatory interaction. **(C)** HEK293T cells were co-transfected with increasing amounts of an expression plasmid for HSF1, along with an empty vector and LTR12D_*DHRS2 Gaussia* luciferase constructs. 24 hours post-transfection, *Gaussia* luciferase activity was measured. A pTAL-Firefly luciferase construct was used for normalization. HEK293T cells were transfected with titrated amounts of the HSF1 plasmid and analyzed via Western blotting. GAPDH served as a loading control. Mean values ± SEM (standard error of the mean) derived from four independent experiments are shown on top. One exemplary Western blot is shown at the bottom. Statistical significance was determined using one-way ANOVA: (* $p < 0.05$, *** $p < 0.001$).

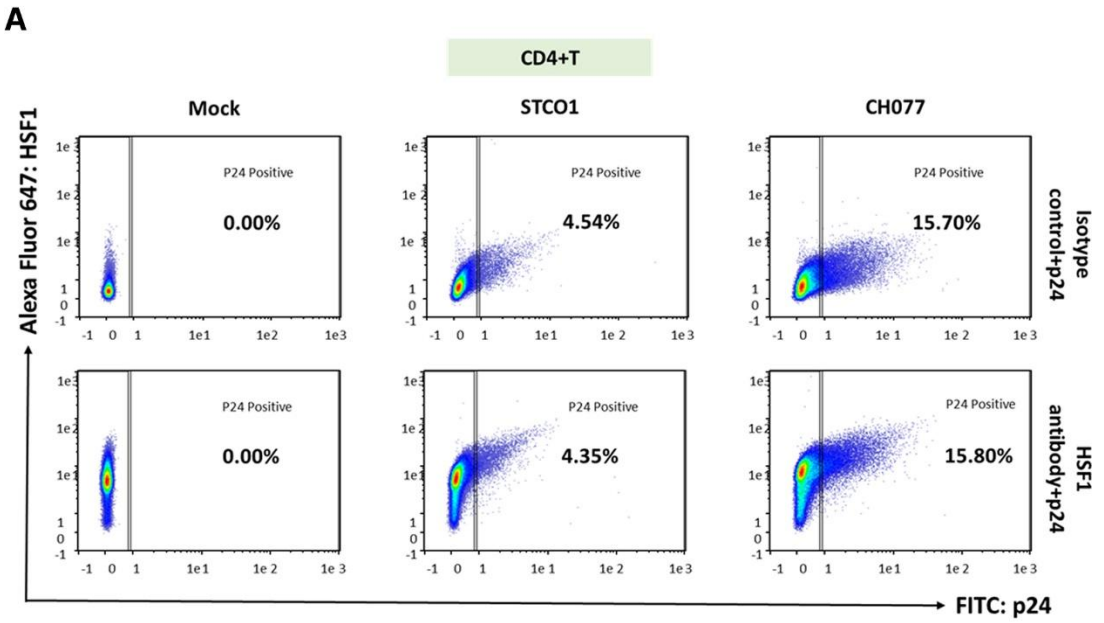
A
CD4+T
Mock
STCO1
CH077
Alexa Fluor 647: HSF1
P24 Positive
0.00%
4.54%
15.70%
Isotype control+p24
0.00%
4.35%
15.80%
HSF1 antibody+p24
FITC: p24

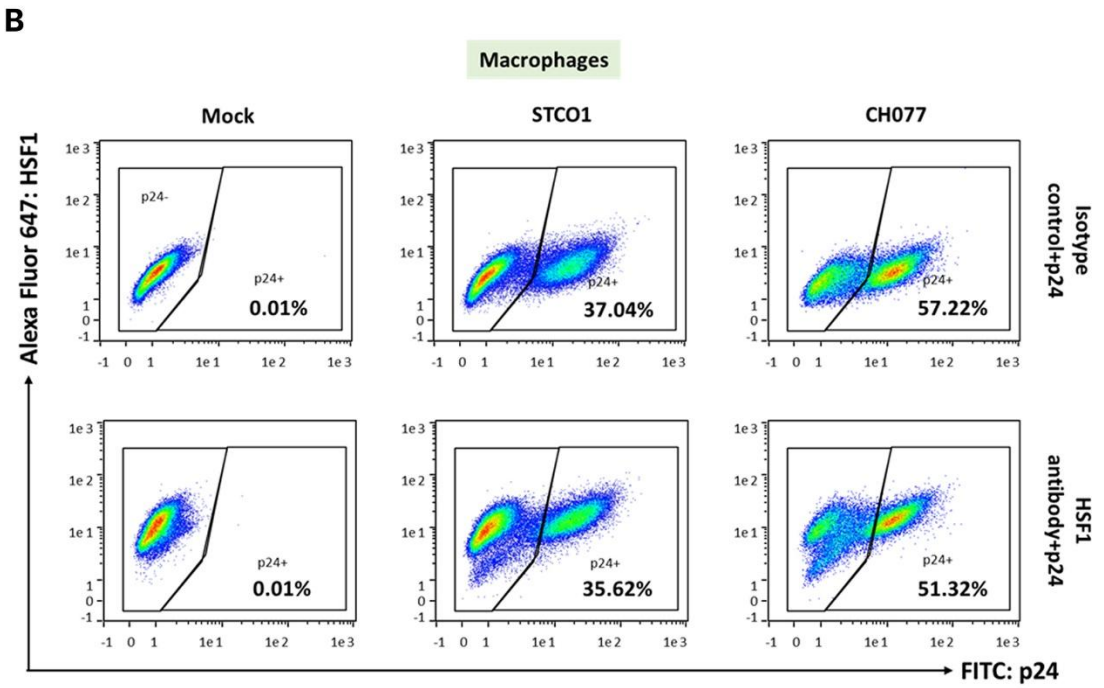
B
Macrophages
Mock
STCO1
CH077
Alexa Fluor 647: HSF1
p24-
p24+
0.01%
37.04%
57.22%
Isotype control+p24
0.01%
35.62%
51.32%
HSF1 antibody+p24
FITC: p24

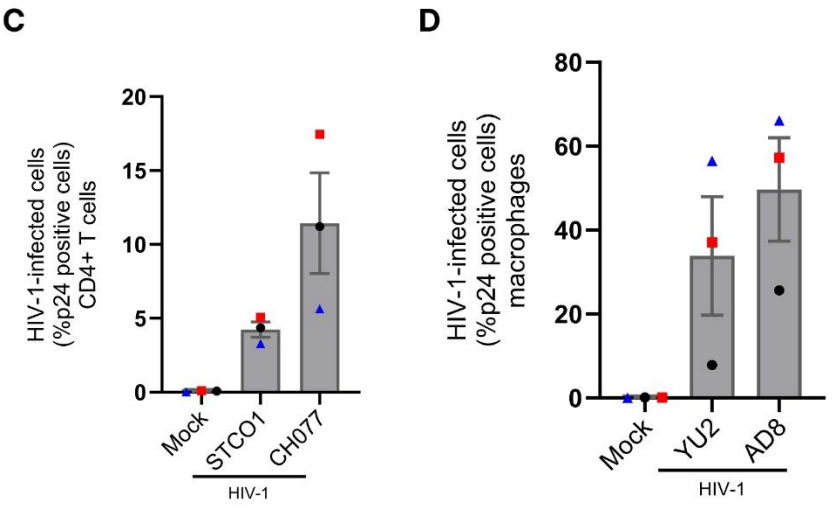
C
HIV-1-infected cells (%p24 positive cells) CD4+ T cells
Mock
STCO1
CH077
HIV-1
D
HIV-1-infected cells (%p24 positive cells) macrophages
Mock
YU2
AD8
HIV-1

Figure 4.15: HIV-1 infection rates of primary CD4⁺ T cells and monocyte-derived macrophages. (A-B) Representative primary FACS plots showing both HSF1 and p24 staining of (A) CD4⁺ T cells and (B) monocyte-derived macrophages. **(C-D)** Quantification of p24-positive cells in (C) primary CD4⁺ T cells and (D) monocyte-derived macrophages infected with the indicated HIV-1 strains. P24-: uninfected; shown on left side of the gating (100 – p24+)%, p24+: HIV-1-infected.

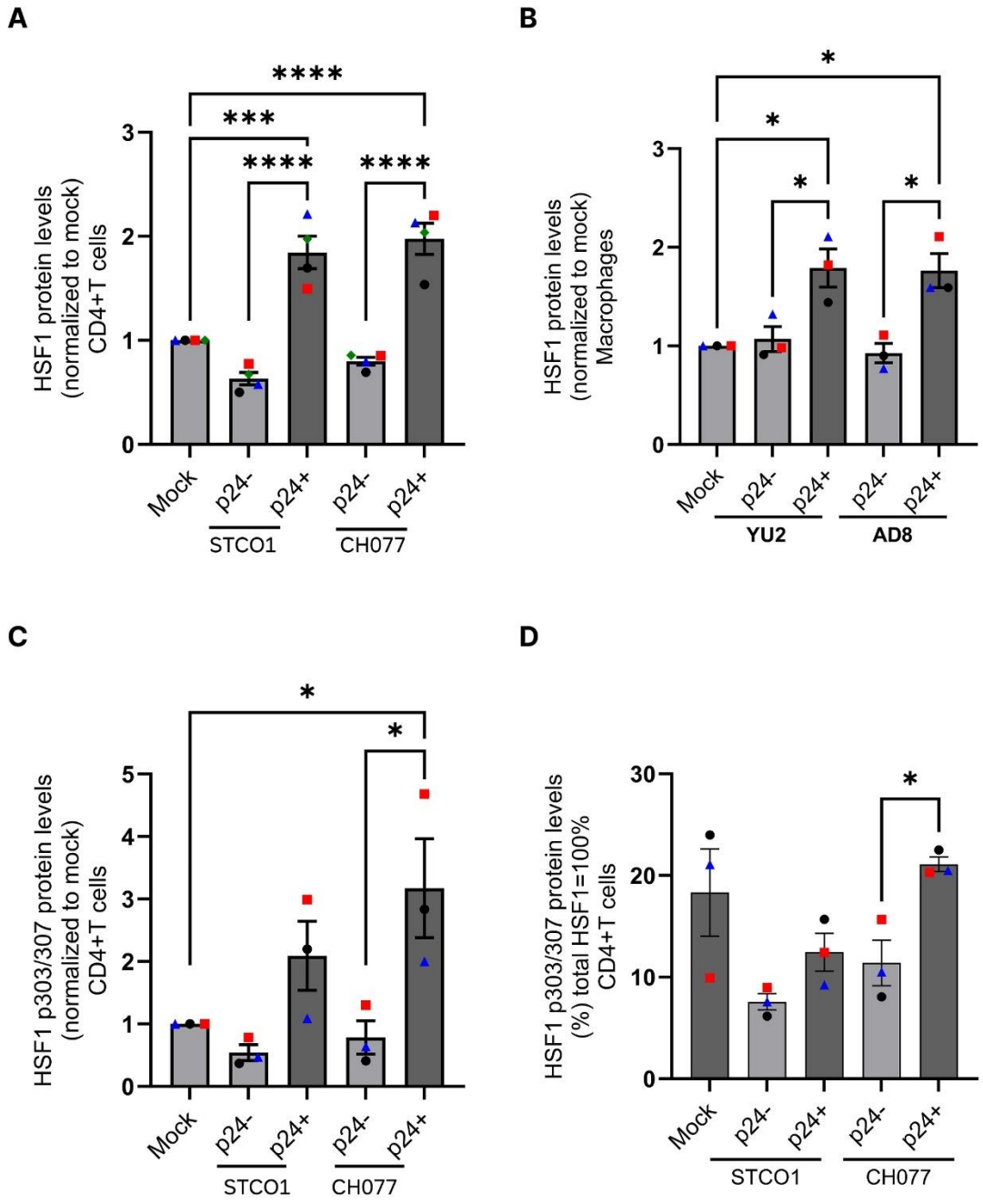

Figure 4.16: HIV-1 increases HSF1 protein levels in both CD4⁺ T cells and macrophages. (A) and **(B)** show HSF1 protein levels (normalized to mock) in the HIV-1-infected CD4⁺ T

cells (STCO1, CH077) and macrophages (YU2, AD8) shown in Fig. 4.15, respectively. **(C)** Phosphorylation of HSF1 at serine 303/307 (normalized to mock) was assessed in $CD4^+$ T cells infected with HIV-1 STCO1 or CH077 using flow cytometry. **(D)** The ratio of phosphorylated HSF1 (serine 303/307) to total HSF1 was calculated to determine its relative activation status. Mean values ± standard error of the mean (SEM) from three to four independent experiments are shown. Statistical significance was determined using one-way ANOVA: (* $p < 0.05$, *** $p < 0.001$, **** $p < 0.0001$), comparing HIV-1-infected cells to mock controls; p303/307- serine phosphorylated at positions 303 and 307.

4.9 LEF1, TCF1, and β-catenin inhibit the LTR12D promoter of *DHRS2*.

After analyzing HSF1 as a potential regulator of LTR12D_*DHRS2*, we next focused on LEF1 and TCF1, which were also identified as candidate transcription factors from the JASPAR database [269]. Using both the JASPAR and HOCOMOCO tools [269, 275], we confirmed predicted binding sites for LEF1 and TCF1 within the LTR12D promoter region upstream of the *DHRS2* gene (Fig. 4.17A, 4.17B). Moreover, analysis of ChIP-seq data from the Cistrome database [270] provided experimental evidence for TCF1 binding to the LTR12D promoter of *DHRS2* (Fig. 4.17C). These findings support a regulatory role for LEF1 and TCF1 in modulating *DHRS2* expression through the LTR12D element.

To validate the regulatory roles of LEF1 and TCF1, we performed LTR12D luciferase reporter assays similar to those conducted for HSF1. Briefly, HEK293T cells were co-transfected with increasing amounts of LEF1 or TCF1 expression plasmids together with the LTR12D_*DHRS2* luciferase construct. Western blot analysis confirmed the efficient overexpression and titration of LEF1 and TCF1 proteins (Fig. 4.17D). I observed a dose-dependent decrease in LTR12D_*DHRS2* activity upon overexpression of LEF1 and TCF1.

LEF1 and TCF1 are transcription factors that function downstream of the Wnt/β-catenin signaling pathway [276]. In the absence of Wnt signaling, LEF1 and TCF1 primarily act as transcriptional repressors [277], whereas in the presence of Wnt, stabilized β-catenin translocates to the nucleus and converts LEF1/TCF1 into transcriptional activators [278]. Based on this, we hypothesized that HIV-1 activates the Wnt/β-catenin pathway [279], leading to LEF1 and TCF1-mediated transcriptional activation of the *DHRS2* gene, which

subsequently triggers downstream events culminating in cellular senescence. To test whether the Wnt/β-catenin pathway is activated during HIV-1 infection, primary $CD4^+$ T cells were infected with HIV-1 clones STCO1 and CH077. Infection rates were assessed by flow cytometry measuring the percentage of p24-positive cells (Fig. 4.18A, 4.18B), and β-catenin protein levels in these infected cells were also measured by flow cytometry (Fig. 4.18C). I observed a significant increase in total β-catenin protein levels in HIV-1-infected cells compared to mock-infected controls.

To assess the effect of β-catenin on LTR12D activity, we performed a luciferase reporter assay using the LTR12D_*DHRS2* construct with increasing amounts of β-catenin expression plasmid. Similar to LEF1 and TCF1, β-catenin overexpression resulted in a dose-dependent decrease in LTR12D_*DHRS2* promoter activity. The combined data demonstrate that LEF1, TCF1, and β-catenin each suppress LTR12D_*DHRS2*-driven transcription in a dose-dependent manner (Fig. 4.18D).

A

Predicted binding sites (LEF1)	Relative score/strand
AAAGAACAAAGCTTC	0.83725804 -
GAAGACCAAAAGAAC	0.7920094 -

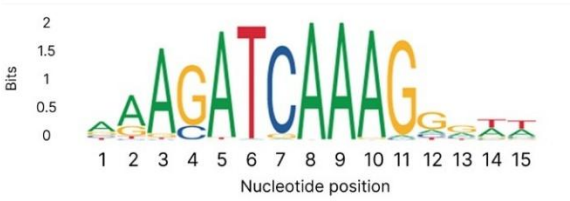

B

Predicted binding sites (TCF1)	Relative score/strand
CTTTTAT	0.8876331 -
CTTTGTT	0.8646873 +
AGCTTTGTTCT	0.8523545 +
AAAGAACAAAGC	0.8502704 -
TGCTTTTATTC	0.82858145 -
CTTTAAG	0.8042876 +

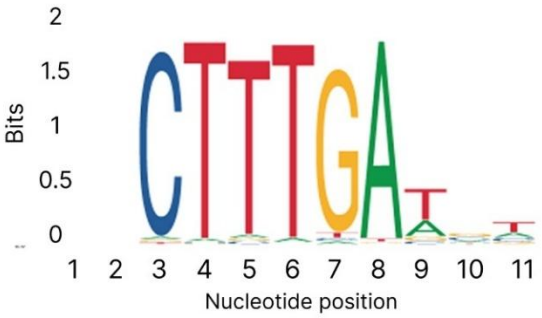

C

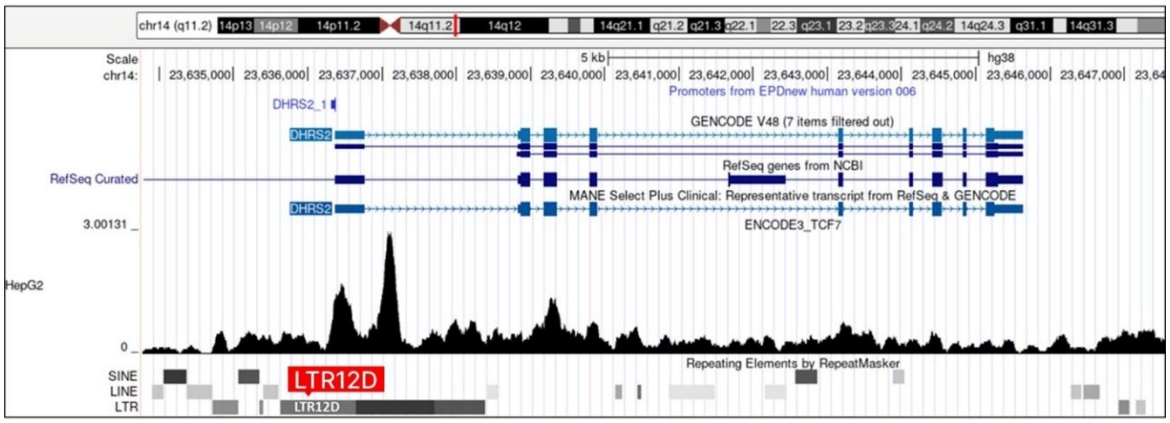

D

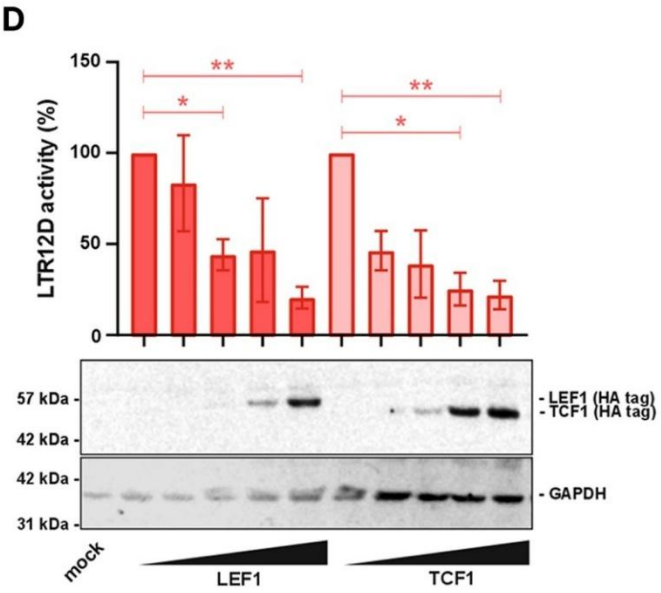

Figure 4.17: LEF1 and TCF1 suppress LTR12D_*DHRS2* promoter activity. (A-B) The left-hand side of the figure presents predicted binding sites for LEF1 and TCF1 within the LTR12D promoter region, identified using the JASPAR database. This includes (A) the top two LEF1 sites (with relative binding scores ≥79%, reaching a maximum of 84%) and (B) the top six TCF1 sites (with relative binding scores ≥79%, reaching a maximum of 89%). On the right-hand side, two sequence logos illustrate the frequency matrices for these human transcription factors. (A) The sequence logo for LEF1 (JASPAR Matrix ID: MA0768.1) and (B) the sequence logo for TCF1 (JASPAR Matrix ID: MA0769.2) are shown. In both logos, the height of each nucleotide within a stack is proportional to its frequency, and the overall height of the stack indicates sequence conservation. **(C)** ChIP-seq data from the Cistrome database revealed an experimentally validated TCF1 binding site within the LTR12D promoter upstream of *DHRS2* in HepG2 cells, indicating potential transcriptional regulation. **(D)** HEK293T cells were co-transfected with increasing amounts of LEF1 or TCF1 expression plasmids, an empty vector control, and the LTR12D_*DHRS2 Gaussia* luciferase reporter construct. Luciferase activity was measured 24 hours post-transfection and normalized to pTAL-Firefly luciferase. (D) The experiment was performed by our technician, Ms. Isabell Haußmann, at Tübingen University. Data represent mean values ± SEM from three independent experiments. Western blot analysis confirmed dose-dependent overexpression of LEF1 and TCF1, with GAPDH as the loading control. Statistical significance was determined using one-way ANOVA (* $p < 0.05$, ** $p < 0.01$).

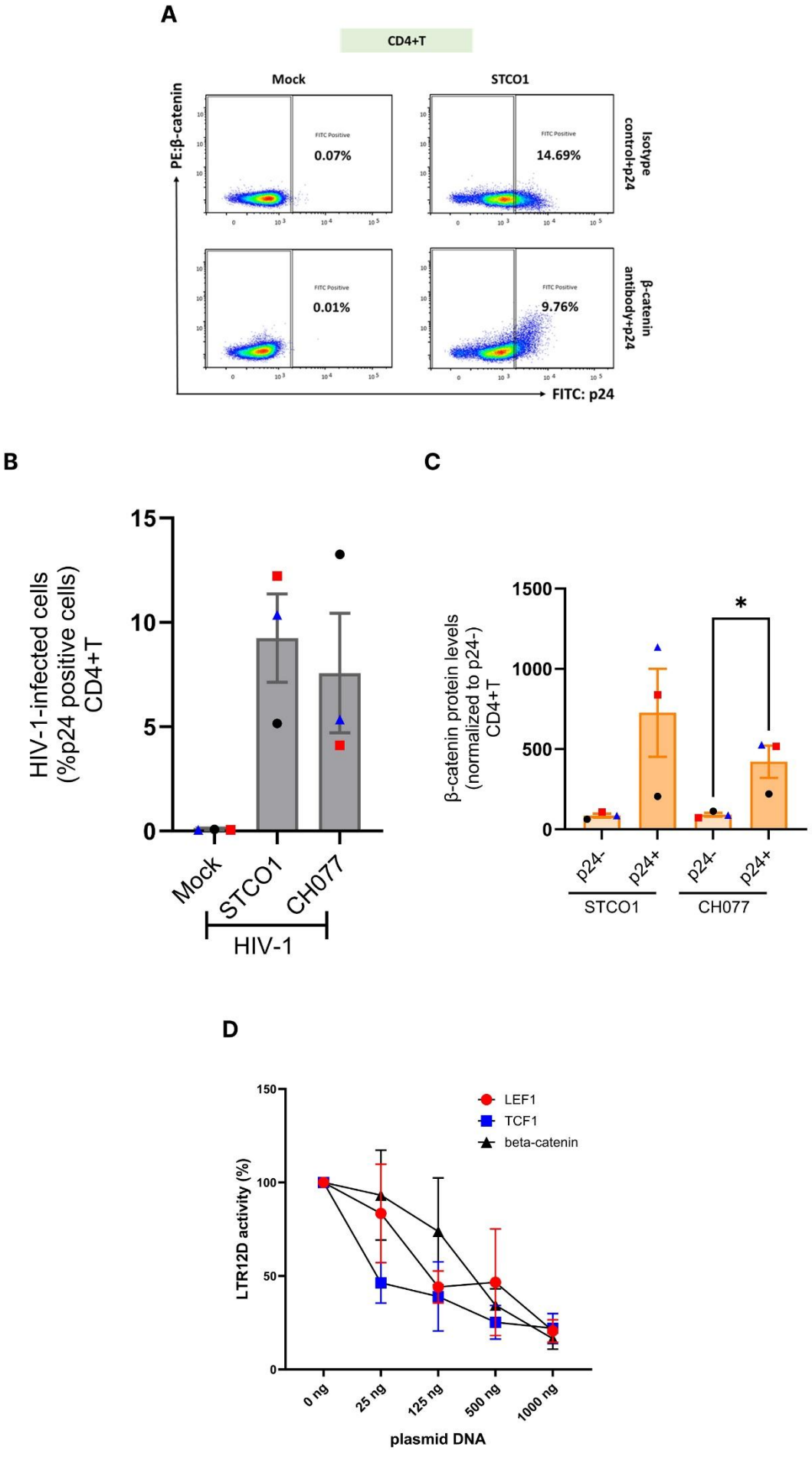
A
CD4+T
Mock
STCO1
PE:β-catenin
FITC Positive
0.07%
14.69%
0.01%
9.76%
Isotype control+p24
β-catenin antibody+p24
FITC: p24
B
HIV-1-infected cells (%p24 positive cells) CD4+T
15
10
5
0
Mock
STCO1
CH077
HIV-1
C
β-catenin protein levels (normalized to p24-) CD4+T
1500
1000
500
0
*
p24-
p24+
p24-
p24+
STCO1
CH077
D
LTR12D activity (%)
150
100
50
0
LEF1
TCF1
beta-catenin
0 ng
25 ng
125 ng
500 ng
1000 ng
plasmid DNA

Figure 4.18: LEF1, TCF1, and β-catenin suppress LTR12D_*DHRS2* activity, and HIV-1 infection increases β-catenin levels. (A–B) Flow cytometry analysis showing infection rates in primary $CD4^+$ T cells infected with HIV-1 strain/s STCO1, (B) CH077 indicated by the percentage of p24-positive cells. **(C)** β-catenin protein levels measured by flow cytometry in $CD4^+$ T cells following infection with STCO1 and CH077. **(D)** HEK293T cells were co-transfected with increasing amounts of LEF1, TCF1, or β-catenin expression plasmids and the LTR12D_*DHRS2 Gaussia* luciferase reporter. Luciferase activity was measured 24 hours post-transfection. Data represent mean ± SEM from three independent experiments. Statistical significance was determined using one-way ANOVA (* $p < 0.05$). p24-: uninfected; shown on left side of the gating (100 – p24+) %, p24+: HIV-1-infected.

4.10 Stressors that cause cellular damage trigger the LTR12D_*DHRS2* senescence pathway.

To determine whether the LTR12D_*DHRS2* senescence cascade is a general feature of stress-induced senescence [280] or specific to HIV infection, I investigated its activation across diverse senescence models. Since different stressors such as oxidative stress, mitochondrial dysfunction, endoplasmic reticulum (ER) stress, oncogene activation, or syncytia formation trigger distinct senescence pathways, examining this cascade in multiple contexts will help identify common and unique mechanisms driving senescence [281, 282].

To investigate LTR12D_*DHRS2* activation across diverse senescence models, I used multiple stress inducers and cell types. $CD4^+$ T cells were treated with H_2O_2 [283], staurosporine [284], thapsigargin [285], and Nutlin-3a [286] to induce oxidative stress, mitochondrial stress, ER stress, and p53-mediated senescence, respectively (Fig. 4.19A). Oncogene-mediated senescence was triggered in primary fibroblasts by expressing $hRas^{G12V}$, a constitutively active Ras mutant [209]. To create a control for true oncogene-mediated senescence, primary BJ fibroblasts were first immortalized with hTERT and then transduced with $hRas^{G12V}$, resulting in a transient growth delay [209]. For fusion-induced senescence, I used BeWo cells, a human placental trophoblast-derived cell line, and treated them with forskolin, a cAMP activator known to promote syncytium formation [287]. Additionally, primary placental cytotrophoblast cells were allowed to naturally differentiate into syncytiotrophoblasts, the multinucleated placental cells associated with fusion-induced senescence [215] (Fig. 4.19B). These models were

selected to determine whether LTR12D_*DHRS2* activation is a common feature of senescence or specific to certain stress conditions.

Senescence markers such as p21/*CDKN1A* (Fig. 4.20A-G) and the activation of the endogenous retroviral LTR12D promoter driving *DHRS2* expression (Fig. 4.21A-F) were measured by qRT-PCR. Treatment with H_2O_2, staurosporine, and thapsigargin resulted in the induction of both LTR12D_*DHRS2* transcripts and p21/*CDKN1A* expression. This indicates a positive correlation between these stress-inducing agents and the upregulation of both LTR12D_*DHRS2* and the cell cycle inhibitor p21/*CDKN1A*. In contrast, when senescence was induced via oncogenic signaling or syncytia formation, the expression of LTR12D_*DHRS2* was observed to be downregulated. Notably, p21/*CDKN1A* expression was not upregulated in either primary trophoblast cells or primary fibroblasts under these specific syncytia-induced or oncogene-induced conditions, respectively.

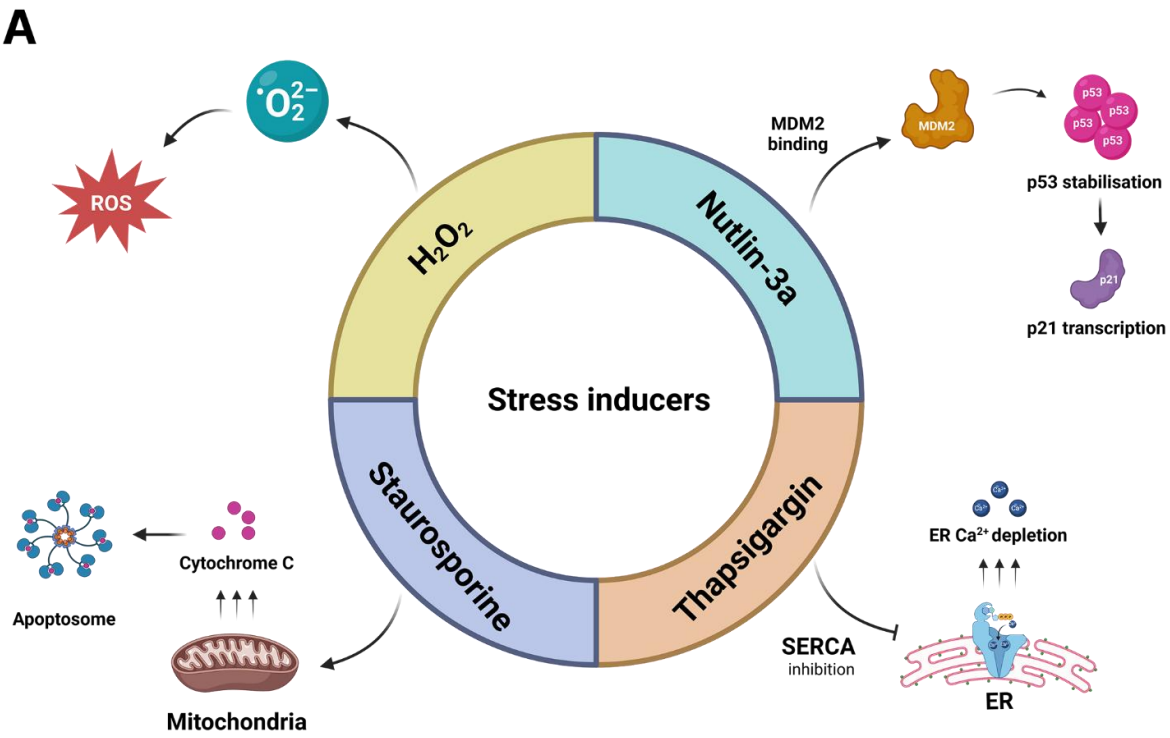
A
O_2^{2-}
ROS
H_2O_2
Nutlin-3a
MDM2 binding
MDM2
p53
p53
p53
p53
p53 stabilisation
p21
p21 transcription
Stress inducers
Staurosporine
Thapsigargin
Cytochrome C
Apoptosome
Mitochondria
ER Ca^{2+} depletion
SERCA inhibition
ER

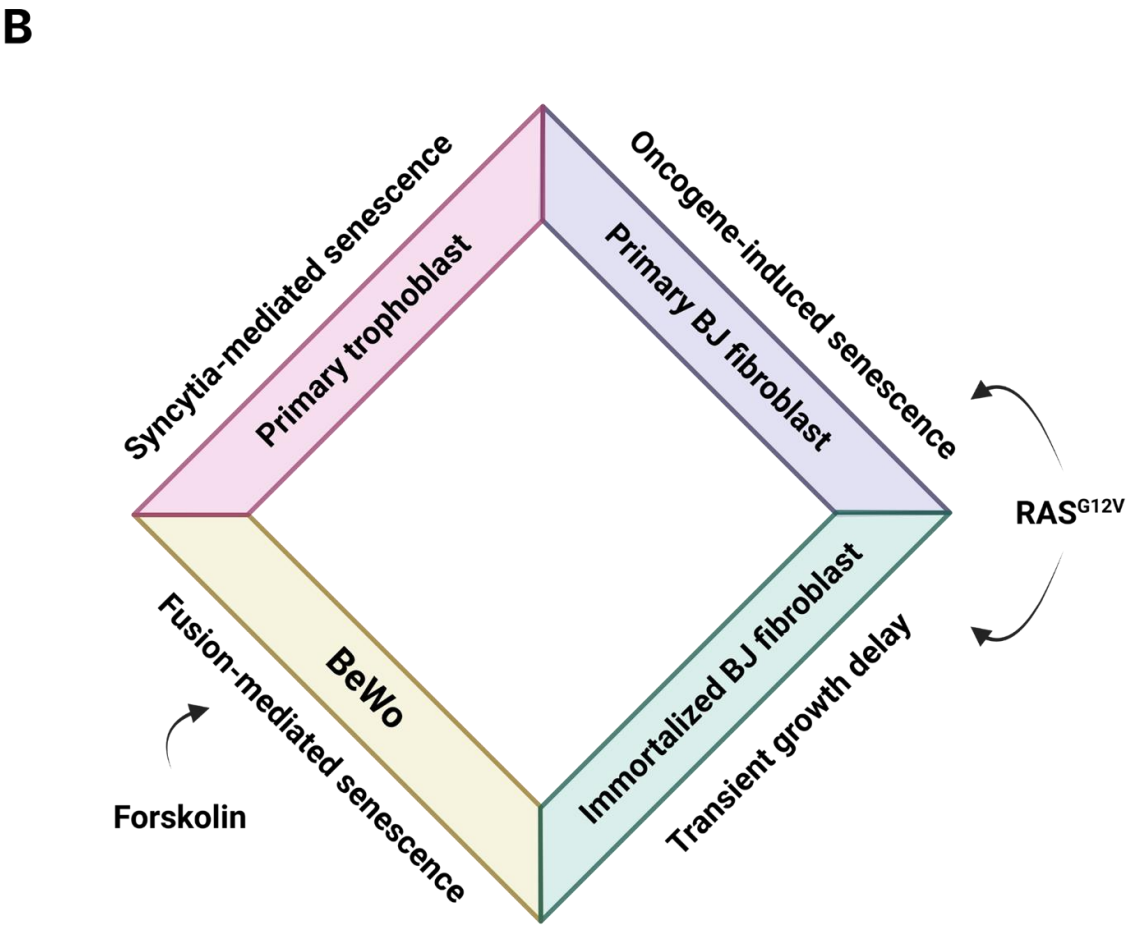
B
Syncytia-mediated senescence
Primary trophoblast
Oncogene-induced senescence
Primary BJ fibroblast
RAS^{G12V}
Fusion-mediated senescence
BeWo
Immortalized BJ fibroblast
Transient growth delay
Forskolin

Figure 4.19: Induction of different types of senescence by various stimuli. (A-B) The schematic diagrams illustrate the induction of transient growth delay or stable senescence in different cell types using various stimuli.

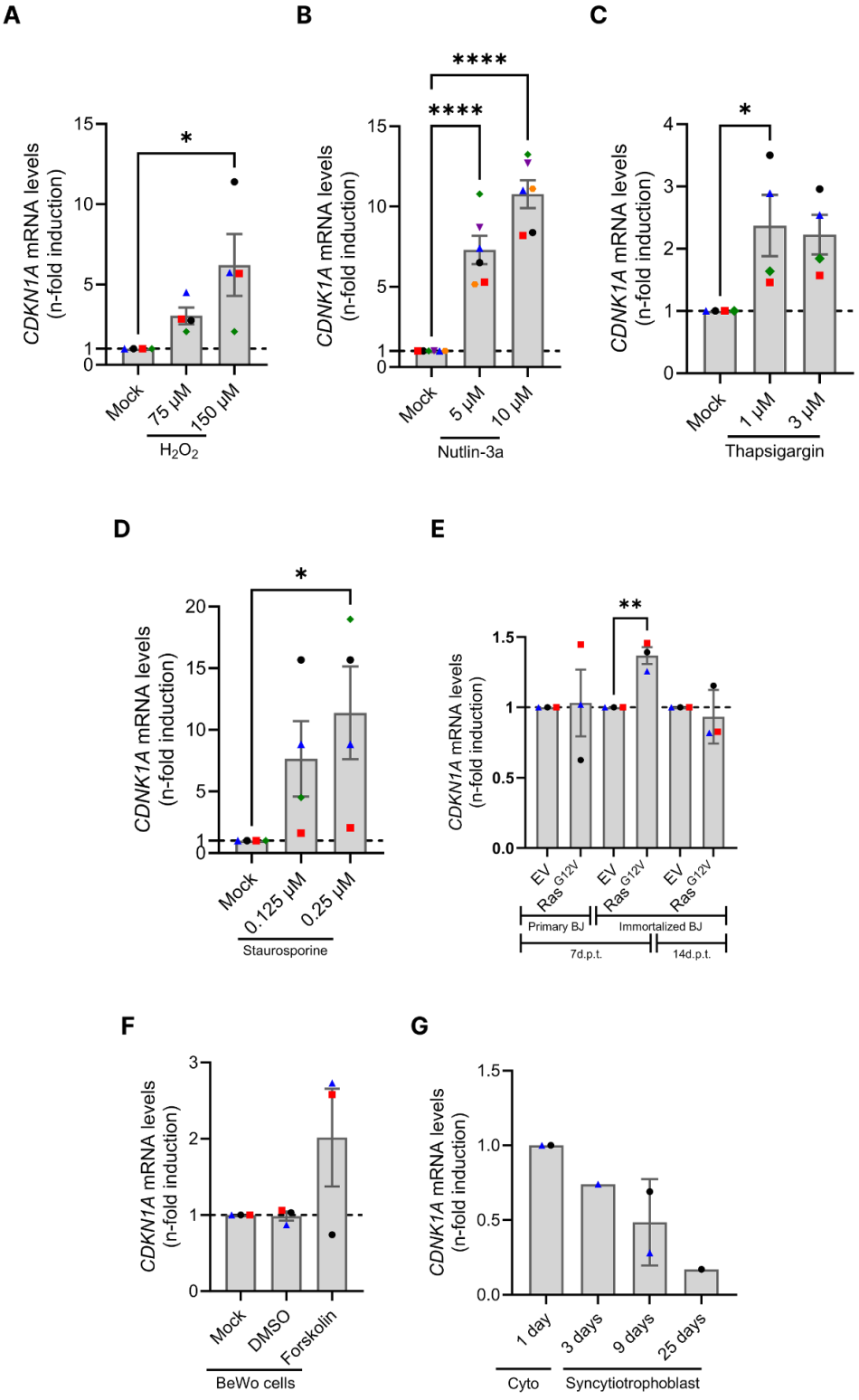

Figure 4.20: Differential induction of *CDKN1A* in transient growth delay/fully senescent cells. *CDKN1A* mRNA levels were quantified by qPCR in **(A-D)** primary $CD4^+$ T cells treated with various chemical stress inducers, **(E)** immortalized and primary BJ fibroblasts transduced with $hRas^{G12V}$, **(F)** BeWo cells treated with forskolin to induce senescence, and **(G)** primary human cytotrophoblasts undergoing natural differentiation into syncytiotrophoblasts over time. $CD4^+$ T cells and BeWo cells were harvested 2 days post-treatment, while BJ fibroblasts were collected at 7- and 14-days post-transduction (d.p.t.). Primary human cytotrophoblasts were cultured and harvested at 1-, 3-, 9-, and 25-days post-initiation of differentiation. **(E)** The transduction experiments in immortalized and primary BJ fibroblasts were performed by Mr. Gregoire Najjar at Ulm University. **(F-G)** The BeWo cells and primary human cytotrophoblasts were cultured by Ph.D. student Ms. Yueshuang Lu in our lab at Tübingen University. Data represent means ± SEM from 1 to 6 independent experiments. Statistical significance was determined using one-way ANOVA (* $p < 0.05$, ** $p < 0.01$, ****$p < 0.0001$) compared to DMSO, EV, mock-treated controls. (EV: empty vector, d.p.t.: days post-transduction, Cyto: cytotrophoblast)

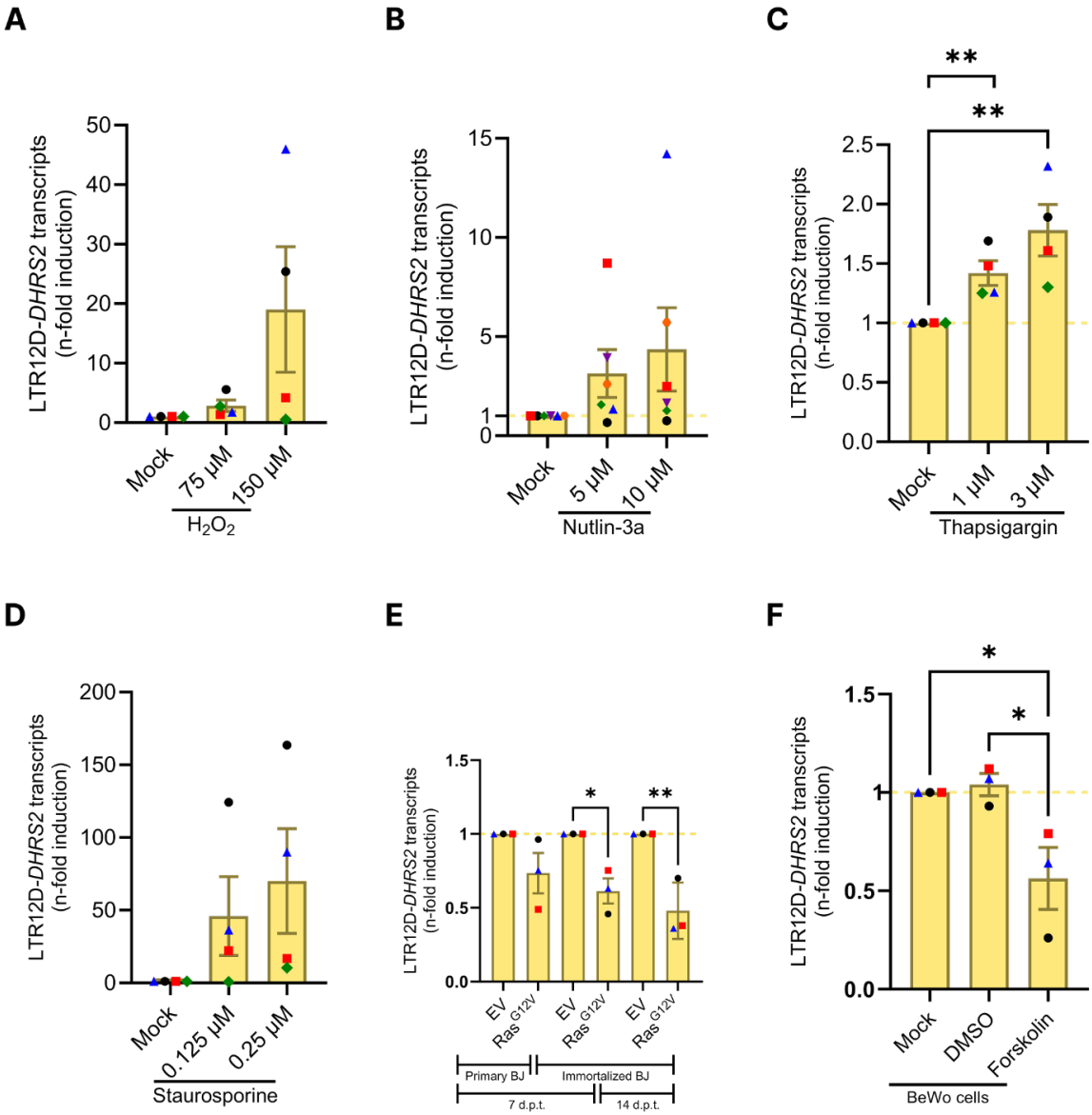

Figure 4.21: Differential induction of LTR12D_*DHRS2* transcription in transient growth delay/fully senescent cells. LTR12D_*DHRS2* transcript levels were assessed by qRT-PCR across various cell types undergoing different forms of senescence: **(A-D)** primary $CD4^+$ T cells exposed to chemical stress inducers, **(E)** immortalized and primary BJ fibroblasts transduced with $hRAS^{G12V}$, and **(F)** BeWo cells treated with forskolin. $CD4^+$ T cells and BeWo cells were collected 2 days post-treatment, while BJ fibroblasts were harvested at 7 and 14 d.p.t. Data represent means ± SEM from 3 to 6 independent experiments. Statistical significance was determined using one-way ANOVA (* $p < 0.05$, ** $p < 0.01$) compared to DMSO, EV, mock-treated controls. EV: empty vector, d.p.t.: days post-transduction.

5 Discussion

5.1 LTR12D_*DHRS2* is also induced by HIV-2

In this study, we identify a specific host response to HIV-1 infection that is mediated by the endogenous retroviral element LTR12D, located on chromosome 14 (hg38 chr14:23636315–23636374) [72]. Using primary $CD4^+$ T cells, we show that HIV-1 infection activates this LTR12D repeat, leading to upregulation of the *DHRS2* gene. DHRS2 stabilizes p53 by inhibiting its degradation via MDM2, thereby promoting p53-mediated transcription of *CDKN1A* (p21) and inducing cellular senescence (figures 1.6, 1.7, 1.8) [175, 182, 186]. This pathway connects retroviral infection to a defined molecular cascade involving cell cycle arrest and aging-like features in immune cells.

Extending these observations, I examined whether HIV-2 infection elicits a similar host response. I observed a consistent increase in DHRS2 protein levels in primary $CD4^+$ T cells infected with three different HIV-2 clones (figure 4.4). Due to low infection rates in this setting, I was unable to directly assess LTR12D promoter activation or downstream markers such as *CDKN1A* via q-RTPCR. Nevertheless, the upregulation of DHRS2 strongly suggests that HIV-2 also engages this host pathway.

The detection of *DHRS2* induction suggests that LTR12D may act as a sensitive, HIV-infection-responsive regulatory element in $CD4^+$ T cells. This is particularly relevant given that HIV-2 infections generally show slower disease progression and reduced pathogenicity compared to HIV-1 [254, 255]. It supports the idea that the LTR12D-DHRS2 axis represents a conserved and early host response to retroviral infection. A stronger or more efficient early host response could help limit viral replication and spread. Although the exact mechanisms remain to be clarified, DHRS2 is known to stabilize p53 and promote cellular senescence, processes that may help control viral activity in infected cells. Therefore, a more robust activation of this axis in response to HIV-2 may contribute to its milder clinical outcomes.

Future work should focus on directly validating LTR12D_*DHRS2* promoter activity in HIV-2-infected primary $CD4^+$ T cells, for example using reporter assays. Increasing HIV-2 infection efficiency, perhaps via concentrating virus particles or spinoculation protocols, could enable more robust analyses of downstream components such as *CDKN1A* or SASP transcripts expression. It would also be valuable to compare the epigenetic accessibility

of the LTR12D locus in HIV-1 versus HIV-2 infection contexts to determine whether differences in chromatin remodeling contribute to variability in *DHRS2* induction. This accessibility can be assessed through techniques such as ATAC-seq (Assay for Transposase-Accessible Chromatin using sequencing) to map open chromatin regions, or ChIP-seq (Chromatin Immunoprecipitation sequencing) to profile specific histone modifications (e.g., active marks such as H3K4me3 and H3K27ac) at the locus.

The consistent induction of LTR12D-driven *DHRS2* expression in response to both HIV-1 and HIV-2 strongly suggests a conserved host response to retroviral infection. Notably, given the attenuated pathogenicity and slower disease progression of HIV-2, it is plausible that this shared LTR12D-DHRS2 cascade serves a protective role. This observation supports the idea that the host has co-opted this endogenous retroviral element to modulate cellular responses during infection, contributing to a more controlled or less harmful disease course. Importantly, the rapid activation of this axis may also act as an early alarm system, alerting the cell to retroviral intrusion and initiating protective programs. Thus, the LTR12D-DHRS2 pathway likely represents a host adaptation aimed at both detecting and mitigating the cellular consequences of chronic retroviral presence.

To definitively determine whether the host or the virus primarily benefits from this cascade, future mechanistic studies are crucial. Prior research by Chowdhury *et al*. demonstrated that the HIV-1 Vpr gene induces a p21-senescence cascade, preventing cell proliferation by causing arrest in the G2/M phase of the cell cycle [288]. Given our findings, it is plausible that Vpr achieves this by activating the LTR12D-DHRS2 axis, thereby linking a viral factor to the initiation of host cellular senescence. While this highlights a potential viral mechanism for activating a host response leading to senescence, further studies are necessary to understand the full spectrum of its regulation and ultimate biological benefit.

For instance, future research should investigate the precise upstream host signaling pathways that trigger LTR12D activation. This could involve assessing whether interferon or other innate immune sensors are involved upon infection, or by challenging cells with specific pathway agonists/antagonists even without viral infection. Such studies would help determine if LTR12D induction is purely host-driven, or if the

host has *co-opted* this cascade as a response to the virus, possibly alongside direct viral triggers.

Analyzing the kinetics of LTR12D and *DHRS2* expression relative to viral replication, would further illuminate the primary orchestrator. For a deeper understanding of viral replication dynamics, quantifying infectious viral titers, measuring proviral DNA integration (for retroviruses), and assessing specific viral gene and protein expression levels are essential to pinpoint exactly which stages of the viral life cycle are affected by this host response. This could be investigated through targeted genetic perturbations of the host, such as *DHRS2* knockout, or by directly perturbing the LTR12D locus in primary $CD4^+$ T cells, for example, through CRISPR-Cas9-mediated deletion. Assessing the impact of such manipulations on both host cellular responses and viral replication dynamics would provide direct evidence of the functional role of the LTR12D-DHRS2 axis.

Together, these data demonstrate that LTR12D-driven *DHRS2* upregulation is a shared host response to both HIV-1 and HIV-2 in primary $CD4^+$ T cells and provide a starting point for deeper mechanistic studies into whether retroviral infections, potentially via factors such as Vpr [288], trigger the host to co-opt endogenous genomic elements such as LTR12D, and how this complex process influences cellular fate and, crucially, to whose ultimate benefit.

5.2 The induction of *DHRS2* is not unique to primary $CD4^+$ T cells

While the investigation of HIV-2 provided valuable insights into *DHRS2* upregulation in $CD4^+$ T cells, it is also essential to explore how HIV-1, the predominant virus responsible for the global HIV pandemic, affects other critical target cells involved in HIV pathogenesis. Among these, primary monocyte-derived macrophages play a central role in the innate immune response and act as important viral reservoirs that contribute to chronic inflammation and immune activation [259, 260]. Given their pivotal role, I also analyzed the activation of the DHRS2 pathway in HIV-1-infected macrophages to understand how viral infection influences cellular aging and immune dysfunction in this key cell type.

My initial experiments using HIV-1 CH077 (dual tropic) and a modified HIV-1 NL4-3 variant (originally CXCR4-tropic) with V3 loop mutations conferring CCR5 tropism and enabling macrophage infection provided a crucial foundation for studying DHRS2

pathway activation in primary macrophages. The modified NL4-3 clone offered a key experimental advantage by enabling the virus to gain entry into this otherwise restrictive cell type, facilitating detailed analysis of host responses [253].

HIV-1 replicates inefficiently in non-dividing cells, such as quiescent $CD4^+$ T cells, dendritic cells, and monocyte-derived macrophages (MDMs) [289]. Pretreating MDMs with Vpx enhances HIV-1 cDNA synthesis by accelerating reverse transcription, which is otherwise limited by SAMHD1-mediated depletion of dNTPs [289]. To enhance viral replication in primary macrophages, which are known for their resistance to HIV-1 due to the antiviral factor SAMHD1, I employed Vpx-mediated SAMHD1 degradation. This strategy effectively increases viral replication, achieving high infection rates and enabling the study of post-entry host responses under conditions of robust infection [289].

My findings indicate that the HIV-1 infection in macrophages, achieved using dual-tropic CH077 or the engineered CCR5-tropic NL4-3 strain in combination with Vpx-mediated SAMHD1 degradation, is not sufficient to activate the *DHRS2* pathway. Specifically, I detected no significant induction of LTR12D_*DHRS2* transcripts in infected macrophages (Figure 4.5). This was observed despite achieving high infection rates with the engineered CCR5-tropic NL4-3 strain (8-85%), and low infection rates (2-6%) with dual-tropic CH077 under these optimized conditions. Therefore, even with successful viral entry and productive infection, the DHRS2 pathway was not activated in macrophages. In contrast, the same CH077 strain led to detectable *DHRS2* induction in HIV-1-infected $CD4^+$ T cells. This difference points strongly toward cell type-specific regulation rather than a purely strain-dependent phenomenon. While the lower infection rates of CH077 in macrophages (2-6%) compared to the generally higher rates achieved in $CD4^+$ T cells (20-40%) could potentially contribute to the observed difference in *DHRS2* induction, the absence of activation even under conditions of high infection achieved with the NL4-3 variant in macrophages further reinforces that cell type-intrinsic factors govern this pathway's activation.

Given the absence of *DHRS2* induction in macrophages, we did not examine downstream components of the pathway, such as *CDKN1A* expression or senescence markers, as DHRS2 acts upstream in this cascade and serves as an early indicator of its activation.

Several possible explanations may account for this differential regulation of DHRS2, though these are complicated by the later observation that M-tropic HIV-1 clones *do* induce DHRS2 in macrophages. One plausible factor initially considered is the chromatin accessibility of the LTR12D element, which might be more epigenetically repressed in macrophages than in $CD4^+$ T cells [186]. In line with this, transposable element activation is known to be tightly controlled by cell type-specific histone modifications and DNA methylation [290]. However, the induction by M-tropic strains suggests this repression is not absolute and can be overcome. Second, macrophages may lack certain transcription factors or co-factors necessary to activate LTR12D-driven transcription following infection; yet, the M-tropic HIV-1 data implies these factors must be present or inducible under specific infection conditions. Third, it is possible that stress-sensing or innate immune pathways, which might act as upstream inducers of the DHRS2-p21 axis, are either not activated or are differently regulated in macrophages compared to $CD4^+$ T cells; this too would need re-evaluation given the observed induction.

Finally, it is important to consider the existence of a more distal, non-LTR promoter within the *DHRS2* locus [221]. This promoter, which has been specifically observed to be active in monocyte-derived dendritic cells (MDDCs) [221], may play a distinct role or exhibit different regulatory mechanisms in macrophages compared to $CD4^+$ T cells. Notably, the expression driven by this non-LTR promoter is not associated with the production of the DHRS2-V1 (300 amino acids) and DHRS2-V2 (280 amino acids) protein isoforms, which are known to bind MDM2, stabilize p53, and induce cellular senescence. Therefore, even if this non-LTR promoter is active in macrophages, it might lead to the production of different DHRS2 variants that do not mediate the same senescence-inducing effects, thus contributing to the observed differential cellular outcomes despite HIV-1 infection. It is also important to note that our LTR12D_*DHRS2* q-RTPCR primers and DHRS2 antibody are very specific and could detect only these two *DHRS2* transcripts/protein isoforms derived from LTR12D.

SAMHD1 restricts HIV-1 replication by lowering the available pool of nucleotides necessary for viral DNA synthesis [291]. The viral protein Vpx counteracts this restriction by degrading SAMHD1, thereby facilitating efficient viral replication in non-dividing cells such as macrophages [292]. Nonetheless, as SAMHD1 also plays a role in cell cycle regulation, its depletion could in theory indirectly affect *DHRS2* expression. However, existing literature such as Pauls *et al*. 2014 [293] indicates that p21 activity is largely

independent of SAMHD1, and I therefore consider this an unlikely explanation for the lack of *DHRS2* induction. Additional experiments, such as reconstituting SAMHD1 in Vpx-treated cells or using *SAMHD1* knockout macrophages, could help clarify this point.

To address the limitations of using modified viral strains and Vpx treatment, I next employed the macrophage-tropic CCR5-using HIV-1 clones YU2 and AD8 [294] (Figure 4.6). Importantly, I did not use Vpx in this context, thereby preserving the physiological integrity of macrophages and minimizing potential confounding effects from SAMHD1 depletion. While infection rates for these macrophage-tropic strains (YU2: 5-12%, AD8: 20-40%) were lower than those achieved with the modified CCR5-tropic NL4-3 strain, these levels are more representative of natural infection dynamics given the absence of Vpx treatment, and were notably higher than the low (2-6%) infection rates observed for CH077. Strikingly, infection with these M-tropic strains led to a marked upregulation of DHRS2 protein levels, providing compelling evidence that the DHRS2 pathway can be activated in macrophages under more physiological conditions and suggesting a key role for viral tropism in modulating host gene expression.

The contrast between the absence of *DHRS2* activation with CH077 or NL4-3 and its induction by YU2 or AD8 raises an important mechanistic question. One possibility is that macrophage-tropic HIV-1 strains induce specific host responses not triggered by the dual-tropic or engineered viruses. For instance, these strains may more effectively engage pattern recognition receptors (PRRs), leading to differential activation of downstream signaling pathways [295]. Alternatively, they may differ in the efficiency or nature of their interaction with macrophage-specific restriction factors, influencing transcriptional responses such as *DHRS2* expression.

While I observed *DHRS2* induction in this setting, downstream components of the cascade were not assessed, including p53, p21 expression, cytokine production, or markers of senescence. Future experiments could directly address these gaps by performing qPCR and protein-level analyses of p53, p21, multiplex cytokine assays, and senescence-associated β-galactosidase staining. These would help determine whether DHRS2 upregulation in macrophages leads to functionally relevant downstream outcomes.

To my knowledge, comprehensive analyses of *CDKN1A* expression or cytokine profiles in M-tropic HIV-1-infected primary macrophages are limited, particularly in the context of *DHRS2* induction. Studies have shown the critical role of *CDKN1A* in restricting HIV replication in MDMs [296, 297]. Additionally, Vázquez *et al*. (2005), working with an HIV-1 CCR5-engineered NL4-3 strain, demonstrated that Vpr independently enhances *CDKN1A* transcription in macrophages [298]. However, none of these works explicitly explored the upstream activation of the LTR12D-DHRS2 axis or its specific connection to *CDKN1A* induction in these contexts. My results therefore provide a new and critical entry point into this area by specifically focusing on the involvement of the LTR12D-DHRS2 pathway in response to HIV-1 infection in macrophages. I also propose that further investigations using ATAC-seq or ChIP-seq could determine whether LTR12D chromatin accessibility differs between macrophages and $CD4^+$ T cells, helping to clarify why *DHRS2* expression is selectively regulated.

Taken together, my two-step experimental design beginning with an optimized infection model and progressing to physiologically relevant M-tropic strains enabled a nuanced dissection of how viral tropism, host restriction factors, and cellular identity shape DHRS2 pathway activation in primary macrophages. These findings extend our understanding of the cell-specific antiviral and senescence responses triggered by HIV-1 and may shed light on the cell-type-specific mechanisms that contribute to chronic inflammation, immune dysfunction, and premature aging in people living with HIV.

To further dissect the mechanistic underpinnings of the LTR12D-DHRS2-p53-p21 senescence cascade observed in primary $CD4^+$ T cells, I investigated HIV-1 and HIV-2 infection in immortalized T cell lines, SupT1 and Jurkat. These models offer advantages in terms of experimental tractability and reproducibility; however, both harbor inactivating mutations in the *TP53* gene. Jurkat cells carry a heterozygous, stop-gained single-nucleotide substitution in codon 196 (R196*) in exon 6 (rs397516435), first reported by Cheng and Haas in 1990 [299]. This mutation is associated with Li-Fraumeni syndrome, a rare autosomal dominant hereditary cancer predisposition disorder that leads to early tumor development [300]. The R196* variant likely contributes to the widely reported p53 deficiency in Jurkat cells by producing a truncated and non-functional protein. As expected, these mutations limit the ability of these cells to execute a full p53-dependent senescence response.

Despite these limitations, HIV-1 infection induced a pronounced upregulation of LTR12D_*DHRS2* transcripts in both cell lines (5- to 20-fold), while *CDKN1A* (p21) expression increased only modestly (2- to 3-fold) (figure 4.2). These results support our proposed cascade in which LTR12D functions upstream of *DHRS2*, which stabilizes p53 and enhances *CDKN1A* transcription. The relatively weak p21 induction in these *TP53*-mutant cell lines confirms that functional p53 is critical for a robust senescence response, while also validating LTR12D_*DHRS2* activation as a p53-independent upstream event. These findings are further supported by similar patterns observed during HIV-2 infection. Both Jurkat and SupT1 cells showed DHRS2 protein upregulation following HIV-2 exposure, suggesting that the LTR12D_*DHRS2* axis responds to both HIV-1 and HIV-2 despite their differences in replication kinetics and pathogenicity [255].

Interestingly, DHRS2 induction was observed in both p27+ and p27- cell populations during HIV-2 infection [301] (figure 4.4). While this may suggest a bystander effect, we cannot exclude the possibility that the p27- population includes infected cells that were not detected due to the relatively low affinity of the anti-HIV-1 p24 antibody for HIV-2 capsid (p27), potentially leading to underestimation of infected cells. Notably, this pattern differs from HIV-1 infection, where DHRS2 upregulation was restricted to productively infected cells in immortalized cell lines. These subtle differences highlight the importance of carefully interpreting marker-based infection assays, especially when comparing divergent retroviruses.

Taken together, our results validate that immortalized T cell lines can effectively model the early transcriptional events of the LTR12D_*DHRS2* cascade during HIV-1 and HIV-2 infection. However, due to their *TP53* mutations, these models are limited in capturing the downstream senescence phenotypes. Future studies should explore whether other stress-related pathways compensate for p53 deficiency in these lines and investigate how different retroviruses modulate the LTR12D_*DHRS2* axis. Improved detection methods for HIV-2 infection, such as optimized antibodies or reporter viruses, would also enable a more precise delineation of infected versus bystander responses. Altogether, our work provides a platform for understanding how endogenous retroelement activation contributes to host responses during HIV infection and opens avenues to explore whether modulating these elements could influence immune activation or aging-related outcomes in people living with HIV.

5.3 *DHRS2* is essential for HIV-induced senescence

Our central question addresses whether *DHRS2* is essential in establishing or maintaining $CD4^+$ T cell senescence in the context of HIV infection. Senescence is increasingly recognized as a key driver of immune aging in people living with HIV [45, 307], and we previously observed elevated *DHRS2* expression in HIV-1- and HIV-2-infected primary $CD4^+$ T cells, macrophages, and T cell lines. Given DHRS2's established link to p53 stabilization, and our preliminary RNA-seq data showing that the LTR12D acts as a promoter for *DHRS2*, we hypothesized that the LTR12D-DHRS2 pathway might be actively involved in driving cellular senescence, particularly in $CD4^+$ T cells during HIV infection.

Recent studies consistently highlight DHRS2 as an important tumor suppressor gene, with its role investigated across several cancer types [176, 177, 182]. Zhou et al. reported frequent deletion of the DHRS2-containing 14q11.2 region in tumors such as esophageal squamous cell carcinoma (ESCC), accompanied by reduced p53 levels upon DHRS2 knockdown [176]. In contrast, overexpression of DHRS2-V1 or V2 stabilized p53 via Ser15 phosphorylation and reduced Rb phosphorylation at Ser795 [176]. Mechanistically, both isoforms bind MDM2, thereby preventing p53 degradation. This interaction increases p53 phosphorylation at Ser15 and promotes cell cycle arrest or apoptosis in response to cellular stress [176].

The *DHRS2* gene produces ten different transcript variants, leading to six distinct protein isoforms [302]. Among these, DHRS2-V1 (300 amino acids) and DHRS2-V2 (280 amino acids) are the most widely expressed and extensively studied. V2 is generated via an alternative splicing event in the 3’ coding region, resulting in a slightly shorter protein [303]. Additionally, it is important to note that DHRS2-V3 (NM_001318835.1) is expressed in monocyte-derived dendritic cells and has not been extensively studied [304]. In our studies, the primers used for detecting *DHRS2* transcripts (e.g., via qPCR) were designed to bind and detect both DHRS2-V1 (NM_182908.5) and V2 (NM_005794.4) variants. However, the flow cytometry antibody used in our experiments specifically detects the amino-acid sequence coded by DHRS2-V1.

Heinz *et al*. previously showed that both DHRS2-V1 and V2 can be transcribed from a single proximal, hepatocyte-specific promoter derived from the endogenous retroviral element LTR12D [304]. This LTR12D-derived promoter has also been reported to be

inducible by the histone deacetylase inhibitor sodium butyrate in several other cell types. They also identified a more distal, non-LTR promoter within the DHRS2 locus that was specifically active in monocyte-derived dendritic cells and transcribed DHRS2 V3 [304]. The presence of diverse transcripts across different cell types (e.g., monocyte-derived dendritic cells, HepG2 cells, and various tissues) can be attributed to alternative splicing and alternative promoter usage [304]. This strategic use of a co-opted LTR promoter to regulate a stress-responsive host gene highlights the remarkable interplay between ancient viral elements and modern gene regulation.

Li *et al*. further reported that *DHRS2* suppresses growth and metastasis in ovarian cancer by downregulating choline kinase alpha (CHKα). CHKα is the first rate-limiting enzyme in choline metabolism, functioning by phosphorylating choline to produce phosphorylcholine (PC). Elevated activity of this enzyme drives the increase in choline compounds, a process linked to malignant transformation in many cancers. By disrupting choline metabolism, DHRS2 highlights additional tumor-suppressive mechanisms beyond p53 regulation [183]. Intriguingly, Tracey *et al*. found elevated levels of choline-containing compounds in the brains of HIV-positive individuals prior to the onset of AIDS dementia complex (ADC), suggesting early dysregulation of choline metabolism during HIV infection [305]. Given DHRS2's role in modulating this pathway, it is plausible that HIV-mediated alterations in DHRS2 expression may contribute to metabolic changes linked to HIV-associated neurodegeneration.

Deisenroth et al. reported that DHRS2, although a mitochondrial protein, translocates to the nucleus where it binds and inhibits MDM2, thereby stabilizing p53 [175]. Together, these studies reveal that DHRS2 plays dual roles in cellular metabolism and in regulating critical signaling pathways such as the p53-MDM2 axis, which are commonly altered in cancer and aging [175]. Deisenroth *et al*. further demonstrated that knocking down endogenous Hep27 (*DHRS2*) in U2OS and MCF7 cells reduced basal p53 levels, indicating that DHRS2 may support steady-state p53 expression even in the absence of stress.

A complementary study by Luo et al. identified DHRS2 as the most upregulated metabolic gene following treatment with trichothecin (TCN), a natural compound that suppresses nasopharyngeal carcinoma (NPC) growth *in vitro* and *in vivo* [177]. They showed that HOXA13, a homeobox transcription factor, normally suppresses *DHRS2*

expression, thereby allowing MDM2 to remain active and p53 inactive. TCN treatment reversed this suppression, increasing *DHRS2* expression, reducing MDM2 activity, and restoring p53-mediated tumor suppression. This finding is particularly intriguing in the context of HIV-1 infection, as Dhamija *et al*. showed that HIV-1 Tat specifically associates with the HOXA13 promoter, leading to HOXA13 upregulation in T cell lines [306]. Given that HOXA13 is an inhibitor of *DHRS2*, it is plausible to speculate that HIV-1 Tat-mediated upregulation of HOXA13 might initially suppress *DHRS2*. However, the subsequent activation of *DHRS2* that we observed in HIV-1 infected cells, leading to increased p53 and *CDKN1A* expression, suggests a complex interplay where host compensatory mechanisms or other viral/cellular factors eventually override HOXA13's repressive effect, or that the interaction of Tat with HOXA13 is context-dependent in primary cells. This potential pathway offers a compelling hypothesis for further understanding the dynamic regulation of *DHRS2* during HIV-1 infection.

To address our main question regarding DHRS2's role in HIV-induced senescence, we employed two distinct CRISPR/Cas9-based knockout strategies in primary CD4+ T cells: electroporation and lentiviral transduction.

Initially, we utilized electroporation to deliver *DHRS2*-specific guide RNA (gRNA) or control gRNA into $CD4^+$ T cells [307]. While this method allowed us to reduce DHRS2 protein levels substantially, it resulted in a mixed population of edited and non-edited cells, limiting the knockout efficiency and introducing heterogeneity in the readouts. Furthermore, DHRS2 knockout cells exhibited lower HIV-1 infection rates, complicating our ability to determine whether observed reductions in SASP cytokines were due to the absence of DHRS2 or simply reflected reduced viral replication (Figure 4.8). This distinction is critical: if a host factor affects viral entry or replication, any downstream changes in immune responses or senescence markers may be secondary effects, not evidence of a direct role in senescence induction. For example, knocking down an entry receptor such as CD4 would also reduce infection and associated immune activation, but it would not imply a role for CD4 in senescence per se. Interestingly, even though SASP factors were reduced, *CDKN1A* transcript levels remained unchanged in DHRS2 knockout cells. This suggests that the canonical p53-p21 senescence pathway may not be transcriptionally regulated by DHRS2 in this context. Alternatively, DHRS2 may influence cytokine production at a post-transcriptional level, such as by modulating stress signaling, translation, or secretion pathways.

Interpretation was complicated by the incomplete editing efficiency of the knockout. This meant that the most heavily infected cells, those likely driving senescence-associated phenotypes, may have escaped editing. Consequently, the observed reduction in infection and SASP factors could reflect the predominance of edited, less permissive cells, obscuring the specific role of DHRS2. To resolve this, future experiments should equalize infection rates between knockout and control groups by adjusting viral input or sorting infected cells for analysis. Additionally, single-cell techniques such as RNA FISH or CyTOF could independently track DHRS2 status, infection, and senescence markers within individual cells. These approaches will help determine whether DHRS2 directly influences senescence or if the effects are secondary to altered viral replication. Our initial CRISPR Cas9 knockout via electroporation reduced DHRS2 protein levels but showed variable editing efficiency and inconsistent HIV-1 infection rates, making it difficult to discern if SASP cytokine reduction resulted directly from DHRS2 loss or from reduced infection, possibly masking its role in senescence.

To overcome these issues, I employed an alternative strategy using lentiviral transduction with the lentiCRISPRv2 system [308]. This approach allowed more consistent delivery of Cas9 and DHRS2-targeting guide RNAs into primary $CD4^+$ T cells, achieving a comparable (~40%) reduction in DHRS2 protein levels as seen with electroporation (Figure 4.10). While transduction does not guarantee complete knockout in every cell, integration of the CRISPR cassette into the host genome enables stable and prolonged Cas9 expression, likely contributing to the more uniform editing outcomes observed across the three donors tested. Importantly, unlike the electroporation-based knockout, *DHRS2*-deficient and control cells showed similar HIV-1 infection rates in this setup (Figure 4.10), minimizing confounding effects of infection variability and allowing a more confident assessment of the role of DHRS2 in modulating senescence independently of viral replication.

This discrepancy in HIV-1 infection rates between the two knockout methods is notable. Although I used the same gRNA sequences and achieved similar reductions in DHRS2 protein levels, HIV-1 infection rates were reduced in the electroporation-based knockout but remained unaffected in the lentiviral system. This difference may stem from distinctions in the duration and intensity of Cas9 expression, where a rapid, transient burst from electroporation might initially stress cells more than the gentler, more sustained delivery of the lentiviral approach [309, 310]. While the overall DHRS2

protein reduction was similar, the different kinetics or associated cellular stress pathways induced by each delivery method could influence early events like viral entry.

It is plausible that electroporation alone would transiently increase DHRS2 protein levels due to the acute physical stress it induces on cell membranes, potentially triggering a broader cellular stress response that includes DHRS2 upregulation, given its known involvement in such pathways. However, in our specific experimental setup, DHRS2 levels were not observed to be increased in non-transduced electroporated cells compared to untreated cells, suggesting that while the stress response hypothesis is plausible, it did not confound our specific measurements of *DHRS2* knockout efficacy. In contrast, the lentiviral approach, being a comparatively gentler and more sustained delivery method, would likely not cause a significant, acute increase in DHRS2 protein levels compared to non-transduced cells, as it generally avoids the intense, immediate cellular perturbation associated with electroporation, unless the transduced gene itself directly influences *DHRS2* expression or high viral loads are employed [309].

Under the improved conditions afforded by the lentiviral transduction approach, I found that *DHRS2* knockout resulted in a consistent reduction of *CDKN1A* (p21) mRNA levels upon HIV-1 infection compared to infected NT control cells. This suggests that DHRS2 influences the canonical p53–p21 senescence axis under viral stress. I then assessed several SASP-associated cytokines known to be upregulated upon HIV-1 infection [311], including *IL-6, TNF, CCL5*, and *CCL17* (Figure 4.11). Notably, DHRS2-deficient cells displayed a decrease in *IL-6* and *TNF*, both hallmark SASP cytokines [312]. Expression of *CCL5* and *CCL17*, which contribute to immune recruitment and chronic inflammation [313], was also reduced. In contrast, *CXCL10*, a chemokine frequently induced in response to viral infections [314], remained unaffected by DHRS2 loss.

This selective pattern of SASP regulation suggests that DHRS2 may influence a defined subset of inflammatory mediators, potentially through p21-dependent mechanisms (i.e., it might affect p21-associated secretory phenotypes, or PASP [315]). For instance, some SASP factors such as IL-6 and TNF are known to be downstream of p21 and the p38 MAPK pathway [316], suggesting a possible route by which DHRS2 could exert control via transcriptional regulation. In contrast, factors such as CXCL10 are more tightly associated with interferon-stimulated gene responses and may operate independently of the p21 axis [317]. DHRS2-mediated p53 stabilization results in

increased *CDKN1A* transcription, as supported by earlier studies demonstrating that DHRS2 attenuates MDM2-mediated p53 degradation, thereby leading to elevated p53 levels and subsequent transcriptional activation of its target gene, *CDKN1A*.

These findings are consistent with previous work by Deisenroth *et al.* [175], who showed that knocking down endogenous Hep27 (*DHRS2*) in U2OS (human osteosarcoma) and MCF7 (human breast adenocarcinoma) cells reduced basal p53 levels, indicating that *DHRS2* may support steady-state p53 expression in the absence of stress. This observation suggests that the influence of DHRS2 on *CDKN1A* transcription is likely an indirect effect mediated through its modulation of p53 stability. Although I did not directly assess p53 levels in my knockout experiments, I did observe changes in downstream targets such as p21 and selected SASP factors, suggesting functional consequences of *DHRS2* loss that may reflect altered p53 pathway activity. Notably, both U2OS and MCF7 cells harbor wild-type p53, making them useful systems for probing the DHRS2-MDM2 interaction and p53 stabilization without interference from p53 mutations. My findings build on this prior work by extending the analysis to primary $CD4^+$ T cells and senescence-associated cytokine regulation, providing a critical *ex-vivo* context.

To address the remaining limitation of incomplete transduction, future experiments could employ T cell lines with stable *DHRS2* knockout and intact p53 function. This would enable more consistent gene disruption and facilitate in-depth analysis of downstream effects using transcriptomics, proteomics, and cytokine profiling. In parallel, alternative strategies could help resolve the heterogeneity in primary cultures. For example, RNA-based sorting methods like PrimeFlow could be used to separate cells based on *DHRS2* transcript levels or p21 induction, thus allowing comparisons between cells with high and low expression within the same population.

Beyond optimizing knockout efficiency and analysis in primary cells, a complete understanding of DHRS2's functional impact also necessitates dissecting the specific contributions of its different protein isoforms and transcript variants, especially since our current detection methods do not fully distinguish between all of them. I have primarily focused on DHRS2 transcript variants transcribed from the LTR12D promoter, specifically DHRS2-V1 and V2. This is because our preliminary RNA-seq data showed the LTR12D_*DHRS2* repeat was significantly upregulated upon HIV-1 infection, suggesting

these transcripts are the dominant isoforms in this context. However, the *DHRS2* gene produces multiple transcript variants from both the LTR12D-derived and non-LTR promoters, and it remains unclear whether the senescence effects we observed are driven solely by the LTR12D-regulated variants (V1 and V2) or whether other transcript variants, potentially expressed under different stress or infection conditions but undetected by our qPCR primers or FACS antibody, also contribute. Prior studies [175, 176] have focused primarily on V1 and V2, demonstrating their ability to bind MDM2 and stabilize p53. However, information regarding MDM2 interaction or p53 stabilization by other transcript variants (e.g., V3, V4, V5, V6) is currently limited or absent. To determine whether the link between DHRS2 and senescence is isoform-specific, future studies employing isoform-specific knockdowns or CRISPR interference targeting distinct transcription start sites would be valuable.

5.4 *DHRS2* is not sufficient to induce senescence

Our knockout experiments clearly demonstrated that DHRS2 plays a critical role in HIV-1-induced senescence in primary $CD4^+$ T cells, as its loss led to a consistent reduction in key senescence markers and SASP cytokine expression. To assess whether *DHRS2* upregulation alone is sufficient to trigger senescence, I employed a CRISPR/dCas9-VP64-based gene activation system in primary $CD4^+$ T cells [267]. This approach achieved a modest 1.5- to 2-fold increase in *DHRS2* mRNA, yet failed to induce significant upregulation of *CDKN1A* (p21) (Figure 4.13). This suggests that either *DHRS2* needs to surpass a critical expression threshold to initiate the senescence program, or that other co-acting signals are required.

However, this result must be interpreted cautiously, as several technical and biological factors could explain the lack of a senescence response. One possibility is that the transcriptional activator VP64 used in this system was not sufficiently potent in the context of primary $CD4^+$ T cells. Other more robust activator systems, such as dCas9-p300, dCas9-HSF1, dCas9-Rta, dCas9-p65 or SAM, SunTag-based amplifiers [318] might achieve stronger and more physiologically relevant induction of *DHRS2*. It is also possible that the chromatin state at the endogenous *DHRS2* locus in $CD4^+$ T cells is not permissive to activation by VP64, especially if LTR12D-driven transcription is epigenetically silenced under basal conditions.

Moreover, it remains plausible that low-level *DHRS2* induction is sufficient but only in the presence of other cofactors or stress signals, such as reactive oxygen species, DNA damage, or viral proteins, which are absent in the artificial activation context. Together with our knockout data, where p21 and SASP factors were reduced but not entirely lost, these findings indicate that *DHRS2* is necessary but not sufficient for cellular senescence.

Interestingly, lentiviral transduction itself did not alter *DHRS2* expression, suggesting that the viral vector alone does not activate the LTR12D promoter driving *DHRS2* transcription. This is reassuring, as it confirms that lentiviral delivery has no unintended effect on *DHRS2* levels and that the gRNAs used are indeed potent for both activation and knockout. This further supports the idea that additional infection-associated stimuli, such as innate immune signaling, chromatin remodeling, or oxidative stress, are required to trigger the endogenous *DHRS2* program during HIV-1 infection. It is an astute observation that HIV-1, through its sophisticated array of accessory proteins (such as Vpr, Vif, Nef, and Vpu), actively works to suppress the host's antiviral immunity, targeting and degrading key components of innate immune pathways [27, 319-322]. While this might initially suggest diminished overall immune signaling, the virus, despite these suppressive strategies, still presents a multitude of pathogen-associated molecular patterns (PAMPs) such as viral RNA, DNA intermediates during reverse transcription, and even nascent viral proteins that can be detected by an intricate network of host pattern recognition receptors (PRRs) [323]. Therefore, even in the face of targeted immune suppression, the sheer presence and replication of the virus can trigger alternative or residual innate immune responses, contributing to a complex inflammatory milieu that might, in turn, influence the expression of host genes such as *DHRS2*.

To rigorously test the hypothesis that these additional infection-associated stimuli beyond lentiviral transduction itself are required to trigger the endogenous DHRS2 program during HIV-1 infection, a multi-pronged experimental strategy could be employed. This could involve dissecting the synergy and specificity of PRR activation by employing combinatorial or sequential administration of different PRR agonists (e.g., poly(I:C) and cGAMP) to mimic the diverse innate sensing during active infection. Furthermore, utilizing viral mutants lacking specific PRR-engaging elements could pinpoint which viral components are critical for robust DHRS2 induction. Finally, to investigate downstream signaling cascade convergence, experiments could employ

pharmacological inhibitors or genetic knockouts/knockdowns of key signaling molecules (e.g., components of MAPK pathways, NF-κB, or the DNA damage response) known to be activated during HIV-1 infection, thereby assessing their impact on LTR12D_*DHRS2* induction and clarifying the interplay between viral protein expression and these host stress-sensing pathways.

5.5 HSF1, LEF1, TCF1 can drive LTR12D_*DHRS2*-mediated senescence

My findings provide important insights into the regulation of *DHRS2* expression during HIV-1 infection, highlighting the interplay between stress and developmental signaling pathways mediated by heat shock factor 1 (HSF1) and the Wnt/β-catenin effectors LEF1 and TCF1. Using computational predictions from the JASPAR and HOCOMOCO databases alongside luciferase reporter assays and western blotting, we identified HSF1, LEF1, TCF1, and β-catenin as direct negative regulators of the LTR12D element upstream of *DHRS2* (figures 4.17, 4.18). Each factor demonstrated dose-dependent repression of promoter activity in the absence of HIV-1. While Oda *et al*. [220] previously reported that HSF1 depletion increases *DHRS2* expression in a p53-dependent manner, our data establish that HSF1 exerts repression specifically through the LTR12D repeat, indicating a direct transcriptional role.

However, a critical observation emerges when comparing these overexpression-based results to the infection context. Despite elevated total HSF1 protein levels in HIV-1-infected $CD4^+$ T cells and macrophages, the proportion of HSF1 phosphorylated at serine 303/307, a known inactivating modification remains unchanged (~20%), indicating that infection does not substantially alter HSF1 inactivation at these sites. This leads to an apparent paradox: if HSF1 suppresses *DHRS2*, why is *DHRS2* upregulated during infection? One possible explanation is that increased total HSF1 levels do not reflect a fully functional transcriptional activator state. Other post-translational modifications (e.g., phosphorylation at serine residues 230, 320, or 326), trimerization, or nuclear translocation may modulate its activity [271, 273, 324]. Indeed, the transcriptional activity of HSF1 is known to be tightly regulated through interactions with co-regulators and stress-induced nuclear translocation [325]. Though we did not assess HSF1 subcellular localization directly, previous studies indicate that HIV-1 Tat triggers nuclear localization of HSF1 and activates HIV-1 LTR-driven gene expression [326]. These

findings, however, focused on the viral LTR and not the LTR12D element upstream of *DHRS2*, underlining the context specificity of HSF1 function.

Similarly, LEF1 and TCF1, key nuclear mediators of the Wnt/β-catenin pathway [276, 278], also repressed *DHRS2* promoter activity upon overexpression. However, HIV-1 infection is associated with β-catenin accumulation in $CD4^+$ T cells, indicative of Wnt pathway activation [279]. This aligns with reports that the HIV-1 protein Vpu stabilizes β-catenin by interfering with βTrCP-mediated degradation, affecting multiple signaling pathways, including NF-κB and Wnt [327]. Notably, while β-catenin was shown to enhance HIV-1 LTR activity through Tat interaction [326], it also represses HIV transcription via TCF-4 binding sites in $CD4^+$ T cells [182] and astrocytes [328, 329], emphasizing cell-type- and promoter-specific context of Wnt signaling.

The dual nature of β-catenin and its cofactors LEF1 and TCF1 as either repressors or activators depending on chromatin environment and cofactor availability [330] supports a model where their repressive activity observed *in vitro* may shift during infection due to viral modulation. For instance, HIV proteins such as Vpu or Nef may reprogram transcriptional responses. While Vpu activates β-catenin [279], Nef inhibits Wnt signaling in HEK293 cells [331], it remains unclear how these viral proteins specifically modulate β-catenin's nuclear localization and transcriptional activity in primary T cells and macrophages.

Moreover, chromatin-level repression of the HIV-1 LTR by Suv39H1, HP1γ, and H3K9me3 [332] highlights the importance of epigenetic regulation in controlling both viral and host gene expression. This is particularly relevant as LTR12D, which drives *DHRS2* transcription, is an endogenous retroviral LTR that shares similar epigenetic silencing mechanisms (e.g., via H3K9me3) with the exogenous HIV-1 LTR [333]. Therefore, changes in host epigenetic landscapes triggered by HIV-1 infection could concomitantly modulate both viral latency and the expression of endogenous retroelement-driven genes like *DHRS2*.

HSF1 acts on the promoters of Wnt-related genes, directly regulating their transcription and thereby influencing Wnt signaling output [334, 335], suggesting the LTR12D_*DHRS2* locus may function as a hub integrating signals from both pathways.

Although overexpression of HSF1 and Wnt effectors repressed *DHRS2 in vitro*, their *in vivo* role during infection may differ due to changes in signaling and chromatin architecture. Additionally, not all TCF family members respond identically to Wnt; some such as LEF1 and TCF1 can act as transcriptional activators depending on the context [336]. Therefore, the observed upregulation of *DHRS2* in HIV-1-infected cells may reflect a functional switch of these regulators, potentially influenced by viral interference with chromatin accessibility, transcription complex assembly, or cofactor recruitment.

Collectively, this suggests a complex regulatory axis where HSF1, LEF1, TCF1, and β-catenin converge on LTR12D to modulate *DHRS2* transcription. Future studies should investigate whether HIV-1 infection alters nuclear localization or post-translational modifications of HSF1, cofactor dynamics of LEF1 and TCF1, or LTR12D chromatin accessibility. Targeted ChIP-seq for HSF1 and Wnt factors in infected versus uninfected T cells, coupled with assays measuring HSF1 trimerization and subcellular distribution, could illuminate how HIV-1 rewires host transcriptional regulation. Understanding this crosstalk may reveal novel mechanisms contributing to premature senescence and immune dysfunction in people living with HIV.

5.6 LTR12D_*DHRS2* activation: A general stress response

To understand the biological significance of the LTR12D_*DHRS2* cascade, we aimed to determine whether its activation is unique to HIV-1 infection or reflects a broader component of stress-induced senescence. Previous studies have consistently shown upregulation of *DHRS2* in response to cellular stress or senescence. For instance, Oda *et al*. demonstrated that experimental depletion of HSF1, a master regulator of the stress response, activates the MDM2-p53-p21 pathway in human diploid fibroblasts [220]; Deisenroth *et al*. described a mitochondrial-to-nuclear signaling axis involving c-Myb-Hep27-MDM2-p53 in breast cancer cells [174], and Zhou *et al*. showed that DHRS2 overexpression leads to p53 phosphorylation (Ser15) and accumulation by inhibiting MDM2-mediated degradation [186]. Additionally, Crean *et al*. reported that DHRS2 is induced during oxidative stress [337]. While these findings consistently link elevated DHRS2 levels to stressed or senescent cellular states and its involvement in stress-related pathways such as p53, it remains unclear whether *DHRS2* induction in these contexts is driven by the LTR12D element. Therefore, identifying the regulatory origin of *DHRS2* expression under stress conditions is important.

To explore whether LTR12D_*DHRS2* activation occurs across diverse stress models, I tested oxidative (H_2O_2), mitochondrial (staurosporine), and ER stress (thapsigargin), as well as oncogene-mediated senescence ($HRas^{G12V}$) and syncytium formation (figure 4.21). My data show that LTR12D_*DHRS2* is consistently upregulated in response to cellular damage-associated stressors, but not during oncogene- or fusion-mediated senescence, suggesting that its activation is not a general hallmark of senescence but rather a specialized response to cellular damage.

Interestingly, p21, a canonical senescence marker, was not uniformly upregulated across all my models, reflecting the complex kinetics of senescence markers (Figure 4.20). For instance, while *CDKN1A* was upregulated at early time points (day 7) in immortalized BJ-hTERT fibroblasts and BeWo cells undergoing senescence, its expression was absent at later time points (day 14) in immortalized BJ-hTERT cells, and not upregulated at all in primary BJ fibroblasts. This variable and often transient nature of *CDKN1A* upregulation, especially when observed at later time points or entirely absent, highlights that its elevation can reflect either temporary cell cycle arrest or the early phase of senescence, but its absence does not necessarily rule out senescence. Therefore, while our data clearly define the specific conditions under which LTR12D_*DHRS2* is induced (i.e., damage-associated stress), the variable and often transient nature of *CDKN1A* upregulation in the other models implies that stable senescence may not have been fully established in all cases given the limited set of senescence markers evaluated. This underscores the necessity of employing a broader panel of senescence markers and evaluating multiple time points in future studies to confirm the robust and irreversible establishment of senescence across diverse experimental conditions.

Further, in BeWo cells treated with forskolin, which boosts intracellular cAMP via adenylyl cyclase activation [338], I observed increased *CDKN1A* mRNA levels following fusion. This signaling cascade activates protein kinase A (PKA), which in turn activates GCM1, a transcription factor essential for trophoblast fusion. GCM1 upregulates syncytin-1 (ERVWE1), β-hCG (CGB), and PP13 (LGALS13), all of which are markers of syncytiotrophoblast formation [339]. Our data, showing increased *CDKN1A* mRNA during forskolin-induced fusion, thus aligns with findings from Lu et al. [340], who demonstrated that p21 and GCM1 cooperatively regulate syncytin-2. This congruence suggests that p21 is indeed an integral component of the syncytiotrophoblast differentiation program, consistent with its previously established interplay with GCM1

in this context. This further confirms that BeWo cells retain the ability to exit the cell cycle, undergo fusion, and adopt differentiated states that reflect *in vivo* syncytiotrophoblast functions such as hormone secretion and pathogen defense.

In the primary placental model, we observed that while cytotrophoblasts began to fuse into syncytiotrophoblasts between 24- and 48-hours post-isolation [341], *CDKN1A* mRNA levels gradually decreased during our time-course experiments. This observed downregulation of *CDKN1A* during fusion is consistent with its proposed role as a modulator of this developmental process. While reports indicate that abnormally reduced or dysregulated *CDKN1A* expression can impair fusion and increase the risk of pre-eclampsia (PE) [342], our findings suggest that a physiological decrease in *CDKN1A* may reflect a programmed developmental transition essential for proper trophoblast fusion, rather than simply indicating stress. For instance, Kreis et al. [342] demonstrated that p21 protein levels are reduced in fusing cytotrophoblasts from early-onset PE placentas, leading to the downregulation of fusion-related proteins such as syncytin-2 and β-hCG, ultimately disrupting placental development. These findings suggest that p21 functions not only as a cell cycle regulator but also as a modulator of trophoblast fusion.

A notable observation came from $CD4^+$ T cells treated with Nutlin-3A, where we observed a concurrent increase in both *CDKN1A* and LTR12D_*DHRS2* transcripts. Nutlin-3A is a potent small-molecule inhibitor of MDM2, the primary negative regulator of p53 [343]. By blocking the MDM2-p53 interaction, Nutlin-3A stabilizes and activates p53, leading to transcriptional upregulation of its downstream targets [344]. This mechanism closely parallels the proposed function of DHRS2, which has also been reported to stabilize p53 by impairing its degradation. The similarity in outcomes between Nutlin-3A treatment and DHRS2 induction suggests that both may converge on a common pathway involving p53 activation. This raises the intriguing possibility of a positive feedback loop, in which p53 activation induces *DHRS2* expression via LTR12D, and DHRS2 in turn enhances p53 stability, thereby amplifying the transcription of p53 target genes such as *CDKN1A*. The concurrent upregulation of LTR12D_*DHRS2* and p21 in response to Nutlin-3A supports this model and suggests a tightly regulated interplay between retroelement-driven gene expression and canonical tumor suppressor pathways.

It is currently unclear whether p21 itself directly contributes to the transcriptional activation of *DHRS2* or whether both genes are co-regulated as part of a broader p53-dependent stress response. Alternatively, it is also possible that the LTR12D repeat functions as a stress-sensitive enhancer whose activity is modulated by the chromatin context or by transcription factors downstream of p53, such as ATF4, GADD45, or others yet to be identified [345]. Further studies such as promoter-reporter assays, chromatin immunoprecipitation (ChIP) for p53 and histone marks, and CRISPR-mediated deletion of LTR12D could help determine whether this element serves as a true regulatory node in the stress response circuit.

Collectively, these findings point toward a potentially self-reinforcing axis between DHRS2, p53, and p21 that likely fine-tunes cellular responses to genotoxic and oxidative stress, thereby linking endogenous retroelement activity to fundamental processes such as cell cycle control and senescence. In the context of HIV-1 infection, the LTR12D-DHRS2 axis appears to represent a host-beneficial response that the virus inadvertently triggers.

Cellular senescence, characterized by cell cycle arrest, primarily functions as a host defense mechanism to limit the proliferation of infected cells, thereby restricting viral spread [346, 347]. Emerging evidence supports senescence as a broad-spectrum antiviral response, though its specific roles in retroviral infection, particularly HIV-1, are still under active investigation. Baz-Martínez and colleagues demonstrated that, independently of the trigger, senescence reduces the replication of Vesicular Stomatitis Virus (VSV), leading to low viral titers, reduced viral protein synthesis, and decreased apoptosis in senescent cells, with conditioned medium from senescent cells conferring protection to proliferating cells, indicating mediation by the SASP [346]. This was validated *in vivo*, where bleomycin-induced senescence in mouse lungs prevented VSV particle detection [346]. Similarly, AbuBakar and others showed that DENV infection induces endothelial cells to undergo a senescent state, suggesting this as a host defense mechanism against DENV, given its inability to establish productive infection in senescent cells [347]. These findings, coupled with our observation of DHRS2-mediated *CDKN1A* induction, strengthen the hypothesis that the LTR12D-DHRS2 axis contributes to a host-beneficial response that can influence HIV-1 infection dynamics and potentially local immune responses through SASP.

Prior research by Chowdhury *et al*. (2003) demonstrated that the HIV-1 Vpr gene induces a p21-senescence cascade, preventing cell proliferation by causing arrest in the G2/M phase of the cell cycle [288]. Given our findings that *DHRS2* is activated by stress and can influence p53/p21, it is plausible that Vpr achieves this by activating the LTR12D-DHRS2 axis, directly linking a viral factor to the initiation of host cellular senescence. This suggests that the LTR12D element, an endogenous retroviral LTR, functions as a stress-responsive promoter that the host has co-opted over evolutionary time to regulate genes such as *DHRS2* in response to cellular threats.

In this intriguing scenario, HIV-1, through the expression of Vpr, inadvertently triggers a pre-existing host defense mechanism: the LTR12D-DHRS2-p21 cascade. While this cascade primarily serves to induce senescence, thereby limiting viral production and protecting the organism from widespread infection, it's an intriguing hypothesis that this host defense could, under certain conditions, inadvertently contribute to the establishment of viral latency. This highlights a delicate balance where a host defense mechanism, meant to curtail infection, might also, under specific circumstances, indirectly promote a state of non-productive infection, a topic that warrants further investigation.

This page is intentionally left blank

6 Summary

Human endogenous retroviruses (HERVs), remnants of ancient infections, make up about 8% of the human genome. While typically epigenetically silenced, specific HERV-derived long terminal repeats (LTRs) can be reactivated by various endogenous or exogenous stimuli and function as cis-regulatory elements, influencing host gene expression [223, 224]. For example, certain endogenous retroviral LTRs regulate the expression of immune genes [79, 225].

Notably, HIV-1 infection also induces the activation of distinct HERV loci. More specifically, previous work of my host laboratory identified a HERV-derived LTR12D element on chromosome 14 (hg38: chr14:23636315–23636374), as being specifically activated by HIV-1 [72]. This activation induces expression of the nearby gene *DHRS2*, which promotes cellular senescence via the p53-p21 axis. The DHRS2 protein stabilizes p53 by inhibiting MDM2, and ultimately enhancing *CDKN1A* (p21) expression. In line with this, HIV-infected cells show increased levels of LTR12D_*DHRS2* transcripts, p53 pathway activation, elevated senescence-associated β-galactosidase activity, and increased release of pro-inflammatory SASP factors such as IL-6, IL-8, and TNF-α.

In my thesis, I validated this LTR12D-DHRS2-driven senescence cascade across diverse models, including primary $CD4^+$ T cells, macrophages, and immortalized cell lines infected with HIV-1 or HIV-2. CRISPR/Cas9-mediated *DHRS2* knockout significantly reduced senescence markers and SASP, confirming its role in senescence. Macrophage-tropic HIV-1 strains also induced *DHRS2* in monocyte-derived macrophages, emphasizing the relevance of this pathway in physiologically relevant target cells of the virus.

Moreover, I found that LTR12D_*DHRS2* activation is not limited to HIV infection. It was also triggered by oxidative, mitochondrial, and ER stress but not by oncogene- or syncytia-induced senescence, suggesting a role in specific cellular damage types. Notably *DHRS2* induction alone was not sufficient to trigger senescence, indicating the need for co-factors or higher threshold levels of activation. Finally, I identified the transcription factors HSF1, LEF1, and TCF1 as repressors of the LTR12D_*DHRS2* promoter, suggesting that their inhibition or displacement may enable *DHRS2* expression during stress or infection.

Together, these findings establish a novel LTR12D-DHRS2-p53-p21 signaling axis in virus- and stress-induced senescence. This work highlights how reactivated endogenous retroelements may contribute to the molecular pathology of HIV-associated aging and opens avenues for therapeutic strategies targeting virus-induced cellular dysfunction.

Zusammenfassung

Humane endogene Retroviren (HERVs), Überbleibsel früherer Infektionen, machen etwa 8 % des menschlichen Genoms aus. Obwohl ihre Aktivität in der Regel epigenetisch unterdrückt wird, können bestimmte von HERVs abgeleitete Long Terminal Repeats (LTRs) durch endogene oder exogene Stimuli reaktiviert werden. Sie können dann als cis-regulatorische Elemente wirken, indem sie die Expression von zellulären Genen beeinflussen. So regulieren etwa bestimmte endogene retrovirale LTRs die Expression von Immungenen.

Bemerkenswerterweise führt auch eine HIV-1-Infektion zur Aktivierung bestimmter HERV-Loci. Frühere Arbeiten meines Gastlabors identifizierten ein von HERVs abgeleitetes LTR12D-Element auf Chromosom 14, das spezifisch durch HIV-1 aktiviert wird. Diese Aktivierung führt zur Expression des benachbarten Gens *DHRS2*, welches über die p53-p21-Kaskade zelluläre Seneszenz induziert. Das DHRS2-Protein stabilisiert p53, indem es MDM2 hemmt, was letztlich die Expression von *CDKN1A* (p21) induziert. Entsprechend zeigen HIV-infizierte Zellen eine erhöhte Expression von LTR12D_*DHRS2*-Transkripten, eine Aktivierung des p53-Signalwegs, vermehrte Aktivität der Seneszenz-assoziierten β-Galactosidase und eine gesteigerte Ausschüttung proinflammatorischer SASP-Faktoren wie IL-6, IL-8 und TNF-α.

In meiner Arbeit habe ich die durch LTR12D-DHRS2 vermittelte Seneszenz-Kaskade in verschiedenen Modellen validiert, darunter primäre $CD4^+$-T-Zellen, Makrophagen und immortalisierte Zelllinien, die mit HIV-1 oder HIV-2 infiziert wurden. Ein CRISPR/Cas9-vermittelter Knockout von DHRS2 führte zu einer signifikanten Reduktion von Seneszenzmarkern und SASP-Faktoren, was die funktionelle Bedeutung von DHRS2 in der Seneszenz bestätigte. Außerdem induzierten Makrophagen-trope HIV-1-Klone DHRS2 in Makrophagen, was die Relevanz dieses Signalwegs in physiologisch wichtigen Zielzellen des Virus unterstreicht.

Darüber hinaus konnte ich zeigen, dass die Aktivierung von LTR12D_*DHRS2* nicht auf HIV-Infektionen beschränkt ist. Sie wurde auch durch oxidativen, mitochondrialen und ER-Stress ausgelöst – jedoch nicht durch Onkogen- oder Synzytium-induzierte Seneszenz-, was auf eine Rolle bei spezifischen Formen zellulärer Schädigung hinweist. Interessanterweise war die alleinige Induktion von DHRS2 nicht ausreichend, um

Seneszenz auszulösen, was auf die Notwendigkeit zusätzlicher Faktoren oder das Erreichen eines bestimmten Aktivierungsschwellenwerts hinweist. Schließlich identifizierte ich die Transkriptionsfaktoren HSF1, LEF1 und TCF1 als Repressoren des LTR12D_*DHRS2*-Promotors, was nahelegt, dass deren Hemmung oder Verdrängung eine Expression von *DHRS2* während Stress oder Infektion ermöglicht.

Insgesamt identifizieren und characterisieren meine Ergebnisse eine LTR12D-DHRS2-p53-p21-Signalkaskade bei Virus- und Stress-induzierter Seneszenz. Meine Arbeit zeigt auch, wie reaktivierte endogene retrovirale Elemente zur Pathogenese der HIV-assoziierten Alterung beitragen könnten und eröffnet neue Ansätze für therapeutische Strategien gegen virusbedingte zelluläre Dysfunktionen.

7 References

Bibliography:

1. Pizzioli, E., et al., *Crosstalk between human endogenous retroviruses and exogenous viruses.* Microbes Infect, 2024: p. 105427.
2. Kyriakou, E. and G. Magiorkinis, *Interplay between endogenous and exogenous human retroviruses.* Trends Microbiol, 2023. **31**(9): p. 933-946.
3. Bao, C., et al., *Human endogenous retroviruses and exogenous viral infections.* Front Cell Infect Microbiol, 2024. **14**: p. 1439292.
4. Greenwood, A.D., et al., *Transmission, Evolution, and Endogenization: Lessons Learned from Recent Retroviral Invasions.* Microbiol Mol Biol Rev, 2018. **82**(1).
5. Ciminale, V., et al., *HTLV-1 and HTLV-2: highly similar viruses with distinct oncogenic properties.* Front Microbiol, 2014. **5**: p. 398.
6. Masenga, S.K., et al., *HIV-Host Cell Interactions.* Cells, 2023. **12**(10).
7. Deeks, S.G., et al., *HIV infection.* Nature Reviews Disease Primers, 2015. **1**(1): p. 15035.
8. Esbjörnsson, J., et al., *HIV-2 as a model to identify a functional HIV cure.* AIDS Research and Therapy, 2019. **16**(1): p. 24.
9. Campbell-Yesufu, O.T. and R.T. Gandhi, *Update on human immunodeficiency virus (HIV)-2 infection.* Clin Infect Dis, 2011. **52**(6): p. 780-7.
10. Iwanaga, M., *Epidemiology of HTLV-1 Infection and ATL in Japan: An Update.* Front Microbiol, 2020. **11**: p. 1124.
11. *HIV*. Available from: https://www.who.int/data/gho/data/themes/hiv-aids.
12. Bassett, M.T. and K. Brudney, *Treating our way out of AIDS?* Am J Public Health, 2014. **104**(2): p. 200-3.
13. Ng'uni, T., C. Chasara, and Z.M. Ndhlovu, *Major Scientific Hurdles in HIV Vaccine Development: Historical Perspective and Future Directions.* Front Immunol, 2020. **11**: p. 590780.
14. Faust, T.B., et al., *Making Sense of Multifunctional Proteins: Human Immunodeficiency Virus Type 1 Accessory and Regulatory Proteins and Connections to Transcription.* Annu Rev Virol, 2017. **4**(1): p. 241-260.
15. Lewitus, E., et al., *HIV-1 Gag, Pol, and Env diversified with limited adaptation since the 1980s.* mBio, 2024. **15**(3): p. e01749-23.
16. Klingler, J., et al., *How HIV-1 Gag Manipulates Its Host Cell Proteins: A Focus on Interactors of the Nucleocapsid Domain.* Viruses, 2020. **12**(8).
17. Yu, F.H., K.J. Huang, and C.T. Wang, *HIV-1 Mutant Assembly, Processing and Infectivity Expresses Pol Independent of Gag.* Viruses, 2020. **12**(1).
18. Pancera, M., et al., *Structure of HIV-1 gp120 with gp41-interactive region reveals layered envelope architecture and basis of conformational mobility.* Proc Natl Acad Sci U S A, 2010. **107**(3): p. 1166-71.
19. Harris, M., et al., *Slow Receptor Binding of the Noncytopathic HIV-2(UC1) Envs Is Balanced by Long-Lived Activation State and Efficient Fusion Activity.* Cell Rep, 2020. **31**(10): p. 107749.
20. Rosen, C.A., *Tat and Rev: positive modulators of human immunodeficiency virus gene expression.* Gene Expr, 1991. **1**(2): p. 85-90.
21. Karn, J. and C.M. Stoltzfus, *Transcriptional and posttranscriptional regulation of HIV-1 gene expression.* Cold Spring Harb Perspect Med, 2012. **2**(2): p. a006916.
22. Andrew, A. and K. Strebel, *HIV-1 accessory proteins: Vpu and Vif.* Methods Mol Biol, 2014. **1087**: p. 135-58.
23. Strebel, K., *HIV accessory proteins versus host restriction factors.* Curr Opin Virol, 2013. **3**(6): p. 692-9.

24. Malim, M.H. and M. Emerman, *HIV-1 Accessory Proteins—Ensuring Viral Survival in a Hostile Environment.* Cell Host & Microbe, 2008. **3**(6): p. 388-398.
25. Li, L., et al., *Roles of HIV-1 auxiliary proteins in viral pathogenesis and host-pathogen interactions.* Cell Research, 2005. **15**(11): p. 923-934.
26. Casartelli, N., et al., *CD4 and major histocompatibility complex class I downregulation by the human immunodeficiency virus type 1 nef protein in pediatric AIDS progression.* J Virol, 2003. **77**(21): p. 11536-45.
27. Sauter, D., et al., *Tetherin-Driven Adaptation of Vpu and Nef Function and the Evolution of Pandemic and Nonpandemic HIV-1 Strains.* Cell Host & Microbe, 2009. **6**(5): p. 409-421.
28. Sheehy, A.M., et al., *Isolation of a human gene that inhibits HIV-1 infection and is suppressed by the viral Vif protein.* Nature, 2002. **418**(6898): p. 646-50.
29. Douglas, J.L., et al., *Vpu directs the degradation of the human immunodeficiency virus restriction factor BST-2/Tetherin via a {beta}TrCP-dependent mechanism.* J Virol, 2009. **83**(16): p. 7931-47.
30. Willey, R.L., et al., *Human immunodeficiency virus type 1 Vpu protein induces rapid degradation of CD4.* J Virol, 1992. **66**(12): p. 7193-200.
31. Fujita, M., et al., *SAMHD1-Dependent and -Independent Functions of HIV-2/SIV Vpx Protein.* Front Microbiol, 2012. **3**: p. 297.
32. Sharifi, H.J., A.M. Furuya, and C.M. de Noronha, *The role of HIV-1 Vpr in promoting the infection of nondividing cells and in cell cycle arrest.* Curr Opin HIV AIDS, 2012. **7**(2): p. 187-94.
33. Checkley, M.A., B.G. Luttge, and E.O. Freed, *HIV-1 envelope glycoprotein biosynthesis, trafficking, and incorporation.* J Mol Biol, 2011. **410**(4): p. 582-608.
34. McCaul, N., et al., *Intramolecular quality control: HIV-1 envelope gp160 signal-peptide cleavage as a functional folding checkpoint.* Cell Reports, 2021. **36**(9): p. 109646.
35. Doores, K.J., *The HIV glycan shield as a target for broadly neutralizing antibodies.* Febs j, 2015. **282**(24): p. 4679-91.
36. Bour, S., R. Geleziunas, and M.A. Wainberg, *The human immunodeficiency virus type 1 (HIV-1) CD4 receptor and its central role in promotion of HIV-1 infection.* Microbiol Rev, 1995. **59**(1): p. 63-93.
37. Kang, B.H., et al., *Analyses of the TCR repertoire of MHC class II-restricted innate CD4+ T cells.* Experimental & Molecular Medicine, 2015. **47**(3): p. e154-e154.
38. Veillette, M., et al., *Interaction with cellular CD4 exposes HIV-1 envelope epitopes targeted by antibody-dependent cell-mediated cytotoxicity.* J Virol, 2014. **88**(5): p. 2633-44.
39. Février, M., K. Dorgham, and A. Rebollo, *CD4+ T cell depletion in human immunodeficiency virus (HIV) infection: role of apoptosis.* Viruses, 2011. **3**(5): p. 586-612.
40. Jasinska, A.J., I. Pandrea, and C. Apetrei, *CCR5 as a Coreceptor for Human Immunodeficiency Virus and Simian Immunodeficiency Viruses: A Prototypic Love-Hate Affair.* Front Immunol, 2022. **13**: p. 835994.
41. Joseph, S.B. and R. Swanstrom, *The evolution of HIV-1 entry phenotypes as a guide to changing target cells.* J Leukoc Biol, 2018. **103**(3): p. 421-431.
42. Ribeiro, R.M., et al., *Naïve and memory cell turnover as drivers of CCR5-to-CXCR4 tropism switch in human immunodeficiency virus type 1: implications for therapy.* J Virol, 2006. **80**(2): p. 802-9.
43. Masenga, S.K., et al., *HIV–Host Cell Interactions.* Cells, 2023. **12**(10): p. 1351.
44. Mu, W., et al., *Examining Chronic Inflammation, Immune Metabolism, and T Cell Dysfunction in HIV Infection.* Viruses, 2024. **16**(2).
45. Montano, M., et al., *Biological ageing with HIV infection: evaluating the geroscience hypothesis.* The Lancet Healthy Longevity, 2022. **3**(3): p. e194-e205.
46. Appay, V., D. Sauce, and A.D. Kelleher, *HIV Infection as a Model of Accelerated Immunosenescence*, in *Handbook of Immunosenescence: Basic Understanding and*

Clinical Implications, T. Fulop, et al., Editors. 2019, Springer International Publishing: Cham. p. 1961-1989.
47. McGettrick, P., E.A. Barco, and P.W.G. Mallon, *Ageing with HIV.* Healthcare (Basel), 2018. **6**(1).
48. Shiau, S., et al., *The Current State of HIV and Aging: Findings Presented at the 10th International Workshop on HIV and Aging.* AIDS Res Hum Retroviruses, 2020. **36**(12): p. 973-981.
49. Kaplan-Lewis, E., J.A. Aberg, and M. Lee, *Aging with HIV in the ART era.* Seminars in Diagnostic Pathology, 2017. **34**(4): p. 384-397.
50. Lazar, M., et al., *The Impact of HIV on Early Brain Aging—A Pathophysiological (Re)View.* Journal of Clinical Medicine, 2024. **13**(23): p. 7031.
51. Schank, M., et al., *The Impact of HIV- and ART-Induced Mitochondrial Dysfunction in Cellular Senescence and Aging.* Cells, 2021. **10**(1).
52. Zhao, J., et al., *Mitochondrial Functions Are Compromised in CD4 T Cells From ART-Controlled PLHIV.* Front Immunol, 2021. **12**: p. 658420.
53. Fields, J.A. and R.J. Ellis, *Chapter Three - HIV in the cART era and the mitochondrial: immune interface in the CNS*, in *International Review of Neurobiology*, P. Fernyhough and N.A. Calcutt, Editors. 2019, Academic Press. p. 29-65.
54. Guo, J., et al., *Aging and aging-related diseases: from molecular mechanisms to interventions and treatments.* Signal Transduction and Targeted Therapy, 2022. **7**(1): p. 391.
55. Sokoya, T., et al., *HIV as a Cause of Immune Activation and Immunosenescence.* Mediators Inflamm, 2017. **2017**: p. 6825493.
56. Paiardini, M. and M. Müller-Trutwin, *HIV-associated chronic immune activation.* Immunol Rev, 2013. **254**(1): p. 78-101.
57. Angajala, A., et al., *Diverse Roles of Mitochondria in Immune Responses: Novel Insights Into Immuno-Metabolism.* Front Immunol, 2018. **9**: p. 1605.
58. Bloch, M., et al., *Managing HIV-associated inflammation and ageing in the era of modern ART.* HIV Med, 2020. **21 Suppl 3**: p. 2-16.
59. Nabatanzi, R., et al., *Effects of HIV infection and ART on phenotype and function of circulating monocytes, natural killer, and innate lymphoid cells.* AIDS Research and Therapy, 2018. **15**(1): p. 7.
60. Colonna Romano, N. and L. Fanti, *Transposable Elements: Major Players in Shaping Genomic and Evolutionary Patterns.* Cells, 2022. **11**(6).
61. Chesnokova, E., A. Beletskiy, and P. Kolosov, *The Role of Transposable Elements of the Human Genome in Neuronal Function and Pathology.* International Journal of Molecular Sciences, 2022. **23**(10): p. 5847.
62. Cordaux, R. and M.A. Batzer, *The impact of retrotransposons on human genome evolution.* Nat Rev Genet, 2009. **10**(10): p. 691-703.
63. Prokopov, D., et al., *Transposable elements as genome regulators in normal and malignant haematopoiesis.* Blood Cancer Journal, 2025. **15**(1): p. 87.
64. Prokopov, D., et al., *Transposable elements as genome regulators in normal and malignant haematopoiesis.* Blood Cancer J, 2025. **15**(1): p. 87.
65. An, W. and J.D. Boeke, *Transposon technology and vertebrate functional genomics.* Genome Biol, 2005. **6**(12): p. 361.
66. Zhang, W., et al., *Retrotransposon: an insight into neurological disorders from perspectives of neurodevelopment and aging.* Translational Neurodegeneration, 2025. **14**(1): p. 14.
67. Boso, G., et al., *The Oldest Co-opted gag Gene of a Human Endogenous Retrovirus Shows Placenta-Specific Expression and Is Upregulated in Diffuse Large B-Cell Lymphomas.* Mol Biol Evol, 2021. **38**(12): p. 5453-5471.

68. Hohn, O., K. Hanke, and N. Bannert, *HERV-K(HML-2), the Best Preserved Family of HERVs: Endogenization, Expression, and Implications in Health and Disease.* Front Oncol, 2013. **3**: p. 246.
69. Kozubek, P., et al., *Human Endogenous Retroviruses and Their Putative Role in Pathogenesis of Alzheimer's Disease, Inflammation, and Senescence.* Biomedicines, 2025. **13**(1): p. 59.
70. Ruprecht, K., et al., *Human endogenous retrovirus family HERV-K(HML-2) RNA transcripts are selectively packaged into retroviral particles produced by the human germ cell tumor line Tera-1 and originate mainly from a provirus on chromosome 22q11.21.* J Virol, 2008. **82**(20): p. 10008-16.
71. Mi, S., et al., *Syncytin is a captive retroviral envelope protein involved in human placental morphogenesis.* Nature, 2000. **403**(6771): p. 785-9.
72. Srinivasachar Badarinarayan, S., et al., *HIV-1 infection activates endogenous retroviral promoters regulating antiviral gene expression.* Nucleic Acids Res, 2020. **48**(19): p. 10890-10908.
73. da Silva, A.L., et al., *Beyond pathogens: the intriguing genetic legacy of endogenous retroviruses in host physiology.* Front Cell Infect Microbiol, 2024. **14**: p. 1379962.
74. Gruchot, J., et al., *Interplay between activation of endogenous retroviruses and inflammation as common pathogenic mechanism in neurological and psychiatric disorders.* Brain, Behavior, and Immunity, 2023. **107**: p. 242-252.
75. Zhang, Q., et al., *Transcriptional Regulation of Endogenous Retroviruses and Their Misregulation in Human Diseases.* Int J Mol Sci, 2022. **23**(17).
76. Balestrieri, E., et al., *Endogenous Retroviruses Activity as a Molecular Signature of Neurodevelopmental Disorders.* Int J Mol Sci, 2019. **20**(23).
77. Shin, W., S. Mun, and K. Han, *Human Endogenous Retrovirus-K (HML-2)-Related Genetic Variation: Human Genome Diversity and Disease.* Genes (Basel), 2023. **14**(12).
78. Li, Y., G. Zhang, and J. Cui, *Origin and Deep Evolution of Human Endogenous Retroviruses in Pan-Primates.* Viruses, 2022. **14**(7).
79. Grandi, N. and E. Tramontano, *Type W Human Endogenous Retrovirus (HERV-W) Integrations and Their Mobilization by L1 Machinery: Contribution to the Human Transcriptome and Impact on the Host Physiopathology.* Viruses, 2017. **9**(7).
80. Gleason, C., et al., *An integrated approach for the accurate detection of HERV-K HML-2 transcription and protein synthesis.* Nucleic Acids Research, 2025. **53**(2): p. gkaf011.
81. Kyriakou, E. and G. Magiorkinis, *Compilation of all known HERV-K HML-2 proviral integrations.* Mobile DNA, 2025. **16**(1): p. 21.
82. Jarosz, A.S. and J.V. Halo, *Transcription of Endogenous Retroviruses: Broad and Precise Mechanisms of Control.* Viruses, 2024. **16**(8).
83. Bergallo, M., et al., *Human Endogenous Retroviruses Are Preferentially Expressed in Mononuclear Cells From Cord Blood Than From Maternal Blood and in the Fetal Part of Placenta.* Front Pediatr, 2020. **8**: p. 244.
84. Krchlikova, V., Y. Lu, and D. Sauter, *Viral influencers: deciphering the role of endogenous retroviral LTR12 repeats in cellular gene expression.* J Virol, 2025. **99**(2): p. e0135124.
85. Ohtani, H., et al., *Efficient activation of hundreds of LTR12C elements reveals cis-regulatory function determined by distinct epigenetic mechanisms.* Nucleic Acids Res, 2024. **52**(14): p. 8205-8217.
86. Krchlikova, V., Y. Lu, and D. Sauter, *Viral influencers: deciphering the role of endogenous retroviral LTR12 repeats in cellular gene expression.* Journal of Virology, 2025. **99**(2): p. e01351-24.
87. Hu, T., et al., *Long non-coding RNAs transcribed by ERV-9 LTR retrotransposon act in cis to modulate long-range LTR enhancer function.* Nucleic Acids Res, 2017. **45**(8): p. 4479-4492.

88. Delcuve, G.P., D.H. Khan, and J.R. Davie, *Roles of histone deacetylases in epigenetic regulation: emerging paradigms from studies with inhibitors.* Clin Epigenetics, 2012. **4**(1): p. 5.
89. Statello, L., et al., *Gene regulation by long non-coding RNAs and its biological functions.* Nat Rev Mol Cell Biol, 2021. **22**(2): p. 96-118.
90. Blikstad, V., et al., *Evolution of human endogenous retroviral sequences: a conceptual account.* Cell Mol Life Sci, 2008. **65**(21): p. 3348-65.
91. Lee, S.K., S.H. Kim, and J. Ahnn, *Human Endogenous Retroviruses: Friends and Foes in Urology Clinics.* Int Neurourol J, 2022. **26**(4): p. 275-287.
92. Rowe, H.M. and D. Trono, *Dynamic control of endogenous retroviruses during development.* Virology, 2011. **411**(2): p. 273-287.
93. Simula, E.R., et al., *Human Endogenous Retroviruses as Novel Therapeutic Targets in Neurodegenerative Disorders.* Vaccines (Basel), 2025. **13**(4).
94. Durnaoglu, S., S.-K. Lee, and J. Ahnn, *Human Endogenous Retroviruses as Gene Expression Regulators: Insights from Animal Models into Human Diseases.* Molecules and Cells, 2021. **44**(12): p. 861-878.
95. Evans, E.F., A. Saraph, and M. Tokuyama, *Transactivation of Human Endogenous Retroviruses by Viruses.* Viruses, 2024. **16**(11): p. 1649.
96. Arora, A., et al., *SARS-CoV-2 infection induces epigenetic changes in the LTR69 subfamily of endogenous retroviruses.* Mobile DNA, 2023. **14**(1): p. 11.
97. Wang, M., et al., *Transcription profile of human endogenous retroviruses in response to dengue virus serotype 2 infection.* Virology, 2020. **544**: p. 21-30.
98. Riedl, P., et al., *Differential presentation of endogenous and exogenous hepatitis B surface antigens influences priming of CD8(+) T cells in an epitope-specific manner.* Eur J Immunol, 2014. **44**(7): p. 1981-91.
99. Liu, H., et al., *Influenza A Virus Infection Reactivates Human Endogenous Retroviruses Associated with Modulation of Antiviral Immunity.* Viruses, 2022. **14**(7).
100. Wieland, L., et al., *Epstein-Barr Virus-Induced Genes and Endogenous Retroviruses in Immortalized B Cells from Patients with Multiple Sclerosis.* Cells, 2022. **11**(22).
101. Pizzioli, E., et al., *Crosstalk between human endogenous retroviruses and exogenous viruses.* Microbes and Infection, 2024: p. 105427.
102. Brinzevich, D., et al., *HIV-1 interacts with human endogenous retrovirus K (HML-2) envelopes derived from human primary lymphocytes.* J Virol, 2014. **88**(11): p. 6213-23.
103. Petrone, V., et al., *The transactivation of human endogenous retroviruses is associated with HIV-1 reservoir, lymphocyte activation and low CD4 count in virologically suppressed PLWH.* Microbes and Infection, 2025: p. 105478.
104. Vincendeau, M., et al., *Modulation of human endogenous retrovirus (HERV) transcription during persistent and de novo HIV-1 infection.* Retrovirology, 2015. **12**: p. 27.
105. O'Carroll, I.P., et al., *Structural Mimicry Drives HIV-1 Rev-Mediated HERV-K Expression.* J Mol Biol, 2020. **432**(24): p. 166711.
106. Mantovani, F., K. Kitsou, and G. Magiorkinis, *HERVs: Expression Control Mechanisms and Interactions in Diseases and Human Immunodeficiency Virus Infection.* Genes (Basel), 2024. **15**(2).
107. Gao, Y., X.F. Yu, and T. Chen, *Human endogenous retroviruses in cancer: Expression, regulation and function.* Oncol Lett, 2021. **21**(2): p. 121.
108. Zhang, M., S. Zheng, and J.Q. Liang, *Transcriptional and reverse transcriptional regulation of host genes by human endogenous retroviruses in cancers.* Front Microbiol, 2022. **13**: p. 946296.
109. Weber, S., et al., *Epigenetic analysis of HIV-1 proviral genomes from infected individuals: predominance of unmethylated CpG's.* Virology, 2014. **449**: p. 181-9.
110. Arumugam, T., et al., *Deciphering DNA Methylation in HIV Infection.* Front Immunol, 2021. **12**: p. 795121.

111. Shah, R., et al., *Activation of HIV-1 proviruses increases downstream chromatin accessibility.* iScience, 2022. **25**(12): p. 105490.
112. Kint, S., et al., *Underestimated effect of intragenic HIV-1 DNA methylation on viral transcription in infected individuals.* Clinical Epigenetics, 2020. **12**(1): p. 36.
113. Liao, Z., et al., *Cellular Senescence: Mechanisms and Therapeutic Potential.* Biomedicines, 2021. **9**(12).
114. Gorgoulis, V., et al., *Cellular Senescence: Defining a Path Forward.* Cell, 2019. **179**(4): p. 813-827.
115. Huang, W., et al., *Cellular senescence: the good, the bad and the unknown.* Nat Rev Nephrol, 2022. **18**(10): p. 611-627.
116. He, S. and N.E. Sharpless, *Senescence in Health and Disease.* Cell, 2017. **169**(6): p. 1000-1011.
117. Kumari, R. and P. Jat, *Mechanisms of Cellular Senescence: Cell Cycle Arrest and Senescence Associated Secretory Phenotype.* Front Cell Dev Biol, 2021. **9**: p. 645593.
118. Pellarin, I., et al., *Cyclin-dependent protein kinases and cell cycle regulation in biology and disease.* Signal Transduction and Targeted Therapy, 2025. **10**(1): p. 11.
119. Chen, J.H., C.N. Hales, and S.E. Ozanne, *DNA damage, cellular senescence and organismal ageing: causal or correlative?* Nucleic Acids Res, 2007. **35**(22): p. 7417-28.
120. Hernández Borrero, L.J. and W.S. El-Deiry, *Tumor suppressor p53: Biology, signaling pathways, and therapeutic targeting.* Biochim Biophys Acta Rev Cancer, 2021. **1876**(1): p. 188556.
121. Sherr, C.J. and F. McCormick, *The RB and p53 pathways in cancer.* Cancer Cell, 2002. **2**(2): p. 103-112.
122. Gire, V. and V. Dulic, *Senescence from G2 arrest, revisited.* Cell Cycle, 2015. **14**(3): p. 297-304.
123. Weng, Z., et al., *Mesenchymal Stem/Stromal Cell Senescence: Hallmarks, Mechanisms, and Combating Strategies.* Stem Cells Transl Med, 2022. **11**(4): p. 356-371.
124. McHugh, D. and J. Gil, *Senescence and aging: Causes, consequences, and therapeutic avenues.* J Cell Biol, 2018. **217**(1): p. 65-77.
125. Coppé, J.P., et al., *The senescence-associated secretory phenotype: the dark side of tumor suppression.* Annu Rev Pathol, 2010. **5**: p. 99-118.
126. Fan, H., et al., *Recent advances in senescence-associated secretory phenotype and osteoporosis.* Heliyon, 2024. **10**(4): p. e25538.
127. Freund, A., et al., *Inflammatory networks during cellular senescence: causes and consequences.* Trends Mol Med, 2010. **16**(5): p. 238-46.
128. Bleve, A., et al., *Immunosenescence, Inflammaging, and Frailty: Role of Myeloid Cells in Age-Related Diseases.* Clin Rev Allergy Immunol, 2023. **64**(2): p. 123-144.
129. Wong, J.J., et al., *Atherosclerotic cardiovascular disease in aging and the role of advanced cardiovascular imaging.* npj Cardiovascular Health, 2024. **1**(1): p. 11.
130. Del Rey, M.J., et al., *Senescent synovial fibroblasts accumulate prematurely in rheumatoid arthritis tissues and display an enhanced inflammatory phenotype.* Immunity & Ageing, 2019. **16**(1): p. 29.
131. Ruhland, M.K., L.M. Coussens, and S.A. Stewart, *Senescence and cancer: An evolving inflammatory paradox.* Biochim Biophys Acta, 2016. **1865**(1): p. 14-22.
132. Sun, R., J. Feng, and J. Wang, *Underlying Mechanisms and Treatment of Cellular Senescence-Induced Biological Barrier Interruption and Related Diseases.* Aging Dis, 2024. **15**(2): p. 612-639.
133. Qin, Y., H. Liu, and H. Wu, *Cellular Senescence in Health, Disease, and Lens Aging.* Pharmaceuticals, 2025. **18**(2): p. 244.
134. Luan, Y., et al., *Cardiac cell senescence: molecular mechanisms, key proteins and therapeutic targets.* Cell Death Discovery, 2024. **10**(1): p. 78.
135. Saito, Y., S. Yamamoto, and T.S. Chikenji, *Role of cellular senescence in inflammation and regeneration.* Inflammation and Regeneration, 2024. **44**(1): p. 28.

136. Lopes-Paciencia, S., et al., *The senescence-associated secretory phenotype and its regulation.* Cytokine, 2019. **117**: p. 15-22.
137. Khavinson, V., et al., *Senescence-Associated Secretory Phenotype of Cardiovascular System Cells and Inflammaging: Perspectives of Peptide Regulation.* Cells, 2022. **12**(1).
138. Flanagan, K.C., et al., *c-Myb and C/EBPβ regulate OPN and other senescence-associated secretory phenotype factors.* Oncotarget, 2018. **9**(1): p. 21-36.
139. Alqahtani, S., et al., *SASP Modulation for Cellular Rejuvenation and Tissue Homeostasis: Therapeutic Strategies and Molecular Insights.* Cells, 2025. **14**(8).
140. Fang, C.L., B. Liu, and M. Wan, *"Bone-SASP" in Skeletal Aging.* Calcif Tissue Int, 2023. **113**(1): p. 68-82.
141. Rattanavirotkul, N., K. Kirschner, and T. Chandra, *Induction and transmission of oncogene-induced senescence.* Cell Mol Life Sci, 2021. **78**(3): p. 843-852.
142. Wallis, R., H. Mizen, and C.L. Bishop, *The bright and dark side of extracellular vesicles in the senescence-associated secretory phenotype.* Mech Ageing Dev, 2020. **189**: p. 111263.
143. Urbanelli, L., et al., *Extracellular Vesicles as New Players in Cellular Senescence.* Int J Mol Sci, 2016. **17**(9).
144. Lee, B.Y., et al., *Senescence-associated beta-galactosidase is lysosomal beta-galactosidase.* Aging Cell, 2006. **5**(2): p. 187-95.
145. Song, P., J. An, and M.H. Zou, *Immune Clearance of Senescent Cells to Combat Ageing and Chronic Diseases.* Cells, 2020. **9**(3).
146. Kale, A., et al., *Role of immune cells in the removal of deleterious senescent cells.* Immunity & Ageing, 2020. **17**(1): p. 16.
147. Yang, J., et al., *The Paradoxical Role of Cellular Senescence in Cancer.* Front Cell Dev Biol, 2021. **9**: p. 722205.
148. Olivieri, F., et al., *Cellular Senescence and Inflammaging in Age-Related Diseases.* Mediators Inflamm, 2018. **2018**: p. 9076485.
149. Tchkonia, T., et al., *Cellular senescence and the senescent secretory phenotype: therapeutic opportunities.* J Clin Invest, 2013. **123**(3): p. 966-72.
150. Alqahtani, S., et al., *SASP Modulation for Cellular Rejuvenation and Tissue Homeostasis: Therapeutic Strategies and Molecular Insights.* Cells, 2025. **14**(8): p. 608.
151. Dong, Z., et al., *Cellular senescence and SASP in tumor progression and therapeutic opportunities.* Mol Cancer, 2024. **23**(1): p. 181.
152. Liu, Y., I. Lomeli, and S.J. Kron, *Therapy-Induced Cellular Senescence: Potentiating Tumor Elimination or Driving Cancer Resistance and Recurrence?* Cells, 2024. **13**(15): p. 1281.
153. Riessland, M., et al., *Therapeutic targeting of senescent cells in the CNS.* Nat Rev Drug Discov, 2024. **23**(11): p. 817-837.
154. Prata, L., et al., *Senescent cell clearance by the immune system: Emerging therapeutic opportunities.* Semin Immunol, 2018. **40**: p. 101275.
155. Hickson, L.J., et al., *Senolytics decrease senescent cells in humans: Preliminary report from a clinical trial of Dasatinib plus Quercetin in individuals with diabetic kidney disease.* EBioMedicine, 2019. **47**: p. 446-456.
156. Wissler Gerdes, E.O., et al., *Discovery, development, and future application of senolytics: theories and predictions.* Febs j, 2020. **287**(12): p. 2418-2427.
157. Yang, B., et al., *Ruxolitinib-based senomorphic therapy mitigates cardiomyocyte senescence in septic cardiomyopathy by inhibiting the JAK2/STAT3 signaling pathway.* Int J Biol Sci, 2024. **20**(11): p. 4314-4340.
158. Zhang, L., et al., *Targeting cellular senescence with senotherapeutics: senolytics and senomorphics.* Febs j, 2023. **290**(5): p. 1362-1383.
159. Mijit, M., et al., *Role of p53 in the Regulation of Cellular Senescence.* Biomolecules, 2020. **10**(3).
160. Rodier, F. and J. Campisi, *Four faces of cellular senescence.* J Cell Biol, 2011. **192**(4): p. 547-56.

161. Kagawa, S., et al., *p53 expression overcomes p21WAF1/CIP1-mediated G1 arrest and induces apoptosis in human cancer cells.* Oncogene, 1997. **15**(16): p. 1903-9.
162. Al Bitar, S. and H. Gali-Muhtasib, *The Role of the Cyclin Dependent Kinase Inhibitor p21(cip1/waf1) in Targeting Cancer: Molecular Mechanisms and Novel Therapeutics.* Cancers (Basel), 2019. **11**(10).
163. Stein, G.H., et al., *Differential roles for cyclin-dependent kinase inhibitors p21 and p16 in the mechanisms of senescence and differentiation in human fibroblasts.* Mol Cell Biol, 1999. **19**(3): p. 2109-17.
164. Roger, L., F. Tomas, and V. Gire, *Mechanisms and Regulation of Cellular Senescence.* International Journal of Molecular Sciences, 2021. **22**(23): p. 13173.
165. Yan, J., et al., *The role of p21 in cellular senescence and aging-related diseases.* Mol Cells, 2024. **47**(11): p. 100113.
166. O'Sullivan, E.A., et al., *The paradox of senescent-marker positive cancer cells: challenges and opportunities.* npj Aging, 2024. **10**(1): p. 41.
167. Herranz, N. and J. Gil, *Mechanisms and functions of cellular senescence.* J Clin Invest, 2018. **128**(4): p. 1238-1246.
168. Chen, X., et al., *Senescence-like changes induced by expression of p21Waf1/Cip1 in NIH3T3 cell line.* Cell Research, 2002. **12**(3): p. 229-233.
169. Azazmeh, N., et al., *Chronic expression of p16INK4a in the epidermis induces Wnt-mediated hyperplasia and promotes tumor initiation.* Nature Communications, 2020. **11**(1): p. 2711.
170. Laberge, R.M., et al., *MTOR regulates the pro-tumorigenic senescence-associated secretory phenotype by promoting IL1A translation.* Nat Cell Biol, 2015. **17**(8): p. 1049-61.
171. Bourgeois, B. and T. Madl, *Regulation of cellular senescence via the FOXO4-p53 axis.* FEBS Lett, 2018. **592**(12): p. 2083-2097.
172. Lee, S.H., et al., *Sirtuin signaling in cellular senescence and aging.* BMB Rep, 2019. **52**(1): p. 24-34.
173. Schieber, M. and N.S. Chandel, *ROS function in redox signaling and oxidative stress.* Curr Biol, 2014. **24**(10): p. R453-62.
174. Deisenroth, C., et al., *Mitochondrial Hep27 is a c-Myb target gene that inhibits Mdm2 and stabilizes p53.* Mol Cell Biol, 2010. **30**(16): p. 3981-3993.
175. Deisenroth, C., et al., *Mitochondrial Hep27 is a c-Myb target gene that inhibits Mdm2 and stabilizes p53.* Mol Cell Biol, 2010. **30**(16): p. 3981-93.
176. Zhou, Y., et al., *DHRS2 inhibits cell growth and motility in esophageal squamous cell carcinoma.* Oncogene, 2018. **37**(8): p. 1086-1094.
177. Luo, X., et al., *DHRS2 mediates cell growth inhibition induced by Trichothecin in nasopharyngeal carcinoma.* J Exp Clin Cancer Res, 2019. **38**(1): p. 300.
178. Abbas, T. and A. Dutta, *p21 in cancer: intricate networks and multiple activities.* Nat Rev Cancer, 2009. **9**(6): p. 400-14.
179. Bray, J.E., B.D. Marsden, and U. Oppermann, *The human short-chain dehydrogenase/reductase (SDR) superfamily: a bioinformatics summary.* Chem Biol Interact, 2009. **178**(1-3): p. 99-109.
180. Bhatia, C., et al., *Towards a systematic analysis of human short-chain dehydrogenases/reductases (SDR): Ligand identification and structure–activity relationships.* Chemico-Biological Interactions, 2015. **234**: p. 114-125.
181. Kedishvili, N.Y., *Enzymology of retinoic acid biosynthesis and degradation.* J Lipid Res, 2013. **54**(7): p. 1744-60.
182. Barbian, H.J., et al., *β-catenin regulates HIV latency and modulates HIV reactivation.* PLoS Pathog, 2022. **18**(3): p. e1010354.
183. *Encyclopedia of Virology*. 2021: Academic Press. 4109.
184. Ma, Y., et al., *DHRS7 Integrates NADP(+)/NADPH Redox Sensing with Inflammatory Lipid Signalling via the Oxoeicosanoid Pathway.* bioRxiv, 2025.

185. Müller, M.R., et al., *Characterization of the dehydrogenase-reductase DHRS2 and its involvement in histone deacetylase inhibition in urological malignancies.* Experimental Cell Research, 2024. **439**(1): p. 114055.
186. Gao, L., et al., *Chromatin Accessibility Landscape in Human Early Embryos and Its Association with Evolution.* Cell, 2018. **173**(1): p. 248-259.e15.
187. Han, Y., et al., *Decreased DHRS2 expression is associated with HDACi resistance and poor prognosis in ovarian cancer.* Epigenetics, 2020. **15**(1-2): p. 122-133.
188. Pei, H., et al., *RAC2-P38 MAPK-dependent NADPH oxidase activity is associated with the resistance of quiescent cells to ionizing radiation.* Cell Cycle, 2017. **16**(1): p. 113-122.
189. Li, Z., et al., *Emerging roles of dehydrogenase/reductase member 2 (DHRS2) in the pathology of disease.* Eur J Pharmacol, 2021. **898**: p. 173972.
190. Toussaint, O., E.E. Medrano, and T. von Zglinicki, *Cellular and molecular mechanisms of stress-induced premature senescence (SIPS) of human diploid fibroblasts and melanocytes.* Exp Gerontol, 2000. **35**(8): p. 927-45.
191. Naka, K., et al., *Stress-induced premature senescence in hTERT-expressing ataxia telangiectasia fibroblasts.* J Biol Chem, 2004. **279**(3): p. 2030-7.
192. Qin, Y., H. Liu, and H. Wu, *Cellular Senescence in Health, Disease, and Lens Aging.* Pharmaceuticals (Basel), 2025. **18**(2).
193. Ahumada-Castro, U., et al., *Keeping zombies alive: The ER-mitochondria Ca2+ transfer in cellular senescence.* Biochimica et Biophysica Acta (BBA) - Molecular Cell Research, 2021. **1868**(11): p. 119099.
194. Cao, S.S. and R.J. Kaufman, *Endoplasmic reticulum stress and oxidative stress in cell fate decision and human disease.* Antioxid Redox Signal, 2014. **21**(3): p. 396-413.
195. Nousis, L., P. Kanavaros, and A. Barbouti, *Oxidative Stress-Induced Cellular Senescence: Is Labile Iron the Connecting Link?* Antioxidants (Basel), 2023. **12**(6).
196. de Almeida, A., et al., *ROS: Basic Concepts, Sources, Cellular Signaling, and its Implications in Aging Pathways.* Oxid Med Cell Longev, 2022. **2022**: p. 1225578.
197. Ransy, C., et al., *Use of H(2)O(2) to Cause Oxidative Stress, the Catalase Issue.* Int J Mol Sci, 2020. **21**(23).
198. Sizek, H., et al., *Unlocking mitochondrial dysfunction-associated senescence (MiDAS) with NAD+ – A Boolean model of mitochondrial dynamics and cell cycle control.* Translational Oncology, 2024. **49**: p. 102084.
199. Vasileiou, P.V.S., et al., *Mitochondrial Homeostasis and Cellular Senescence.* Cells, 2019. **8**(7).
200. Wiley, C.D., et al., *Mitochondrial Dysfunction Induces Senescence with a Distinct Secretory Phenotype.* Cell Metab, 2016. **23**(2): p. 303-14.
201. Almanza, A., et al., *Endoplasmic reticulum stress signalling - from basic mechanisms to clinical applications.* Febs j, 2019. **286**(2): p. 241-278.
202. Chen, X., et al., *Endoplasmic reticulum stress: molecular mechanism and therapeutic targets.* Signal Transduction and Targeted Therapy, 2023. **8**(1): p. 352.
203. Pluquet, O., A. Pourtier, and C. Abbadie, *The unfolded protein response and cellular senescence. A review in the theme: cellular mechanisms of endoplasmic reticulum stress signaling in health and disease.* Am J Physiol Cell Physiol, 2015. **308**(6): p. C415-25.
204. Pong, K., et al., *Attenuation of staurosporine-induced apoptosis, oxidative stress, and mitochondrial dysfunction by synthetic superoxide dismutase and catalase mimetics, in cultured cortical neurons.* Exp Neurol, 2001. **171**(1): p. 84-97.
205. Kumamoto, K., et al., *Nutlin-3a activates p53 to both down-regulate inhibitor of growth 2 and up-regulate mir-34a, mir-34b, and mir-34c expression, and induce senescence.* Cancer Res, 2008. **68**(9): p. 3193-203.
206. Haronikova, L., et al., *Resistance mechanisms to inhibitors of p53-MDM2 interactions in cancer therapy: can we overcome them?* Cellular & Molecular Biology Letters, 2021. **26**(1): p. 53.

207. Brugarolas, J., et al., *Radiation-induced cell cycle arrest compromised by p21 deficiency.* Nature, 1995. **377**(6549): p. 552-7.
208. Drakos, E., et al., *Activation of the p53 pathway by the MDM2 inhibitor nutlin-3a overcomes BCL2 overexpression in a preclinical model of diffuse large B-cell lymphoma associated with t(14;18)(q32;q21).* Leukemia, 2011. **25**(5): p. 856-67.
209. Bianchi-Smiraglia, A. and M.A. Nikiforov, *Controversial aspects of oncogene-induced senescence.* Cell Cycle, 2012. **11**(22): p. 4147-51.
210. Zhu, B., et al., *PPARß/δ promotes HRAS-induced senescence and tumor suppression by potentiating p-ERK and repressing p-AKT signaling.* Oncogene, 2014. **33**(46): p. 5348-59.
211. Di Micco, R., et al., *Interplay between oncogene-induced DNA damage response and heterochromatin in senescence and cancer.* Nat Cell Biol, 2011. **13**(3): p. 292-302.
212. Olan, I., T. Handa, and M. Narita, *Beyond SAHF: An integrative view of chromatin compartmentalization during senescence.* Current Opinion in Cell Biology, 2023. **83**: p. 102206.
213. Narita, M., *Cellular senescence and chromatin organisation.* British Journal of Cancer, 2007. **96**(5): p. 686-691.
214. Zhou, H., et al., *Regulators involved in trophoblast syncytialization in the placenta of intrauterine growth restriction.* Front Endocrinol (Lausanne), 2023. **14**: p. 1107182.
215. Higuchi, S., et al., *Trophoblast type-specific expression of senescence markers in the human placenta.* Placenta, 2019. **85**: p. 56-62.
216. Gal, H., et al., *Molecular pathways of senescence regulate placental structure and function.* Embo j, 2019. **38**(18): p. e100849.
217. Suvakov, S., et al., *Women With a History of Preeclampsia Exhibit Accelerated Aging and Unfavorable Profiles of Senescence Markers.* Hypertension, 2024. **81**(7): p. 1550-1560.
218. Saleh, T., et al., *Therapy-Induced Senescence: An "Old" Friend Becomes the Enemy.* Cancers (Basel), 2020. **12**(4).
219. Shafqat, N., et al., *Hep27, a member of the short-chain dehydrogenase/reductase family, is an NADPH-dependent dicarbonyl reductase expressed in vascular endothelial tissue.* Cell Mol Life Sci, 2006. **63**(10): p. 1205-13.
220. Oda, T., et al., *Acute HSF1 depletion induces cellular senescence through the MDM2-p53-p21 pathway in human diploid fibroblasts.* J Cell Sci, 2018. **131**(9).
221. Heinz, S., et al., *Genomic Organization of the Human Gene HEP27: Alternative Promoter Usage in HepG2 Cells and Monocyte-Derived Dendritic Cells.* Genomics, 2002. **79**(4): p. 608-615.
222. Evans, E.F., A. Saraph, and M. Tokuyama, *Transactivation of Human Endogenous Retroviruses by Viruses.* Viruses, 2024. **16**(11).
223. Nakamura, A., et al., *Human endogenous retroviruses with transcriptional potential in the brain.* Journal of Human Genetics, 2003. **48**(11): p. 575-581.
224. Durnaoglu, S., S.K. Lee, and J. Ahnn, *Human Endogenous Retroviruses as Gene Expression Regulators: Insights from Animal Models into Human Diseases.* Mol Cells, 2021. **44**(12): p. 861-878.
225. Chuong, E.B., N.C. Elde, and C. Feschotte, *Regulatory evolution of innate immunity through co-option of endogenous retroviruses.* Science, 2016. **351**(6277): p. 1083-7.
226. Ormsby, C.E., et al., *Human endogenous retrovirus expression is inversely associated with chronic immune activation in HIV-1 infection.* PLoS One, 2012. **7**(8): p. e41021.
227. Graham, F.L., et al., *Characteristics of a human cell line transformed by DNA from human adenovirus type 5.* J Gen Virol, 1977. **36**(1): p. 59-74.
228. Mücke, K., et al., *Human Cytomegalovirus Major Immediate Early 1 Protein Targets Host Chromosomes by Docking to the Acidic Pocket on the Nucleosome Surface.* Journal of Virology, 2014. **88**(2): p. 1228-1248.
229. Fouchier, R.A.M., et al., *HIV-1 infection of non-dividing cells: evidence that the amino-terminal basic region of the viral matrix protein is important for Gag processing but not for post-entry nuclear import.* The EMBO Journal, 1997. **16**(15): p. 4531-4539-4539.

230. Parrish, N.F., et al., *Phenotypic properties of transmitted founder HIV-1.* Proc Natl Acad Sci U S A, 2013. **110**(17): p. 6626-33.
231. Ochsenbauer, C., et al., *Generation of transmitted/founder HIV-1 infectious molecular clones and characterization of their replication capacity in CD4 T lymphocytes and monocyte-derived macrophages.* J Virol, 2012. **86**(5): p. 2715-28.
232. Theodore, T.S., et al., *Short Communication: Construction and Characterization of a Stable Full-Length Macrophage-Tropic HIV Type 1 Molecular Clone That Directs the Production of High Titers of Progeny Virions.* AIDS Research and Human Retroviruses, 1996. **12**(3): p. 191-194.
233. Theodore, T.S., et al., *Construction and characterization of a stable full-length macrophage-tropic HIV type 1 molecular clone that directs the production of high titers of progeny virions.* AIDS Res Hum Retroviruses, 1996. **12**(3): p. 191-4.
234. Li, Y., et al., *Molecular characterization of human immunodeficiency virus type 1 cloned directly from uncultured human brain tissue: identification of replication-competent and -defective viral genomes.* J Virol, 1991. **65**(8): p. 3973-85.
235. O'Brien, W.A., et al., *HIV-1 tropism for mononuclear phagocytes can be determined by regions of gp120 outside the CD4-binding domain.* Nature, 1990. **348**(6296): p. 69-73.
236. Clavel, F., et al., *Molecular cloning and polymorphism of the human immune deficiency virus type 2.* Nature, 1986. **324**(6098): p. 691-5.
237. Ryan-Graham, M.A. and K.W. Peden, *Both virus and host components are important for the manifestation of a Nef- phenotype in HIV-1 and HIV-2.* Virology, 1995. **213**(1): p. 158-68.
238. Clavel, F., et al., *Isolation of a new human retrovirus from West African patients with AIDS.* Science, 1986. **233**(4761): p. 343-6.
239. Gao, F., et al., *Human infection by genetically diverse SIVSM-related HIV-2 in west Africa.* Nature, 1992. **358**(6386): p. 495-9.
240. Shibata, R., et al., *Mutational analysis of the human immunodeficiency virus type 2 (HIV-2) genome in relation to HIV-1 and simian immunodeficiency virus SIV (AGM).* J Virol, 1990. **64**(2): p. 742-7.
241. Marr, R.A., et al., *Neprilysin regulates amyloid Beta peptide levels.* J Mol Neurosci, 2004. **22**(1-2): p. 5-11.
242. Gándara, C., V. Affleck, and E.A. Stoll, *Manufacture of Third-Generation Lentivirus for Preclinical Use, with Process Development Considerations for Translation to Good Manufacturing Practice.* Hum Gene Ther Methods, 2018. **29**(1): p. 1-15.
243. Kearns, N.A., et al., *Cas9 effector-mediated regulation of transcription and differentiation in human pluripotent stem cells.* Development, 2014. **141**(1): p. 219-23.
244. Suzuki, H., et al., *Recurrent noncoding U1 snRNA mutations drive cryptic splicing in SHH medulloblastoma.* Nature, 2019. **574**(7780): p. 707-711.
245. Sanjana, N.E., O. Shalem, and F. Zhang, *Improved vectors and genome-wide libraries for CRISPR screening.* Nat Methods, 2014. **11**(8): p. 783-784.
246. Zhang, M., et al., *MSAID: multiple sequence alignment based on a measure of information discrepancy.* Computational Biology and Chemistry, 2005. **29**(2): p. 175-181.
247. Owczarzy, R., et al., *IDT SciTools: a suite for analysis and design of nucleic acid oligomers.* Nucleic Acids Res, 2008. **36**(Web Server issue): p. W163-9.
248. Safwan-Zaiter, H., N. Wagner, and K.D. Wagner, *P16INK4A-More Than a Senescence Marker.* Life (Basel), 2022. **12**(9).
249. Rayess, H., M.B. Wang, and E.S. Srivatsan, *Cellular senescence and tumor suppressor gene p16.* Int J Cancer, 2012. **130**(8): p. 1715-25.
250. Herold, N., et al., *HIV-1 entry in SupT1-R5, CEM-ss, and primary CD4+ T cells occurs at the plasma membrane and does not require endocytosis.* J Virol, 2014. **88**(24): p. 13956-70.
251. Abraham, R.T. and A. Weiss, *Jurkat T cells and development of the T-cell receptor signalling paradigm.* Nature Reviews Immunology, 2004. **4**(4): p. 301-308.

252. Cristofalo, V.J., et al., *Relationship between donor age and the replicative lifespan of human cells in culture: a reevaluation.* Proc Natl Acad Sci U S A, 1998. **95**(18): p. 10614-9.
253. Srivastava, K.K., et al., *Human immunodeficiency virus type 1 NL4-3 replication in four T-cell lines: rate and efficiency of entry, a major determinant of permissiveness.* J Virol, 1991. **65**(7): p. 3900-2.
254. Boswell, M.T. and S.L. Rowland-Jones, *Delayed disease progression in HIV-2: the importance of TRIM5α and the retroviral capsid.* Clin Exp Immunol, 2019. **196**(3): p. 305-317.
255. Vidya Vijayan, K.K., et al., *Pathophysiology of CD4+ T-Cell Depletion in HIV-1 and HIV-2 Infections.* Front Immunol, 2017. **8**: p. 580.
256. Kong, R., et al., *Broad and potent neutralizing antibody responses elicited in natural HIV-2 infection.* J Virol, 2012. **86**(2): p. 947-60.
257. Bour, S., et al., *Naturally occurring amino acid substitutions in the HIV-2 ROD envelope glycoprotein regulate its ability to augment viral particle release.* Virology, 2003. **309**(1): p. 85-98.
258. Ayisi, N.K., *Differential cytopathicity and susceptibility of Ghanaian highly divergent HIV-2 -GH2-, prototype HIV-2 -GH1-, and prototype HIV-1 -GH3- to inhibition by ddCyd and ddIno.* East Afr Med J, 1995. **72**(10): p. 654-7.
259. Woottum, M., et al., *Macrophages: Key Cellular Players in HIV Infection and Pathogenesis.* Viruses, 2024. **16**(2).
260. Koppensteiner, H., R. Brack-Werner, and M. Schindler, *Macrophages and their relevance in Human Immunodeficiency Virus Type I infection.* Retrovirology, 2012. **9**: p. 82.
261. Laakso, M.M., et al., *V3 loop truncations in HIV-1 envelope impart resistance to coreceptor inhibitors and enhanced sensitivity to neutralizing antibodies.* PLoS Pathog, 2007. **3**(8): p. e117.
262. Berkowitz, R.D., et al., *CCR5- and CXCR4-utilizing strains of human immunodeficiency virus type 1 exhibit differential tropism and pathogenesis in vivo.* J Virol, 1998. **72**(12): p. 10108-17.
263. Hofmann, H., et al., *The Vpx lentiviral accessory protein targets SAMHD1 for degradation in the nucleus.* J Virol, 2012. **86**(23): p. 12552-60.
264. Duncan, C.J. and Q.J. Sattentau, *Viral determinants of HIV-1 macrophage tropism.* Viruses, 2011. **3**(11): p. 2255-79.
265. Rashid, F., et al., *Interactions between HIV proteins and host restriction factors: implications for potential therapeutic intervention in HIV infection.* Front Immunol, 2024. **15**: p. 1390650.
266. Ishibashi, A., et al., *A simple method using CRISPR-Cas9 to knock-out genes in murine cancerous cell lines.* Scientific Reports, 2020. **10**(1): p. 22345.
267. Cai, R., et al., *CRISPR/dCas9 Tools: Epigenetic Mechanism and Application in Gene Transcriptional Regulation.* Int J Mol Sci, 2023. **24**(19).
268. Omachi, K. and J.H. Miner, *Comparative analysis of dCas9-VP64 variants and multiplexed guide RNAs mediating CRISPR activation.* PLoS One, 2022. **17**(6): p. e0270008.
269. Rauluseviciute, I., et al., *JASPAR 2024: 20th anniversary of the open-access database of transcription factor binding profiles.* Nucleic Acids Research, 2024. **52**(D1): p. D174-D182.
270. Zheng, R., et al., *Cistrome Data Browser: expanded datasets and new tools for gene regulatory analysis.* Nucleic Acids Research, 2018. **47**(D1): p. D729-D735.
271. Yasuda, K., et al., *Phosphorylation of HSF1 at serine 326 residue is related to the maintenance of gynecologic cancer stem cells through expression of HSP27.* Oncotarget, 2017. **8**(19): p. 31540-31553.
272. Gabriel, S., T. Czerny, and E. Riegel, *Repression motif in HSF1 regulated by phosphorylation.* Cellular Signalling, 2023. **110**: p. 110813.

273. Jin, X., D. Moskophidis, and N.F. Mivechi, *Targeted Replacement of HSF1 Phosphorylation Sites at S303/S307 with Alanine Residues in Mice Increases Cell Proliferation and Drug Resistance.* Methods Mol Biol, 2023. **2693**: p. 81-94.
274. Kline, M.P. and R.I. Morimoto, *Repression of the heat shock factor 1 transcriptional activation domain is modulated by constitutive phosphorylation.* Mol Cell Biol, 1997. **17**(4): p. 2107-15.
275. Kulakovskiy, I.V., et al., *HOCOMOCO: towards a complete collection of transcription factor binding models for human and mouse via large-scale ChIP-Seq analysis.* Nucleic Acids Res, 2018. **46**(D1): p. D252-d259.
276. Wild, S.L., et al., *The Canonical Wnt Pathway as a Key Regulator in Liver Development, Differentiation and Homeostatic Renewal.* Genes (Basel), 2020. **11**(10).
277. Kim, S., et al., *The Distinct Role of Tcfs and Lef1 in the Self-Renewal or Differentiation of Mouse Embryonic Stem Cells.* Int J Stem Cells, 2020. **13**(2): p. 192-201.
278. Lien, W.H. and E. Fuchs, *Wnt some lose some: transcriptional governance of stem cells by Wnt/β-catenin signaling.* Genes Dev, 2014. **28**(14): p. 1517-32.
279. Besnard-Guerin, C., et al., *HIV-1 Vpu sequesters beta-transducin repeat-containing protein (betaTrCP) in the cytoplasm and provokes the accumulation of beta-catenin and other SCFbetaTrCP substrates.* J Biol Chem, 2004. **279**(1): p. 788-95.
280. Mylonas, A. and A. O'Loghlen, *Cellular Senescence and Ageing: Mechanisms and Interventions.* Front Aging, 2022. **3**: p. 866718.
281. Salminen, A., et al., *Mitochondrial dysfunction and oxidative stress activate inflammasomes: impact on the aging process and age-related diseases.* Cell Mol Life Sci, 2012. **69**(18): p. 2999-3013.
282. Gorbunova, V., et al., *The role of retrotransposable elements in ageing and age-associated diseases.* Nature, 2021. **596**(7870): p. 43-53.
283. Chen, Q. and B.N. Ames, *Senescence-like growth arrest induced by hydrogen peroxide in human diploid fibroblast F65 cells.* Proc Natl Acad Sci U S A, 1994. **91**(10): p. 4130-4.
284. Jalava, A., K. Akerman, and J. Heikkilä, *Protein kinase inhibitor, staurosporine, induces a mature neuronal phenotype in SH-SY5Y human neuroblastoma cells through an alpha-, beta-, and zeta-protein kinase C-independent pathway.* J Cell Physiol, 1993. **155**(2): p. 301-12.
285. Lindner, P., et al., *Cell death induced by the ER stressor thapsigargin involves death receptor 5, a non-autophagic function of MAP1LC3B, and distinct contributions from unfolded protein response components.* Cell Communication and Signaling, 2020. **18**(1): p. 12.
286. Efeyan, A., et al., *Induction of p53-dependent senescence by the MDM2 antagonist nutlin-3a in mouse cells of fibroblast origin.* Cancer Res, 2007. **67**(15): p. 7350-7.
287. Orendi, K., et al., *The choriocarcinoma cell line BeWo: syncytial fusion and expression of syncytium-specific proteins.* Reproduction, 2010. **140**(5): p. 759-66.
288. Chowdhury, I.H., et al., *HIV-1 Vpr activates cell cycle inhibitor p21/Waf1/Cip1: a potential mechanism of G2/M cell cycle arrest.* Virology, 2003. **305**(2): p. 371-7.
289. Antonucci, J.M., C. St Gelais, and L. Wu, *The Dynamic Interplay between HIV-1, SAMHD1, and the Innate Antiviral Response.* Front Immunol, 2017. **8**: p. 1541.
290. Lippman, Z., et al., *Distinct mechanisms determine transposon inheritance and methylation via small interfering RNA and histone modification.* PLoS Biol, 2003. **1**(3): p. E67.
291. Mohamed, A., et al., *HIV-2 Vpx neutralizes host restriction factor SAMHD1 to promote viral pathogenesis.* Scientific Reports, 2021. **11**(1): p. 20984.
292. Fu, W., et al., *Immune Activation Influences SAMHD1 Expression and Vpx-mediated SAMHD1 Degradation during Chronic HIV-1 Infection.* Scientific Reports, 2016. **6**(1): p. 38162.
293. Pauls, E., et al., *p21 regulates the HIV-1 restriction factor SAMHD1.* Proc Natl Acad Sci U S A, 2014. **111**(14): p. E1322-4.

294. Klein, F., et al., *Enhanced HIV-1 immunotherapy by commonly arising antibodies that target virus escape variants.* J Exp Med, 2014. **211**(12): p. 2361-72.
295. Mukhopadhyay, S., A. Plüddemann, and S. Gordon, *Macrophage pattern recognition receptors in immunity, homeostasis and self tolerance.* Adv Exp Med Biol, 2009. **653**: p. 1-14.
296. Bergamaschi, A., et al., *The CDK inhibitor p21Cip1/WAF1 is induced by FcgammaR activation and restricts the replication of human immunodeficiency virus type 1 and related primate lentiviruses in human macrophages.* J Virol, 2009. **83**(23): p. 12253-65.
297. Allouch, A., et al., *p21-mediated RNR2 repression restricts HIV-1 replication in macrophages by inhibiting dNTP biosynthesis pathway.* Proc Natl Acad Sci U S A, 2013. **110**(42): p. E3997-4006.
298. Vázquez, N., et al., *Human immunodeficiency virus type 1-induced macrophage gene expression includes the p21 gene, a target for viral regulation.* J Virol, 2005. **79**(7): p. 4479-91.
299. Gioia, L., et al., *A genome-wide survey of mutations in the Jurkat cell line.* BMC Genomics, 2018. **19**(1): p. 334.
300. Miranda Alcalde, B., et al., *The importance of Li-Fraumeni syndrome, a hereditary cancer predisposition disorder.* Arch Argent Pediatr, 2021. **119**(1): p. e11-e17.
301. Horton, R., P. Spearman, and L. Ratner, *HIV-2 viral protein X association with the GAG p27 capsid protein.* Virology, 1994. **199**(2): p. 453-7.
302. ; Available from: https://may2025.archive.ensembl.org/Homo_sapiens/Gene/Summary?db=core;g=ENSG00000100867;r=14:23630115-23645639.
303. Gabrielli, F. and S. Tofanelli, *Molecular and functional evolution of human DHRS2 and DHRS4 duplicated genes.* Gene, 2012. **511**(2): p. 461-9.
304. Heinz, S., et al., *Genomic organization of the human gene HEP27: alternative promoter usage in HepG2 cells and monocyte-derived dendritic cells.* Genomics, 2002. **79**(4): p. 608-15.
305. Tracey, I., et al., *Brain choline-containing compounds are elevated in HIV-positive patients before the onset of AIDS dementia complex: A proton magnetic resonance spectroscopic study.* Neurology, 1996. **46**(3): p. 783-8.
306. Dhamija, N., et al., *Tat predominantly associates with host promoter elements in HIV-1-infected T-cells - regulatory basis of transcriptional repression of c-Rel.* Febs j, 2015. **282**(3): p. 595-610.
307. Laustsen, A. and R.O. Bak, *Electroporation-Based CRISPR/Cas9 Gene Editing Using Cas9 Protein and Chemically Modified sgRNAs.* Methods Mol Biol, 2019. **1961**: p. 127-134.
308. Lu, J. and S. Wang, *CRISPR/Cas9-Mediated Gene Knockout in Cells and Tissues Using Lentivirus.* Curr Protoc, 2023. **3**(5): p. e772.
309. Jamour, P., et al., *Comparing chemical transfection, electroporation, and lentiviral vector transduction to achieve optimal transfection conditions in the Vero cell line.* BMC Mol Cell Biol, 2024. **25**(1): p. 15.
310. Hamada, T., et al., *Electroporation Induces Unexpected Alterations in Gene Expression: A Tip for Selection of Optimal Transfection Method.* Curr Issues Mol Biol, 2025. **47**(2).
311. Casanova, V., et al., *HIV-Tat upregulates the expression of senescence biomarkers in CD4(+) T-cells.* Front Immunol, 2025. **16**: p. 1568762.
312. Rodrigues, L.P., et al., *Hallmarks of aging and immunosenescence: Connecting the dots.* Cytokine & Growth Factor Reviews, 2021. **59**: p. 9-21.
313. Bozic, T., et al., *Gene electrotransfer of proinflammatory chemokines CCL5 and CCL17 as a novel approach of modifying cytokine expression profile in the tumor microenvironment.* Bioelectrochemistry, 2021. **140**: p. 107795.
314. Elemam, N.M., I.M. Talaat, and A.A. Maghazachi, *CXCL10 Chemokine: A Critical Player in RNA and DNA Viral Infections.* Viruses, 2022. **14**(11).

315. Sturmlechner, I., et al., *p21 produces a bioactive secretome that places stressed cells under immunosurveillance.* Science, 2021. **374**(6567): p. eabb3420.
316. Li, Z., et al., *DHRS2 inhibits cell growth and metastasis in ovarian cancer by downregulation of CHKα to disrupt choline metabolism.* Cell Death & Disease, 2022. **13**(10): p. 845.
317. Yeruva, S., G. Ramadori, and D. Raddatz, *NF-kappaB-dependent synergistic regulation of CXCL10 gene expression by IL-1beta and IFN-gamma in human intestinal epithelial cell lines.* Int J Colorectal Dis, 2008. **23**(3): p. 305-17.
318. Chen, M. and L.S. Qi, *Repurposing CRISPR System for Transcriptional Activation.* Adv Exp Med Biol, 2017. **983**: p. 147-157.
319. Gibbons, J.M., et al., *HIV-1 Accessory Protein Vpr Interacts with REAF/RPRD2 To Mitigate Its Antiviral Activity.* J Virol, 2020. **94**(4).
320. Mouzakis, A., et al., *Mechanisms of Immune Evasion in HIV-1: The Role of Virus-Host Protein Interactions.* Current Issues in Molecular Biology, 2025. **47**(5): p. 367.
321. Byeon, I.-J.L., et al., *Structure of HIV-1 Vpr in complex with the human nucleotide excision repair protein hHR23A.* Nature Communications, 2021. **12**(1): p. 6864.
322. Langer, S., et al., *HIV-1 Vpu is a potent transcriptional suppressor of NF-κB-elicited antiviral immune responses.* eLife, 2019. **8**: p. e41930.
323. Yin, X., et al., *Sensor Sensibility-HIV-1 and the Innate Immune Response.* Cells, 2020. **9**(1).
324. Trivedi, R. and D.A. Jurivich, *A molecular perspective on age-dependent changes to the heat shock axis.* Exp Gerontol, 2020. **137**: p. 110969.
325. Vladimirova, S.A., et al., *Unveiling the HSF1 Interaction Network: Key Regulators of Its Function in Cancer.* Cancers (Basel), 2024. **16**(23).
326. Rawat, P. and D. Mitra, *Cellular heat shock factor 1 positively regulates human immunodeficiency virus-1 gene expression and replication by two distinct pathways.* Nucleic Acids Res, 2011. **39**(14): p. 5879-92.
327. Spiegelman, V.S., et al., *Wnt/β-Catenin Signaling Induces the Expression and Activity of βTrCP Ubiquitin Ligase Receptor.* Molecular Cell, 2000. **5**(5): p. 877-882.
328. Narasipura, S.D., et al., *Role of β-catenin and TCF/LEF family members in transcriptional activity of HIV in astrocytes.* J Virol, 2012. **86**(4): p. 1911-21.
329. Henderson, L.J., et al., *Human immunodeficiency virus type 1 (HIV-1) transactivator of transcription through its intact core and cysteine-rich domains inhibits Wnt/β-catenin signaling in astrocytes: relevance to HIV neuropathogenesis.* J Neurosci, 2012. **32**(46): p. 16306-13.
330. Cadigan, K.M. and M.L. Waterman, *TCF/LEFs and Wnt signaling in the nucleus.* Cold Spring Harb Perspect Biol, 2012. **4**(11).
331. Weiser, K., et al., *HIV's Nef interacts with β-catenin of the Wnt signaling pathway in HEK293 cells.* PLoS One, 2013. **8**(10): p. e77865.
332. du Chéné, I., et al., *Suv39H1 and HP1gamma are responsible for chromatin-mediated HIV-1 transcriptional silencing and post-integration latency.* Embo j, 2007. **26**(2): p. 424-35.
333. Zhao, S., et al., *TNRC18 engages H3K9me3 to mediate silencing of endogenous retrotransposons.* Nature, 2023. **623**(7987): p. 633-642.
334. Rossin, F., et al., *Transglutaminase Type 2 regulates the Wnt/β-catenin pathway in vertebrates.* Cell Death Dis, 2021. **12**(3): p. 249.
335. Chou, S.D., et al., *HSF1 regulation of β-catenin in mammary cancer cells through control of HuR/elavL1 expression.* Oncogene, 2015. **34**(17): p. 2178-2188.
336. Eastman, Q. and R. Grosschedl, *Regulation of LEF-1/TCF transcription factors by Wnt and other signals.* Current Opinion in Cell Biology, 1999. **11**(2): p. 233-240.
337. Crean, D., et al., *Glucose reintroduction triggers the activation of Nrf2 during experimental ischemia reperfusion.* Molecular and Cellular Biochemistry, 2012. **366**(1): p. 231-238.

338. Motawea, H.K.B., et al., *Human Placenta Expresses α(2)-Adrenergic Receptors and May Be Implicated in Pathogenesis of Preeclampsia and Fetal Growth Restriction.* Am J Pathol, 2018. **188**(12): p. 2774-2785.
339. Iwai, K., et al., *Transglutaminase 2-dependent deamidation of glyceraldehyde-3-phosphate dehydrogenase promotes trophoblastic cell fusion.* J Biol Chem, 2014. **289**(8): p. 4989-99.
340. Lu, X., et al., *Fine-Tuned and Cell-Cycle-Restricted Expression of Fusogenic Protein Syncytin-2 Maintains Functional Placental Syncytia.* Cell Reports, 2017. **21**(5): p. 1150-1159.
341. Ma, H., et al., *Conditioned medium from primary cytotrophoblasts, primary placenta-derived mesenchymal stem cells, or sub-cultured placental tissue promoted HUVEC angiogenesis in vitro.* Stem Cell Res Ther, 2021. **12**(1): p. 141.
342. Kreis, N.N., et al., *Functional Analysis of p21(Cip1/CDKN1A) and Its Family Members in Trophoblastic Cells of the Placenta and Its Roles in Preeclampsia.* Cells, 2021. **10**(9).
343. Trino, S., et al., *Targeting the p53-MDM2 interaction by the small-molecule MDM2 antagonist Nutlin-3a: a new challenged target therapy in adult Philadelphia positive acute lymphoblastic leukemia patients.* Oncotarget, 2016. **7**(11): p. 12951-61.
344. Shen, H. and C.G. Maki, *Pharmacologic activation of p53 by small-molecule MDM2 antagonists.* Curr Pharm Des, 2011. **17**(6): p. 560-8.
345. Baniulyte, G., et al., *Shared gene targets of the ATF4 and p53 transcriptional networks.* bioRxiv, 2023.
346. Baz-Martínez, M., et al., *Cell senescence is an antiviral defense mechanism.* Scientific Reports, 2016. **6**(1): p. 37007.
347. AbuBakar, S., et al., *Senescence Affects Endothelial Cells Susceptibility to Dengue Virus Infection.* International Journal of Medical Sciences, 2014. **11**(6): p. 538-544.

8 Acknowledgements

Looking back on my Ph.D. journey fills me with deep emotions. I still vividly remember the moment I received the long-awaited email from Prof. Dr. Daniel Sauter. His positive response marked the beginning of an incredible chapter in my life. I am truly grateful to him for giving me the opportunity to pursue research in Germany and for believing in my potential.

Prof. Dr. Sauter not only offered me the chance to work in an international and intellectually stimulating environment but also constantly challenged me with new research questions. His mentorship, guidance, and trust helped shape the scientist in me. I am especially thankful for the intellectual freedom, critical feedback, and patience he provided throughout this journey.

I would also like to express my sincere gratitude to my thesis advisory committee members, Prof. Dr. Michael Schindler and Prof. Dr. Michelle Vincendeau, for their valuable input, innovative ideas, and timely guidance, which helped strengthen this project at every stage. My thanks extend to the Interfaculty Graduate School of Infection Biology and Microbiology (IGIM) for offering a well-structured Ph.D. program and equipping me with both fundamental and advanced research skills essential for my scientific development.

I am deeply thankful to Smitha and Rishikesh, who supported me immensely during my initial days in Germany and played a key role in helping me settle down mentally and emotionally. A heartfelt thank you to Siddhesh, who supported me from the very beginning from applying to Ph.D. positions to the final stages of thesis writing. His constant support made my journey much smoother.

My deepest gratitude goes to my family: Mommy, papa, Gaurav (brother) and bai (grandmother), for their unconditional love and constant encouragement. Among all these incredible people, I am especially thankful to my mother and my mother-in-law, whose unwavering support, even from afar, gave me strength throughout this journey. I am also grateful to my siblings-in-law, Sahil and Shrushti, and the entire Gandhi and Munot families for their unwavering support.

I am especially grateful to all members of the AG Sauter group: Moritz, Kristina, Martin, Isabell, Sharmeen and others for making work enjoyable, sharing laughter, and engaging in enriching scientific discussions. Yueshuang and Daniel also added greatly to this collaborative environment. It brought me immense happiness to work with such a dedicated and kind team. I would also like to thank Matteo, Johanna, Rabea, Vincent and Elena, interacting with each of you was always a pleasure. I would also like to thank the technical and administrative staff who was always there to support me in this journey.

To my dear friends in Tübingen and across Germany, Yogesh, Utkarsh, Vaibhavi, Azdah, Sisi, Shruthi, Hardeep, Yashika, and Karan, thank you for making this foreign land feel like home. A big thanks to Ashwini ji, Sunil ji, and the Shaha family for their warmth and generosity, which created a strong sense of belonging and comfort for us.

I would like to express my heartfelt appreciation to my husband, Shubham, who stood by me through every high and low, offering unwavering love, strength, and support. His constant presence gave me the courage to persevere, even during the most challenging times. This accomplishment would not have been possible without his patience, steadfast belief in me, and quiet resilience, thank you, Shubham, for being my rock.

This page is intentionally left blank

9 Statutory declaration

I hereby declare that I wrote the present dissertation with the title

“Activation of an LTR12D repeat by HIV and other stress inducers leads to DHRS2-mediated cellular senescence”

independently and used no other aids than those cited. In each individual case, I have clearly identified the source of the passages that are taken word for word or paraphrased from other works.

I also hereby declare that I have carried out my scientific work according to the principles of good scientific practice in accordance with the current „Satzung der Universität Tübingen zur Sicherung guter wissenschaftlicher Praxis“ (Rules of the University of Tübingen for Assuring Good Scientific Practice).

Tübingen _____

_____ Daksha Munot

This page is intentionally left blank

10 Supplements

Research manuscripts:

1. Arora, A., Kolberg, J.E., Srinivasachar Badarinarayan, S., Savytska, N., Munot, D., Müller, M., Krchlíková, V., Sauter, D., & Bansal, V. (2023). SARS-CoV-2 infection induces epigenetic changes in the LTR69 subfamily of endogenous retroviruses. *Mob DNA*, *14*(1), 11. doi: 10.1186/s13100-023-00299-1. **PMID: 37667401**.

2. Munot, D., Najjar, G., Singh, M., Günes, C., Sauter, D., & Arora, A. (2025). Antagonistic Regulation of LINE-1/Alu Elements and Their Repressor APOBEC3B in Cellular Senescence. *bioRxiv*. doi: https://doi.org/10.1101/2025.03.27.645653. (**Preprint, in revision**).

3. Srinivasachar Badarinarayan, S., Munot, D., Ikonomi, N., Prelli Bozzo, C., Müller, M., Meckes, L.M., Leyens, J., Werle, S.D., Schwab, J.D., Kirchhoff, F., Kestler, H.A., & Sauter, D. (n.d.). HIV-1 activates an endogenous retroviral promoter regulating p53 signaling and senescence. (**Manuscript in preparation**).

This page is intentionally left blank

11 Contributions

Experiment	Contributor	Contribution	Significance
Determination of LTR12D_*DHRS2* transcript levels in HIV-1-infected primary macrophages	Dr. Martin Müller and Ms. Lea Meckes, Tübingen	They cultured MDMs and performed some of the infection experiments (HIV-1 (CH077 and modified NL4-3))	It provided a helpful contribution to the project.
***DHRS2* knockout (KO) in primary CD4+ T cells via electroporation**	Dr. Caterina Prelli Bozzo, Ulm	She performed the electroporation, and monitored infection rates and DHRS2 protein levels via flow cytometry	Her established protocol for the initial KO experiment was beneficial for the subsequent KO approaches
Effects of LEF1, TCF1, and β-catenin on the LTR12D promoter of *DHRS2*	Ms. Isabell Haußmann, Tübingen	She performed the overexpression experiments.	It provided a helpful contribution to the project.
Induction of the LTR12D-DHRS2-p21 cascade in immortalized and primary BJ fibroblasts	Mr. Gregoire Najjar, Ulm	He performed the transduction experiments and provided RNA.	It enabled me to investigate the LTR12D-DHRS2 cascade in oncogene-induced senescence.
Induction of the LTR12D-DHRS2-p21 cascade in BeWo cells and primary human cytotrophoblasts	Ms. Yueshuang Lu, Tübingen	She cultured both primary trophoblasts and trophoblast cell lines	It enabled me to investigate the LTR12D-DHRS2 cascade upon syncytia formation.